R. & M. No. 2811
(13,240, 13,395, 13,460, 13,533)
A.R.C. Technical Report

MINISTRY OF SUPPLY

AERONAUTICAL RESEARCH COUNCIL
REPORTS AND MEMORANDA

The Two-dimensional Subsonic Flow of an Inviscid Fluid about an Aerofoil of Arbitrary Shape

Part I. Incompressible Flow about a Symmetrical Aerofoil in a Channel or Free Stream.

Part II. Incompressible Flow about an Asymmetric Aerofoil in a Free Stream.

Part III. The Influence Factor Method of Calculating Incompressible Flow.

Part IV. Compressible Flow.

By

L. C. Woods, M.A., D.Phil.

LONDON: HER MAJESTY'S STATIONERY OFFICE

1953

FIFTEEN SHILLINGS NET

The Two-dimensional Subsonic Flow of an Inviscid Fluid about an Aerofoil of Arbitrary Shape

Parts I to IV

By

L. C. Woods, M.A., D.Phil.

COMMUNICATED BY PROFESSOR G. TEMPLE

Reports and Memoranda No. 2811

November, 1950

Summary.—The paper describes and applies exact methods of calculating the incompressible flow about thick aerofoils of general shape in a free stream, and about symmetrical aerofoils between channel walls. One of these methods is extended to an approximate treatment of subsonic compressible flow by making use of von Kármán's transformation.

General Introduction.—The paper introduces new and exact methods of calculating the inviscid flow about two-dimensional aerofoils. Parts 1, 2 and 3 are concerned with incompressible flow, but with only slight modifications the work is applied to compressible flow in Part 4. Part 1 deals with a symmetric aerofoil at zero incidence in a channel or free stream, while the asymmetric case and the effect of circulation are dealt with in Part 2. The method gives velocities throughout the field of flow, and, at least for incompressible flow, is much quicker than the relaxation methods that have been applied to this problem. The principle is to replace the aerofoil by a series of small arcs on which it is assumed that the product of the radius of curvature and the velocity is constant. It is almost equivalent to replacing the aerofoil by a many-sided polygon, for, at some distance from the aerofoil, the field due to a polygon and that due to a profile composed of arcs as defined above, is sensibly the same. The method is termed the Polygon Method. The number of arcs selected to replace the aerofoil is governed by the accuracy required in the final results. In Part 2 the problem is solved first for zero circulation, and then solutions for any desired circulation can be obtained almost immediately.* This feature gives the method a marked superiority over ' relaxation ' for which each angle of incidence is a separate problem.

In Part 3 we describe and extend a method of calculating incompressible two-dimensional flow similar in character to the Polygon Method developed in Parts 1 and 2. It was originated by Thom and termed by him the ' Influence Factor Method '. His work on symmetrical aerofoils is extended to asymmetric aerofoils, and his approximate equations for the bounded stream are replaced by the exact forms.

Part 4 contains two new approximate treatments of compressible flow. The first is similar to the linear pertubation theory but gives results a little more accurate than this theory. The second is similar to von Kármán's well-known approximation, and appears to be more accurate. In both methods the equations are reduced by approximations and transformations to Laplace's equation which is then solved by the methods of Parts 1 and 2.* Finally an exact relaxation treatment is outlined which has some advantages over relaxation methods already developed.

Examples illustrating the methods are given throughout the paper.

* A summary of the Polygon Method equations and details of their application to the calculation of the compressible subsonic flow about aerofoils is given in Ref. 21. This reference, written some time after the present paper, also contains tables which considerably reduce the labour involved in applying the method to given aerofoil shapes.

PART 1

Incompressible Flow about a Symmetrical Aerofoil in a Channel or Free Stream

1. *Introduction.*—' Relaxation '[3], and ' Squaring '[11] have been employed in various ways to find the incompressible flow about a two-dimensional aerofoil. The relaxation method outlined in section 2 is new in some features although the general principles have been employed by Thom[11] for many years. He initiated the method of using the network composed of velocity equipotentials and streamlines (the (ϕ,ψ)-plane) as the square grid on which to solve the usual difference equations for a Laplacian field. Working in this (ϕ,ψ)-plane has two outstanding advantages:—

(a) From the point of view of relaxation, it avoids the irregular ' stars ' in the (x, y) or physical plane, with their consequent interpolation formulae.

(b) It makes possible the method of calculating incompressible flow described in sections 3 and 4 below.

The basic principle of the method described in this paper is the replacement of the aerofoil by a polygon with an infinite number of sides, *i.e.*, a polygon for which the change in direction of adjacent sides is an infinitesimal angle $\delta\theta_0$. (The suffix 0 will be used to denote surface values.) The exception to this is at the trailing and leading edges at which, in general, re-entrant finite angles of τ_a and τ_b occur. There may be other sharp corners on the profile, and these can all be included in the term τ_i, $i = a,b,c, \ldots$. The fields in the (ϕ,ψ)-plane due to these angles $\delta\theta_0$ are combined by an integration along the aerofoil boundary and the result added to the sum of the fields due to τ_i. It proves convenient in practice to assume that the product Rq_0, where R is the radius of curvature of the boundary, and q_0 is the velocity magnitude on the boundary, is constant over small ranges. The integration is then performed for each range and the results added to give the total effect due to the whole aerofoil. The number of such ranges is governed by the accuracy required in the final results. In the typical example given in section 9 the author found that twelve were sufficient to give accuracies better than one per cent in the velocity increment due to the aerofoil.

Working in the (ϕ,ψ)-plane involves the difficulty that initially the exact boundary conditions are not known, *i.e.*, the exact relation $\theta_0 = \theta_0(\phi)$ is unknown, and remains so until the exact solution has been found. However starting from some assumption for $q_0(\phi)$, *e.g.*, that q_0 is the same as the free-stream value at infinity, U, we can calculate approximate boundary conditions. These can be used in the polygon method to find a more accurate relation $q_0 = q_0(\phi)$, and hence to find more accurate boundary conditions and so on. This iterative process converges rapidly as demonstrated by the examples in sections 8 and 9. Only two or three rounds of the process prove necessary. Once $q_0(\phi)$ is determined accurate values of $q = q(\theta,\psi)$ can be found immediately without further iteration. The relations $x = x(\phi,\psi)$, $y = y(\phi,\psi)$ can then be found and the solution is complete.

The relaxation method described in section 2 below has two disadvantages:—

(i) There is no convenient method of dealing with the outer boundary condition, $\log(U/q) = 0$ at infinity. Inversion is the only exact method, and this is clumsy numerically. The difficulty is much greater for the unbounded field than for the field confined between channel walls.

(ii) Relaxation is very slow for this type of problem, in which normal boundary gradients are specified rather than boundary values. Furthermore the only fixed value is at infinity and so the errors are likely to be the greatest on the aerofoil surface.

2. *The Differential Equation and Boundary Conditions.*—Let (q,θ) be the velocity vector in polar co-ordinates, $z = x + iy$, and $w = \phi + i\psi$, then $qe^{-i\theta} = \dfrac{dw}{dz}$. Therefore $\log\left(\dfrac{U}{q}\right) + i\theta = \log\left(U\dfrac{dz}{dw}\right) = f$, say. Thus, apart from possible singularities, f is an analytic

function and it therefore satisfies $\nabla^2 f = 0$ in both the z and w-planes. We shall write $L \equiv \log\left(\frac{U}{q}\right)$, and so $f = L + i\theta$. The Cauchy-Riemann equations hold, *e.g.*, in the w-plane

$$\frac{\partial L}{\partial \phi} = \frac{\partial \theta}{\partial \psi}, \qquad \frac{\partial L}{\partial \psi} = -\frac{\partial \theta}{\partial \phi}. \qquad (1)$$

On the aerofoil boundary θ_0 is specified or can be calculated from the aerofoil co-ordinates. The distance measured from an origin along a streamline or boundary will be denoted by s, then $\left(\frac{\partial \phi}{\partial s}\right)_0 = q_0$, and $\left(\frac{\partial s}{\partial \theta}\right)_0 = -R$. Thus from (1) the normal boundary gradient can be written

$$\left(\frac{\partial L}{\partial \psi}\right)_0 = -\left(\frac{\partial \theta}{\partial s}\right)_0 \left(\frac{\partial s}{\partial \phi}\right)_0 = \frac{1}{Rq_0} \qquad (2)$$

The other aerofoil boundary conditions are the locations of the stagnation points and sharp corners, if any. The rear stagnation point will be fixed at the trailing edge (Joukowski condition), while, for the general asymmetric aerofoil, the location of the front stagnation point will depend upon the incidence (or circulation) imposed. For a symmetrical aerofoil the non-linear boundary conditions (2) can be dealt with as follows.

Initially an approximate relation $q_0 = q_0(\phi)$ is assumed. The origin for ϕ and s is taken to be the trailing edge. Let the value of ϕ at the front stagnation point be $\bar{\phi}$. The distance $s(\phi)$ from the trailing edge to ϕ is found from

$$s(\phi) = \int_0^{\phi} d\phi / q_0, \qquad (3)$$

since $q_0 = \left(\frac{\partial \phi}{\partial s}\right)_0$. Let the known relationship between the semi-perimeter p and the chord c be $p = mc$, say, then $c = \frac{1}{m}\int_0^{\bar{\phi}} \frac{d\phi}{q_0}$, and using this in (3) we have $\frac{s}{c} = \frac{s}{c}(\phi)$. Using this relationship in $\frac{c}{R} = \frac{c}{R}\left(\frac{s}{c}\right)$, which can be calculated from the aerofoil co-ordinates, enables us to calculate $\frac{c}{R} = \frac{c}{R}(\phi)$. From the assumed values of $q_0(\phi)$ and the derived values of c and $\frac{c}{R}(\phi)$ we then find the approximate boundary conditions $\left(\frac{\partial L}{\partial \psi}\right)_0 = \left(\frac{c}{R}\right)\frac{1}{cq_0}$. The values of the boundary gradient found in this way are reasonably close to the true values; *e.g.*, an overestimate in the value of q_0 reduces the value of c subsequently determined, and so the product (cq_0) remains reasonably close to the true value. Furthermore along the greater part of the aerofoil chord R varies slowly. With these approximate boundary conditions, either the usual relaxation treatment or the method developed in this paper can be used to calculate new and more accurate values of $q_0(\phi)$, which are then used to determine more accurate boundary conditions by the method described above. Relaxation or the polygon method is again applied to find a new relationship $q_0(\phi)$, and so on. The process converges rapidly and even if the initial assumption $q_0 = U$, is made, only two or three integrations along the surface are necessary. In section 7 this is made the initial assumption for a circular-arc aerofoil. The first approximation is compared with the exact analytical solution and the agreement is very good.

Before dealing with the new method of this paper two further difficulties peculiar to the relaxation treatment will be mentioned.

(a) *The Outer Boundary Conditions.*—Some remarks have already been made about this in the introduction. For the bounded field the difficulty is not so great. On the channel walls R is specified, so $\partial L/\partial \phi$ can be found. Now $L = 0$ at infinity upstream and downstream, but it is sufficient to assume that $L = 0$ at distances of two or three chords upstream and downstream from the aerofoil centre, for it is known that the channel walls rapidly damp out the influence of the aerofoil[12].

For the unbounded field the boundary condition is $L = 0$ at infinity in every direction. Short of inverting the plane to limit its extent, we can only use approximate methods, such as replacing the aerofoil by a substitution vortex and calculating theoretically the values of L on an outer boundary, say two to three chords radius from the centroid of circulation. Inversion produces a curved boundary and is thus clumsy numerically. A substitution vortex has been used by the author for an asymmetric aerofoil and it proved to be sufficiently accurate provided the outer boundary was taken to be at a radius of at least two chords[18]. This resulted in a large field in which to 'relax' and therefore the calculations were very slow.

(b) *The Singularities in* $\log(U/q)$ *at the Stagnation Points.*—Methods of dealing with these infinities have been dealt with at length elsewhere[16], but the principle will be briefly indicated in the appendix.

3. *The Velocity Field Due to a Symmetrical Aerofoil.*—The aerofoil is at zero incidence midway between symmetrical channel walls. Fig. 2 shows the w-plane field repeated at intervals of h in the ϕ direction. In this extended field the aerofoil is a slit on $w = 0, \pm ih, \pm 2ih, \ldots$, and so $f(w) = f(w + irh)$, $r = \pm 1, \pm 2, \ldots$, where $f \equiv \log(U/q) + i\theta$. From symmetry $f(w) = \bar{f}(irh + \bar{w})$, the bar denoting conjugates; in particular

$$f(\phi_0 + i0) = \bar{f}(\phi_0 + irh - i0); \quad f(\phi_0 + \tfrac{1}{2}ih - i0) = \bar{f}(\phi_0 + ih(r - \tfrac{1}{2}) + i0) \qquad .. \qquad (4)$$

$+ i0$ and $- i0$ denoting the upper and lower edges respectively of $\phi = 0$. We shall assume that $f(w)$ has singularities at $w = \phi_s$, $s = 1, 2, \ldots$, due to discontinuities in θ, *i.e.*, sharp corners on the aerofoil surface. Elsewhere f is analytic, and so if the singularities are excluded by small semi-circular indentations, Cauchy's integral taken around the contour 0 in Fig. 2, gives

$$f(w) = \frac{1}{2\pi i}\Big[\Big\{\int_{-R}^{\phi_1 - \rho} + \sum_{r=1}^{n-1}\int_{\phi_r + \rho}^{\phi_{r+1} - \rho} + \int_{\phi_n + \rho}^{R}\Big\}\frac{f(\phi_0 + i0)}{(\phi_0 - w)}\,d\phi_0 - \int_{-R}^{R}\frac{f(\phi_0 + \frac{1}{2}ih - i0)}{\phi_0 + \frac{1}{2}ih - w}\,d\phi_0$$

$$+ \sum_s I_s + I_a + I_b\Big], \qquad .. \qquad .. \qquad .. \qquad (5)$$

where w is a point within the contour, I_s is the contribution to the integral from the indentation about the singularity at $w = \phi_s$, and I_a, I_b are the contributions from the ends of the rectangle.

Referring to Fig. 1, in which there is a corner of angle $-\tau$ at the origin, we see that the Schwarz-Christoffel transformation from the z to the w-plane is

$$\frac{dz}{dw} = \frac{1}{K}\,e^{i\lambda}w^{-\tau/\pi},$$

where K and λ are real constants. Thus

$$f \equiv \log\left(U\frac{dz}{dw}\right) = -\frac{\tau}{\pi}\log w + \text{constant}.$$

This result shows that in the neighbourhood of a discontinuity in θ on an aerofoil we can expand $f(w)$ thus:—

$$f(w) = -\frac{\tau}{\pi}\log(w - \phi_s) + a + b(w - \phi_s) + c(w - \phi_s)^2 + \ldots,$$

where $a, b, c \ldots$ are independent of $|w - \phi_s|$. Thus for small values of ρ, $|f(\phi_s + \rho e^{i\varepsilon})| = -|\log\rho + 0(1)|$. Since w is within the contour $|\phi_s + \rho e^{i\varepsilon} - w|$ has a lower bound, k say, and so $|I_s| \leqslant \frac{\tau}{\pi}\int_0^{\pi}\frac{|\log\rho + 0(1)|}{|\phi_s + \rho e^{i\varepsilon} - w|}\,d\varepsilon \leqslant \frac{\tau}{k}\rho\,|\log\rho + 0(1)| \to 0$ as $\rho \to 0$.

In the limit then as $\rho \to 0$, (5) becomes

$$f(w) = \frac{1}{2\pi i}\left\{\int_{-R}^{R} \frac{f(\phi_0 + i0)}{(\phi_0 - w)}\, d\phi_0 - \int_{-R}^{R} \frac{f(\phi_0 + \frac{1}{2}ih - i0)}{\phi_0 + \frac{1}{2}ih - w}\, d\phi_0 + i\int_0^{h/2} \frac{f(R + i\psi_0)}{R + i\psi_0 - w}\, d\psi_0 \right.$$
$$\left. - i\int_0^{h/2} \frac{f(-R + i\psi_0)}{-R + i\psi_0 - w}\, d\psi_0\right\} \quad .. \quad .. \quad .. \quad (6)$$

The conjugate point $\bar{w}$ lies outside contour ' 0 ', and so

$$0 = \frac{1}{2\pi i}\int_{-R}^{R} \frac{f(\phi_0 + i0)}{\phi_0 - \bar{w}}\, d\phi_0 - \int_{-R}^{R} \frac{f(\phi_0 + \frac{1}{2}ih - i0)}{\phi_0 + \frac{1}{2}ih - \bar{w}}\, d\phi_0 + i\int_0^{h/2} \frac{f(R + i\psi_0)}{R + i\psi_0 - \bar{w}}\, d\psi_0$$
$$\left. - i\int_0^{h/2} \frac{f(-R + i\psi_0)}{-R + i\psi_0 - \bar{w}}\, d\psi_0\right\} \quad .. \quad .. \quad .. \quad (7)$$

Adding the conjugate of this equation to (6) and using $2i\theta = f - \bar{f}$, we find

$$f(w) = \frac{1}{\pi}\int_{-R}^{R}\left\{\frac{\theta(\phi_0 + i0)}{\phi_0 - w} - \frac{\theta(\phi_0 + \frac{1}{2}ih - i0)}{\phi_0 + \frac{1}{2}ih - w} + \frac{\bar{f}(\phi_0 + \frac{1}{2}ih - i0)}{\phi_0 - \frac{1}{2}ih - w} - \frac{\bar{f}(\phi_0 + \frac{1}{2}ih - i0)}{\phi_0 + \frac{1}{2}ih - w}\right\} d\phi_0$$
$$+ \frac{1}{2\pi}\int_0^{h/2}\left\{\frac{f(R + i\psi_0)}{R - i\psi_0 - w} + \frac{\bar{f}(R + i\psi_0)}{R + i\psi_0 - w} + \frac{f(-R + i\psi_0)}{R - i\psi_0 + w} + \frac{\bar{f}(-R + i\psi_0)}{R + i\psi_0 + w}\right\} d\psi_0.$$

Applying the same method to the r^{th} contour, and making use of (4), we have

$$0 = \frac{1}{\pi}\int_{-R}^{R}\left\{\frac{\theta(\phi_0 + i0)}{\phi_0 + irh - w} - \frac{\theta(\phi_0 + \frac{1}{2}ih - i0)}{\phi_0 + i(r + \frac{1}{2})h - w} + \frac{\bar{f}(\phi_0 + \frac{1}{2}ih - i0)}{\phi_0 + i(r - \frac{1}{2})h - w} - \frac{\bar{f}(\phi_0 + \frac{1}{2}ih - i0)}{\phi_0 + i(r + \frac{1}{2})h - w}\right\} d\phi_0$$
$$+ \frac{1}{2\pi}\int_0^{h/2}\left\{\frac{f(R + i\psi_0)}{R + irh - i\psi_0 - w} + \frac{\bar{f}(R + i\psi_0)}{R + irh + i\psi_0 - w} + \frac{f(-R + i\psi_0)}{R + irh - i\psi_0 + w}\right.$$
$$\left. + \frac{\bar{f}(-R + i\psi_0)}{R + irh + i\psi_0 + w}\right\} d\psi_0.$$

Adding these equations for $r = \pm 1, \pm 2, \ldots \pm n$ to the equation for $f(w)$ we get

$$f(w) = \frac{1}{\pi}\int_{-R}^{R} \sum_{r=-n}^{n}\left\{\frac{\theta(\phi_0 + i0)}{\phi_0 + irh - w} - \frac{\theta(\phi_0 + \frac{1}{2}ih - i0)}{\phi_0 + i(r + \frac{1}{2})h - w}\right\} d\phi_0 + \frac{1}{\pi}\int_{-R}^{R} \frac{\bar{f}(\phi_0 + \frac{1}{2}ih - i0)}{\phi_0 - i(n + \frac{1}{2})h - w}\, d\phi_0$$
$$- \frac{1}{\pi}\int_{-R}^{R} \frac{\bar{f}(\phi_0 + \frac{1}{2}ih - i0)}{\phi_0 + i(n + \frac{1}{2})h - w}\, d\phi_0 + \frac{1}{2\pi}\int_0^{h/2} \sum_{r=-n}^{n}\left\{\frac{f(R + i\psi_0)}{R + irh - i\psi_0 - w} + \frac{\bar{f}(R + i\psi_0)}{R + irh + i\psi_0 - w}\right\} d\psi_0$$
$$+ \frac{1}{2\pi}\int_0^{h/2} \sum_{r=-n}^{n}\left\{\frac{f(-R + i\psi_0)}{R + irh - i\psi_0 + w} + \frac{\bar{f}(-R + i\psi_0)}{R + irh + i\psi_0 + w}\right\} d\psi_0.$$

In the limit as $n \to \infty$ this becomes

$$f(w) = \frac{1}{h}\int_{-R}^{R}\left\{\theta(\phi_0 + i0)\coth\frac{\pi}{h}(\phi_0 - w) - \theta(\phi_0 + \tfrac{1}{2}ih - i0)\tanh\frac{\pi}{h}(\phi_0 - w)\right\} d\phi_0$$
$$+ \frac{1}{2h}\int_0^{h/2}\left\{f(R + i\psi_0)\coth\frac{\pi}{h}(R - i\psi_0 - w) + \bar{f}(R + i\psi_0)\coth\frac{\pi}{h}(R + i\psi_0 - w)\right\} d\psi_0$$
$$+ \frac{1}{2h}\int_0^{h/2}\left\{f(-R + i\psi_0)\coth\frac{\pi}{h}(R - i\psi_0 + w) + \bar{f}(-R + i\psi_0)\coth\frac{\pi}{h}(R + i\psi_0 + w)\right\} d\psi_0.$$

If at $\phi = \infty$, $L = \log U/a$, and at $\phi = -\infty$, $L = \log U/b$, then in the limit as $R \to \infty$ we have finally

$$f(w) = \frac{1}{h}\int_{-\infty}^{\infty} \left\{\theta \coth \frac{\pi}{h}(\phi_0 - w) - \theta^* \tanh \frac{\pi}{h}(\phi_0 - w)\right\} d\phi_0 + \tfrac{1}{2}\log\left(\frac{U^2}{ab}\right),$$

where θ refers to the aerofoil and θ^* to the channel wall. Selecting $U = \sqrt{(ab)}$, we have for the flow in an asymmetric channel, width $h/2$ in the w-plane,*

$$f(w) = \frac{1}{h}\int_{-\infty}^{\infty} \left\{\theta \coth \frac{\pi}{h}(\phi_0 - w) - \theta^* \tanh \frac{\pi}{h}(\phi_0 - w)\right\} d\phi_0. \quad .. \quad .. \quad .. \quad (8)$$

The functions θ and θ^* must satisfy

$$-\log\left(\frac{U}{a}\right) = \frac{1}{h}\int_{-\infty}^{\infty} (\theta - \theta^*)\, d\phi_0 = \tfrac{1}{2}\log\left(\frac{a}{b}\right), \quad .. \quad .. \quad .. \quad .. \quad .. \quad (9)$$

obtained from (8) by putting $|w| = \infty$.

Putting $\theta^* = 0$, and then letting $h \to \infty$, we find for a symmetrical aerofoil at zero incidence in an unbounded stream

$$f(w) = \frac{1}{\pi}\int_{-\infty}^{\infty} \frac{\theta\, d\phi_0}{(\phi_0 - w)}. \quad .. \quad .. \quad .. \quad .. \quad .. \quad .. \quad .. \quad .. \quad (10)$$

We can reduce the range of integration to (A,H) for if the aerofoil lies in this interval, then outside (A,H), $\theta = 0$.

$$\int_{\phi_0=H}^{A} d\theta(\phi_0) = 0, \quad .. \quad .. \quad .. \quad .. \quad .. \quad .. \quad .. \quad .. \quad .. \quad (11)$$

another useful result, is simply one of the conditions that the profile is closed.

If instead of adding the conjugate of (7) to (6) we subtract it, we find corresponding to (8) the conjugate equation*

$$f(w) = -\frac{i}{h}\int_{-\infty}^{\infty} \left\{L \coth \frac{\pi}{h}(\phi_0 - w) - L^* \tanh \frac{\pi}{h}(\phi_0 - w)\right\} d\phi_0, \quad .. \quad .. \quad .. \quad (12)$$

where the axes in the z-plane are adjusted to make $\theta(\infty) = \theta(-\infty)$, *i.e.*, the flow directions at infinity make equal angles with the x-axis. The functions L and L^* must satisfy

$$\frac{1}{h}\int_{-\infty}^{\infty} (L - L^*)\, d\phi_0 = \theta(\infty) - \theta(-\infty) = 0.$$

In an unbounded stream

$$f(w) = -\frac{i}{h}\int_{-\infty}^{\infty} \frac{L\, d\phi_0}{\phi_0 - w}, \quad \int_{-\infty}^{\infty} L\, d\phi_0 = 0. \quad .. \quad .. \quad .. \quad .. \quad .. \quad .. \quad (13)$$

These conjugate equations play the same role in aerofoil design as do (8) and (10) in the calculation of the flow about a specified aerofoil.

The appropriate value to use for h in the above formulae is clearly

$$h = H_a a, \quad .. \quad .. \quad .. \quad .. \quad .. \quad .. \quad .. \quad .. \quad .. \quad .. \quad (14)$$

where H_a is the channel width in the z-plane at a point where the velocity is known to be uniform and equal to a. The prescribed conditions at infinity fix these quantities.

---

* Equations (8) and (12) are applied to a number of fluid motion problems in Ref. 22.

4. *Numerical Solution of the Equations.*—(a) *Unbounded Field.*—Integrating (10) by parts

$$f(w) = -\frac{1}{\pi}\int_{\phi_0=H}^{A} \log(\phi_0 - w)\, d\theta(\phi_0), \qquad (15)$$

since $\theta = 0$ at $\phi_0 = \pm\infty$. Now $\theta(\phi_0)$ is continuous except at a number of points $\phi_0 = \phi_s$, where there is jump in θ of τ_s say. From (1) and (2)

$$d\theta(\phi_0) = -\left(\frac{\partial L}{\partial \psi}\right)_0 d\phi_0 = -\frac{1}{Rq_0}\, d\phi_0. \qquad (16)$$

Subdividing the range (A,H) into $(\phi_1, \phi_2, \ldots, \phi_r, \ldots \phi_n)$ and using (16), we can transform the Steiltjes integral in (15) into

$$f(w) = \frac{1}{\pi}\int_H^A \left(\frac{1}{Rq}\right)_0 \log(\phi_0 - w)\, d\phi_0 - \frac{1}{\pi}\sum_s \tau_s \log(\phi_s - w) \qquad (17)$$

$$= \frac{1}{\pi}\sum_{i=1}^{n-1}\int_{\phi_i}^{\phi_{i+1}} \left(\frac{1}{Rq}\right) \log(\phi_0 - w)\, d\phi_0 - \frac{1}{\pi}\sum_s \tau_s \log(\phi_s - w) \qquad (18)$$

If the subdivision is carefully made with n large enough, we can write approximately

$$f(w) = \frac{1}{\pi}\sum_{i=1}^{n-1}\left(\frac{\delta\phi}{Rq}\right)_i [\log(\phi_0 - w)]_{mi} - \frac{1}{\pi}\sum_s \tau_s \log(\phi_s - w), \qquad (18)$$

where $\left(\frac{\delta\phi}{Rq}\right)_i$ is the mean value of $\frac{\delta\phi}{Rq}$ in the i^{th} range, $[\log(\phi_0 - w)]_{mi}$ is the mean value of the logarithm in the i^{th} range, and $\delta\phi_i = \phi_{i+1} - \phi_i$. On $\psi = 0$, (18) becomes

$$\log\left(\frac{U}{q}\right) = \frac{1}{\pi}\sum_{i=1}^{n-1}\left(\frac{\delta\phi}{Rq}\right)_i [\log(\phi_0 - \phi)]_{mi} - \frac{1}{\pi}\sum_s \tau_s \log(\phi_s - \phi), \qquad (19)$$

an equation which must be solved by an iterative process as q appears on both sides of the equation. This iteration has been described in section 1 and is summarized in section 7. When (19) has been solved (18) can be used without further iteration to determine $L(\phi,\psi)$ and $\theta(\phi,\psi)$ throughout the field. For example the real part of (18) is

$$L(\phi,\psi) = \frac{1}{\pi}\sum_{i=1}^{n-1}\left(\frac{\delta\phi}{Rq}\right)_i [\log\{(\phi_0 - \phi)^2 + \psi^2\}^{1/2}]_{mi} - \frac{1}{\pi}\sum_s \tau_s \log\{(\phi_s - \phi)^2 + \psi^2\})^{1/2}.$$

The mid-range values of the logarithm may be taken instead of the mean value except near the singularity $(\phi_0,0)$.

(b) *Bounded Field.*—Assuming for simplicity that $\theta^* = 0$ in (8) we find

$$f(w) = -\frac{1}{\pi}\int_{0=H}^{A} \log\sinh\frac{\pi}{h}(\phi_0 - w)\, d\phi(\phi_0), \qquad (20)$$

then as before

$$f(w) = \frac{1}{\pi}\sum_{i=1}^{n-1}\left(\frac{\delta\phi}{Rq}\right)_i [\log\sinh\frac{\pi}{h}(\phi_0 - w)]_{mi} - \frac{1}{\pi}\sum_s \tau_s \log\sinh\frac{\pi}{h}(\phi_s - w), \qquad (21)$$

and in particular

$$\log\left(\frac{U}{q}\right)=\frac{1}{\pi}\sum_{i=1}^{n-1}\left(\frac{\delta\phi}{Rq}\right)_i[\log\sinh\frac{\pi}{h}(\phi_0-\phi)]_{mi}-\frac{1}{\pi}\sum_s\tau_s\log\sinh\frac{\pi}{h}(\phi_s-\phi). \quad .. \quad (22)$$

An alternative approach to the bounded field is given in section 6, which avoids the need to compute $[\log\sinh\frac{\pi}{h}(\phi_0-\phi)]_{mi}$.

5. *Doublets.*—Near a nose with a small radius of curvature it is useful to have formulae for the effect of a corner τ at a distance $\delta\phi_0$ from an equal and opposite corner $-\tau$. The influence of a doublet between parallel channel walls is from equation (20)

$$f(w) = -\frac{\tau}{\pi}[\log\sinh\frac{\pi}{h}(\phi_0+\delta\phi_0-w)-\log\sinh\frac{\pi}{h}(\phi_0-w)]$$

$$\simeq -\frac{(\tau\delta\phi_0)}{\pi}\frac{\partial}{\partial\phi_0}\{\log\sinh\frac{\pi}{h}(\phi_0-w)\},$$

i.e.,
$$f(w) = -\frac{(\tau\,\delta\phi_0)}{h}\coth\frac{\pi}{h}(\phi_0-w). \quad .. \quad .. \quad .. \quad .. \quad .. \quad .. \quad .. \quad (23)$$

For the unbounded field this becomes

$$f(w) = \frac{(\tau\,\delta\phi_0)}{\pi(w-\phi_0)}. \quad .. \quad .. \quad .. \quad .. \quad .. \quad .. \quad .. \quad .. \quad .. \quad (24)$$

The effect of the channel walls on the doublet is

$$\Delta f = \frac{(\tau\,\delta\phi_0)}{h}\left\{\coth\frac{\pi}{h}(w-\phi_0)-\frac{1}{\frac{\pi}{h}(w-\phi_0)}\right\}$$

$$\simeq \frac{(\tau\,\delta\phi_0)}{3h}(w-\phi_0)\left\{1-\frac{1}{15}\left(\frac{\pi}{h}\right)^2(w-\phi_0)^2\right\}. \quad .. \quad .. \quad .. \quad .. \quad .. \quad (25)$$

6. *Increment due to Straight Parallel Walls.*—From (8) and (15) this increment is

$$\Delta f(w) = -\frac{1}{\pi}\int_{\phi_0=H}^{A}\log\sinh\frac{\pi}{h}(\phi_0-w)\,d\underline{\theta}(\phi_0)+\frac{1}{\pi}\int_{\phi_0=H}^{A}\log(\phi_0-w)\,d\theta(\phi_0)$$

$$-\frac{1}{\pi}\int_{\phi_0=D}^{C}\log\cosh\frac{\pi}{h}(\phi_0-w)\,d\theta^*(\phi_0),$$

assuming the walls are straight and parallel outside the range (C,D). Now the functions $d\underline{\theta}(\phi_0)$ and $d\theta(\phi_0)$ occurring in this equation are not quite the same, but since the blockage effect is fairly uniformly distributed over the aerofoil, only a very small error is committed in assuming $d\underline{\theta}(\phi_0)=d\theta(\phi_0)$. Doing this and making use of (11) we find

$$\Delta f = -\frac{1}{\pi}\int_{\phi_0=H}^{A}\log\frac{\sinh(\pi/h)(\phi_0-w)}{(\pi/h)(\phi_0-w)}\,d\theta(\phi_0)-\frac{1}{\pi}\int_{\phi_0=D}^{C}\log\cosh\frac{\pi}{h}(\phi_0-w)\,d\theta^*(\phi_0)$$

$$\simeq -\frac{\pi}{6h^2}\int_{\phi_0=H}^{A}(\phi_0-w)^2\left\{1-\frac{1}{30}\left(\frac{\pi}{h}\right)^2(\phi_0-w)^2\right\}d\theta(\phi_0)$$

$$-\frac{\pi}{2h^2}\int_{\phi_0=D}^{C}(\phi_0-w)^2\left\{1-\frac{1}{6}\left(\frac{\pi}{h}\right)^2(\phi_0-w)^2\right\}d\theta^*(\phi_0) \quad .. \quad .. \quad .. \quad (26)$$

Now $h = HU$ (*see* (14)), and so if $\theta^* = 0$, then with the aid of (16), (26) becomes

$$\Delta L = \log\left(\frac{U}{q_b}\right) - \log\left(\frac{U}{q_u}\right) = \frac{\pi}{6(HU)^2}\left\{\int_H^A\left(\frac{1}{Rq}\right)_0(\phi_0-\phi)^2\left[1-\frac{\pi^2}{3(HU)^2}\right]d\phi_0\right.$$

$$\left.-\sum_s \tau_s(\phi_s-\phi)^2\left[1-\frac{\pi^2}{3(HU)^2}(\phi_s-\phi)^2\right]\right.,$$

where q_b and q_u are the velocities in the bounded and unbounded streams respectively.

Now $\Delta L = -\log(q_b/q_u) = -\log(q_u+q_b-q_u)/q_u = -\log\left(1+\frac{\Delta q}{q_u}\right) \simeq -\frac{\Delta q}{q_u}$, and so with the approximation $\phi_0 \simeq Us_0 \simeq Ux_0$, *i.e.*, $q_0 = 1$, we have

$$\frac{\Delta q}{q_u} = \frac{\pi}{6H^2}\left\{\sum_s \tau_s(x_s-x)^2\left[1-\frac{1}{3}\left(\frac{\pi}{H}\right)^2(x_s-x)^2\right]-\int_H^A\frac{(x_0-x)^2}{R}\left[1-\frac{1}{3}\left(\frac{\pi}{H}\right)^2\right.\right.$$

$$\left.\left.\times(x_0-x)^2\,dx_0\right]\right\} \quad .. \quad .. \quad .. \quad .. \quad .. \quad .. \quad .. \quad .. \quad (27)$$

from which the effect of blockage on the aerofoil surface can be found immediately. If doublets are employed in the calculation an additional term, readily calculable from (25), will appear in (27).

7. *Summary of Iterative Method of Solution.*—Take the origin of s and ϕ to be at the trailing edge say, and let $\phi = \bar{\phi}$ at the leading edge.

(a) From the aerofoil co-ordinates find (i) $\frac{c}{R} = \frac{c}{R}\left(\frac{s}{c}\right)$,

(ii) semi-perimeter $p = mc$.

(b) Assume a relation $q_0 = q_0(\phi)$ ($q_0 = 1$ for example), and calculate

$$s(\phi) = \int_0^{\phi}\frac{d\phi}{q_0},\ c = \frac{1}{m}\int_0^{\bar{\phi}}\frac{d\phi}{q_0},\ \text{and}\ \frac{s}{c} = \frac{s}{c}(\phi).$$

From this the relationship $\frac{c}{R} = \frac{c}{R}(\phi)$ can then be deduced.

(c) Using the assumed $q_0(\phi)$ and the deduced values of c and $\frac{c}{R}(\phi)$ calculate approximately $\left(\frac{c}{R}\right)\frac{1}{cq_0}$ as a function of ϕ_0. Substituting this value in the right-hand side of equation (19) yields $L_0^1(\phi)$ say, from which $q_0^1(\phi)$ can be found.

(d) Repeat steps (b) and (c), using $q_0^1(\phi)$ to find $q_0^2(\phi)$, which will be more accurate.

(e) Repeat step (d) until $q_0(\phi)$ remains unchanged in successive steps.

(f) Values of L and θ in the outer field can now be found directly from (18) using the accurate values of $\left(\frac{c}{R}\right)\frac{1}{cq_0}$ from the last calculation of step (e).

(g) The (ϕ,ψ) and (x,y)-planes are now related by

$$x = x(\phi,\psi) = \int_{\phi_0}^{\phi} \frac{\cos\theta}{q}\, d\phi - \int_0^{\psi} \frac{\sin\theta}{q}\, d\psi,$$

$$y = y(\phi,\psi) = \int_{\phi_0}^{\phi} \frac{\sin\theta}{q}\, d\phi + \int_0^{\psi} \frac{\cos\theta}{q}\, d\psi,$$

and hence from step (f) we finally have the solution $L = L(\phi,\psi)$, $\theta = \theta(\phi,\psi)$.

Section 15 gives an alternative method of calculating θ in step (f).

A similar process applies to the bounded field. One important point arises in step 3. The trailing and leading-edge angles, $2\tau_h$, and $2\tau_a$ say, should not be given their actual values in (19), otherwise the equation corresponding to (11), *i.e.*,

$$\sum_{i=1}^{n-1}\left(\frac{\delta\phi}{Rq}\right)_i - \sum_s \tau_s = 0, \qquad (28)$$

will not be satisfied. It is clearly satisfied by the true values of τ_a and τ_h only if $n = \infty$. The best method of determining appropriate values of τ_a and τ_h is to find the position of that tangent to the aerofoil which is parallel to the x-axis, and then τ_a is taken to be equal to the sum of the $(\delta\phi/Rq)_i$ between this point and the leading edge, while τ_h is the sum of the remainder of the $(\delta\phi/Rq)_i$.

8. *Example: A Circular-Arc Aerofoil.*—(a) *Exact Theory.*—The approximation derived from the initial assumption that $q_0 = 1$, will be compared with the exact theory for the von Kármán-Trefftz profile shown in Fig. 3. The following notation will be used:—

t the maximum thickness

2τ the trailing and leading-edge angle

a the radius of the circle in the ζ-plane into which the profile is transformed

$k = \frac{2}{\pi}(\pi - \tau)$.

The following expansions correct to $(t/c)^2$ will be used:—

$$\tau = \frac{2t}{c},\ R = \frac{c^2}{4t},\ k = 2\left\{1 - \frac{2}{\pi}\left(\frac{t}{c}\right)\right\}. \qquad (29)$$

The transformation from the z-plane to the ζ-plane is

$$\frac{z}{ka} = \frac{(1 + a/\zeta)^k + (1 - a/\zeta)^k}{(1 + a/\zeta)^k - (1 - a/\zeta)^k},\ \text{therefore}\ \frac{dz}{d\zeta} = \frac{z^2 - (ka)^2}{\zeta^2 - a^2}.$$

Also $w = \zeta + a^2/\zeta$, (stream function for cylinder radius a),

$$\text{therefore } \frac{dw}{dz} = 1 - \frac{a^2}{\zeta^2}.$$

If $\zeta = ae^{i\varepsilon}$, then $\left|\frac{dw}{d\zeta}\right| = |1 - e^{-2i\varepsilon}| = 2\sin\varepsilon$,

$$\text{and } \left|\frac{d\zeta}{dz}\right| = \frac{|z^2 - (ka)^2|}{2a^2\sin\varepsilon}.$$

Thus the surface velocity $q_0 = \left|\frac{dw}{dz}\right| = \left|\frac{dw}{d\zeta}\right|\left|\frac{d\zeta}{dz}\right| = \frac{4\sin^2\varepsilon}{k^2\,|(z/ka)^2 - 1|}$.

Now $\frac{z}{ka} = \frac{(1 + e^{-i\varepsilon})^k + (1 - e^{-i\varepsilon})^k}{(1 + e^{-i\varepsilon})^k - (1 - e^{-i\varepsilon})^k} = i\cot\left\{\frac{\pi}{4}k + \tfrac{1}{2}i\log(\tan^k\tfrac{1}{2}\varepsilon)\right\}$,

therefore $1\Big/\left|\left(\frac{z}{ka}\right)^2 - 1\right| = \left|\sin^2\left\{\frac{\pi}{4}k + i\log[\tan^{k/2}(\varepsilon/2)]\right\}\right|$

$$= \left[\left(\frac{\tan^k\tfrac{1}{2}\varepsilon - 1}{2\tan^{k/2}(\tfrac{1}{2}\varepsilon)}\right)^2 + \sin^2\left(\frac{\pi k}{4}\right)\right].$$

With $\zeta = ae^{i\varepsilon}$, $w = \phi = 2a\cos\varepsilon$, which is used to eliminate ε from the above equations giving finally

$$q_0 = \frac{1 - (2\phi/c)^2}{k^2}\left[\left(\frac{1 - 2\phi/c}{1 + 2\phi/c}\right)^{k/2} + \left(\frac{1 - 2\phi/c}{1 + 2\phi/c}\right)^{-k/2} - 2 + 4\sin^2\left(\frac{\pi k}{4}\right)\right]. \quad \ldots \quad (30)$$

At the point of maximum thickness on the profile $\varepsilon = \frac{1}{2}\pi$,

$$\text{therefore } q = \frac{4\sin^2(\pi k/4)}{k^2},$$

and using (29) we have approximately

$$q = 1 + \frac{4}{\pi}\left(\frac{t}{c}\right) + \frac{24 - \pi^2}{2\pi^2}\left(\frac{t}{c}\right)^2. \quad \ldots \quad (31)$$

(b) *Polygon Method.*—The first approximation is $q_0 = 1$. Therefore from (29) $\frac{1}{Rq_0} = \frac{4t}{c^2}$. Thus from (17), with origin at the midpoint of the chord,

$$L_0(\phi) = \frac{1}{\pi}\left\{\int_{c/2}^{c/2}\left(\frac{4t}{c^2}\right)\log(\phi - \phi_0)\,d\phi_0 - \frac{2t}{c}\log(\tfrac{1}{2}c + \phi) - \frac{2t}{c}\log(\tfrac{1}{2}c - \phi)\right\},$$

$$= \frac{4t}{\pi c}\left[\log\left(\frac{1 + 2\phi/c}{1 - 2\phi/c}\right)\right]\left(\frac{\phi}{c}\right) - \frac{4t}{\pi c},$$

$$\text{therefore} \quad q_0 = \exp\left(\frac{4t}{\pi c}\right)\exp\left\{\frac{4t\phi}{\pi c^2}\log\left(\frac{1 - 2\phi/c}{1 + 2\phi/c}\right)\right\} \quad \ldots \quad (32)$$

$$\simeq 1 + \frac{4}{\pi}\left(\frac{t}{c}\right)\left\{1 + \left(\frac{\phi}{c}\right)\log\left(\frac{1 - 2\phi/c}{1 + 2\phi/c}\right)\right\}, \quad \ldots \quad (33)$$

correct to the first power of t/c. At $\phi = 0$, (32) becomes

$$q_0 = 1 + \frac{4}{\pi}\left(\frac{t}{c}\right) + \frac{8}{\pi^2}\left(\frac{t}{c}\right)^2 + \ldots \text{ cf. (31)}. \quad \ldots \quad \ldots \quad \ldots \quad \ldots \quad \ldots \quad \ldots \quad (34)$$

Equations (30) and (32) are compared in Fig. 3. The greatest error in the second approximation (32) is only 7 per cent of the velocity increment. The third approximation cannot be found algebraically, but using arithmetical methods we find that it is indistinguishable on Fig. 3 from the exact theoretical result. This illustrates the rapidity of convergence of the method.

9. *Example: An Aerofoil Inverted from a Hyperbola.*—This aerofoil is one of the series developed by Piercy, Piper and Preston[10], and having a theoretical solution is thus a suitable example to illustrate the polygon method. The results obtained here are

(a) velocity distribution on the aerofoil surface, and

(b) a few values of the velocity at representative points in the field, for both the open and bounded fields.

The velocity distribution for the open field is compared with the exact theoretical curve, while the other results are compared with the values given by Thom and Klanfer[14] obtained by more laborious ' squaring ' methods.

The aerofoil co-ordinates and the derived values of $1/(R \log 10)$ and s are given in Table 1. (log 10 was introduced as it was convenient to use logarithms to base 10.) The curve $\frac{c}{2{\cdot}3R}\, v\, \frac{x}{c}$ is shown in Fig. 4. The initial assumptions are:—

(i) $\phi = 0$ at the leading edge, and $\phi = 10$ at the trailing edge.

(ii) $q_0 = 1$, i.e., $c = 10$.

The aerofoil is represented by arcs of constant Rq_0 centred at $\phi = \frac{1}{2}, 1, 1\frac{1}{2}, 2\frac{1}{8}, 3, 4, 5, 6, 7, 8, 9, 9\frac{3}{4}$. The range $\phi = 0 - \frac{1}{4}$ is not included as it was more convenient to introduce a doublet at $\phi = 0$ to represent this small range.

Open Field.—Fig. 5 shows the first approximation to $q_0 = q_0(x/c)$ based on the assumption $q_0 = 1$. The second and third approximations together with the correct theoretical curve are also shown. Table 2 sets out the integration of $d\phi/q_0$, based on the second approximation, to determine new values of $1/(Rq_0)$ to be used in the third, and in this case, final approximation. The columns of this table that are not obvious will now be described.

Column 3: obtained from the second approximation.

Column 4: $s = \delta\phi/q_0$, calculated from columns 2 and 3. One difficulty here is the integration from $\phi = 0$ to $\frac{1}{2}$, (and $\phi = 10$ to 9) since at the lower limit the integrand becomes infinite. This difficulty is dealt with in the Appendix. The trailing-edge angle for this aerofoil is 21 deg, and so from (165)

$$s = \frac{(\bar{\phi}/\bar{q})}{1 - 0{\cdot}058} = \frac{1{\cdot}002 \times 1}{0{\cdot}942} = 1{\cdot}066, \text{ (cf. col. 4)}$$

Column 7: x/c determined from column 6 and Table 1.

Column 8: From column 7 and Fig. 4 $c/2{\cdot}3R$ can be found for each point, then from columns 2 and 3, with $c = 8{\cdot}861$, $\delta\phi/(2{\cdot}3Rq_0)$ can be deduced.

Table 3 sets out in matrix form (to save space) the solution of

$$L_0(\phi) = \frac{1}{\pi}\left\{\sum_{i=1}^{n-1}\left(\frac{\delta\phi}{Rq}\right)_i [\log(\phi - \phi_0)]_{mi} - \sum_{s=a,h}\tau_s \log(\phi - \phi_s) - \frac{(\tau\,\delta\phi)}{\phi}\right\},$$

which follows from (18) and (24), a doublet being introduced at the nose. This equation can be written in the matrix form

$$\{L_0(\phi_k)\} = \frac{1}{\pi}\Big([A_{ki}]\,\{B_i\} + \{C_k\}\Big),$$

where $B_i = \left(\frac{\delta\phi}{Rq}\right)_i$, $i = 1,2, \ldots n\text{–}1$,

$= -\tau_i$, $i = a,h$, (Note: From (28) $\sum_i B_i$ must be zero)

$C_k = -(\tau\,\delta\phi)/\phi_k$, $k = 1, \ldots n-1$,

$A_{ki} = \log(\phi_k - \phi_i)$, $k = 1, \ldots n-1$, $i = a,h$,

$= [\log(\phi_k - \phi_0)]_{mi}$, $k,i = 1, \ldots n-1$.

In Table 3 logarithms to base 10 are used, and the matrices in the table are related to those defined above by

$$A' = \frac{10^3 A}{2\cdot 3},\quad B' = \frac{10^4 B}{2\cdot 3},\quad C' = \frac{10^4 C}{2\cdot 3},\quad L_0' = \frac{10^4 L_0}{2\cdot 3},$$

and so $\{L_0'(\phi_k)\} = \frac{2\cdot 3}{10^3}[A']\,\{B'\} + \{'C\}$.

Now from (16) $\frac{10^4}{2\cdot 3}(\tau\,\delta\phi) = \left(\frac{10^4}{2\cdot 3}\frac{\delta\phi}{Rq_0}\right)\delta\phi$, and extrapolation of the values of $\left\{\frac{10^4}{2\cdot 3}\frac{\delta\phi}{Rq_0}\right\}_i$ in B′ to $\phi = \frac{1}{8}$ yields a value of 1020, also $\delta\phi = -\frac{1}{4}$, and therefore $C_k' = -\frac{80}{\phi_k}$.

Bounded Field.—H in (26) was taken equal to 20 units. The first approximation based on the unbounded field results and calculated from equation (26), is compared in Fig. 5 with the results obtained by ' relaxation '. Table 5 sets out the results for the bounded and unbounded fields on the aerofoil surface, while Table 4 gives outer field results at four representative points.

TABLE 1

The Piercy, Preston and Piper Aerofoil

x	y	$\frac{s}{c} \times 10^4$	$\frac{c}{2 \cdot 3R}$	$\frac{x}{c} \times 10^3$
50438	0	0		0
49866	982	225	10·12	11
49291	1375	365	2·75	23
48142	1901	613	2·05	45*
46990	2275	853	1·19	68
45834	2565	1089	0·863	90*
44674	2799	1323	0·738	115
43511	2990	1557	0·493	138*
42344	3147	1790	0·457	161
41174	3275	2023	0·382	184*
40000	3379	2257	0·348	207
38822	3461	2491	0·305	231
37639	3524	2725	0·265	253
36453	3570	2960	0·265	278*
35263	3599	3196	0·241	300
34068	3613	3433	0·213	325
31663	3600	3910	0·191	372*
29239	3536	4391	0·165	420
26793	3426	4877	0·155	469*
24323	3272	5368	0·142	518
21828	3077	5867	0·132	567*
19303	2841	6370	0·116	618
18028	2709	6624	0·119	643
16745	2567	6880	0·112	668*
15452	2415	7138	0·101	694
14149	2254	7400	0·103	720
12835	2082	7665	0·100	746
11509	1901	7930	0·110	772*
10169	1709	8198	0·089	799
8813	1507	8469	0·097	825
7439	1294	8745	0·107	853
6043	1068	9025	0·077	880*
4621	830	9311	0·085	908
3164	578	9604	0·092	937
1654	307	9907	0·082	967
0	0	10240	—	1000

Trailing-edge angle = 21 deg

TABLE 2

Integration to Determine Boundary Gradients

ϕ	ϕ	$1/q_0$	δs	s	s/c	x/c	$\frac{1}{2\cdot3}\left(\frac{\delta\phi}{Rq}\right)_0$
(1)	(2)	(3)	(4)	(5)	(6)	(7)	(8)
0				0	0	0	—
	½		0·554				
½		0·894		0·554	0·062	0·046	0·0932
	½		0·432				
1		0·839		0·986	0·111	0·092	0·0405
	½		0·420				
1½		0·840		1·406	0·158	0·140	0·0245
	½		0·419				
2		0·837		1·825	0·205	0·186	0·0267
	1		0·838				
3		0·840		2·663	0·299	0·279	0·0240
	1		0·846				
4		0·852		3·509	0·393	0·374	0·0176
	1		0·858				
5		0·868		4·367	0·491	0·471	0·0150
	1		0·878				
6		0·888		5·245	0·589	0·570	0·0130
	1		0·898				
7		0·907		6·143	0·689	0·669	0·0113
	1		0·935				
8		0·962		7·078	0·794	0·773	0·0106
	1		0·982				
9		1·002		8·060	0·904	0·881	0·0099
	1		1·066				
10				9·126=p	1·024=m	1·000	—

$$c = p/m = 9\cdot126/1\cdot024 = 8\cdot861$$

Note: The results in column 7 should be compared with the results in Table 1 marked with a star, which are for the same values of ϕ, and it will be seen that the maximum error in the location of the equipotentials is 0·3 per cent of the chord.

TABLE 3

Third Approximation, Unbounded Field

A'

														ϕ_i
−301	−1036	−321	−5	207	+395	+544	+653	+740	+813	+875	+929	+966	+978	$\frac{1}{2}$
0	−321	−1036	−321	−43	296	475	602	699	778	845	903	942	954	$1\frac{1}{2}$
+176	−5	−321	−1036	−234	+168	395	544	653	740	813	875	917	929	1
301	+174	−5	−321	−894	−20	+296	475	602	699	778	845	889	903	2
477	398	+300	+174	−59	−735	−20	+296	475	602	699	778	829	845	3
602	544	477	398	+273	−20	−735	−20	+296	475	602	699	756	778	4
699	653	602	544	459	+296	−20	−735	−20	+296	475	602	677	699	5
778	740	699	653	588	475	+296	−20	−735	−20	+296	475	574	602	6
845	813	778	740	688	602	475	296	−20	−735	−20	+296	439	477	7
903	875	845	813	796	699	602	475	+296	−20	−735	−20	+243	+301	8
+954	+929	+903	+875	+837	+778	+699	+602	+475	+296	−20	−735	−175	0	9
$\phi_j = 0$	$\frac{1}{2}$	1	$1\frac{1}{2}$	$2\frac{1}{8}$	3	4	5	6	7	8	9	$9\frac{3}{4}$	10	

$$\times \begin{bmatrix} -2112 \\ +932 \\ 405 \\ 245 \\ 267 \\ 240 \\ 176 \\ 150 \\ 130 \\ 113 \\ 106 \\ 99 \\ +46 \\ -797 \end{bmatrix} \frac{2\cdot3}{10^3\pi} + \begin{bmatrix} -164 \\ -82 \\ -55 \\ -41 \\ -27 \\ -20 \\ -16 \\ -14 \\ -12 \\ -10 \\ -9 \end{bmatrix} = \begin{bmatrix} -511 \\ -760 \\ -778 \\ -788 \\ -747 \\ -680 \\ -600 \\ -502 \\ -374 \\ -212 \\ +39 \end{bmatrix}$$

B' C' L'

TABLE 4

Velocities in the Outer Field

Position Origin L.E. (ϕ,ψ)	Open Field		Bounded Field	
	'Squaring' Results	Polygon Method	'Squaring' Results	Polygon Method
(−5, 0)	0·9804	0·9813	0·9883	0·9899
(1, 4)	1·0253	1·025	1·0373	1·038
(6, 10)	1·0119	1·012	1·0305	1·030
(11, 2)	0·9757	0·9759	0·9906	0·9910

TABLE 5

Velocity Increments on the Aerofoil Surface

ϕ	$\frac{1}{2}$	1	$1\frac{1}{2}$	2	3	4	5	6	7	8	9
Open Field — Polygon	0·125	0·191	0·196	0·199	0·188	0·169	0·148	0·123	0·090	0·051	−0·009
Open Field — Exact	—	0·191	—	0·200	0·188	0·171	0·148	0·122	0·090	0·050	−0·009
Bounded Fielded — Polygon	0·137	0·204	0·210	0·213	0·201	0·184	0·162	0·137	0·103	0·061	0·002
Bounded Fielded — 'Squaring'	—	0·204	—	0·213	0·202	0·184	0·162	0·135	0·102	0·061	0·001

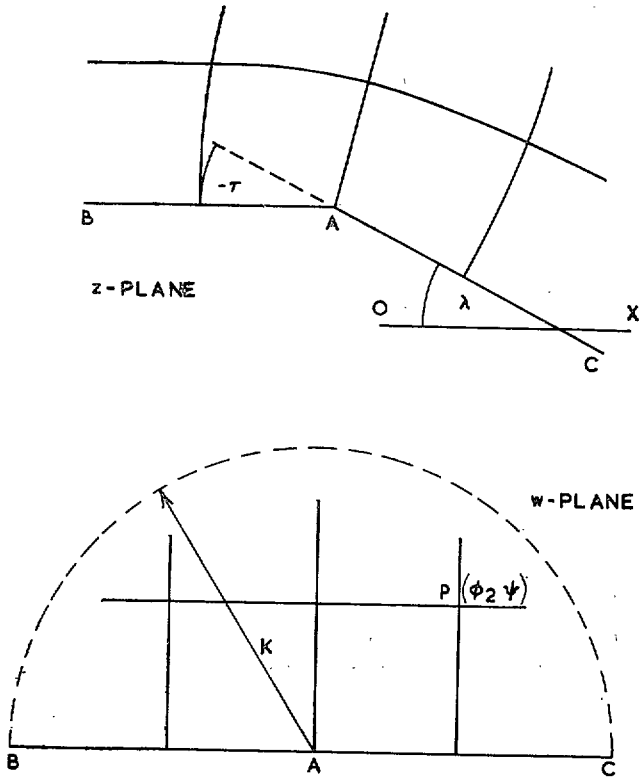

FIG. 1.

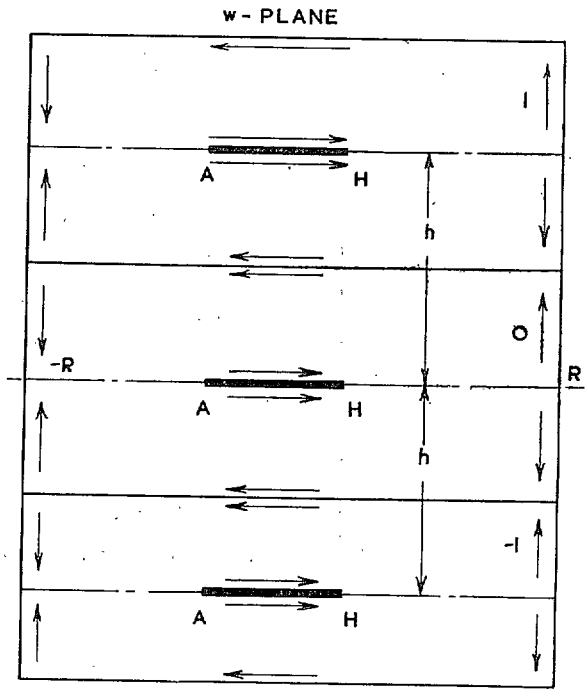

FIG. 2.

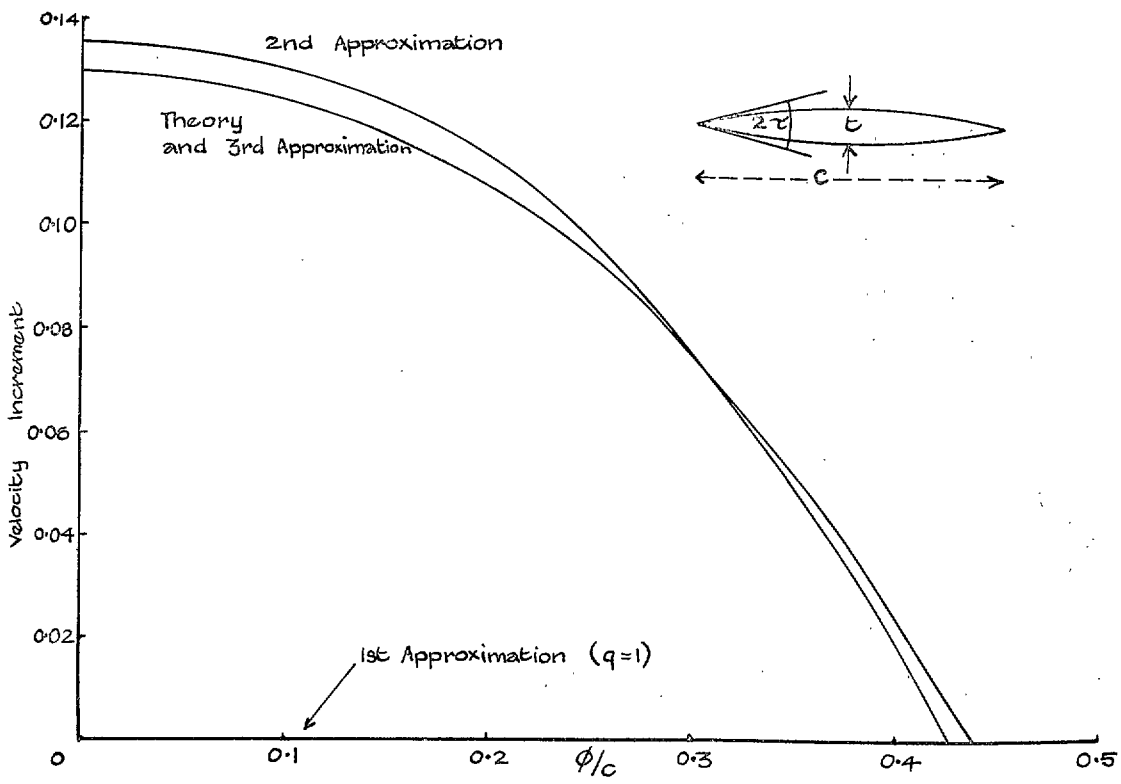

FIG. 3. 10 per cent circular-arc symmetrical aerofoil.

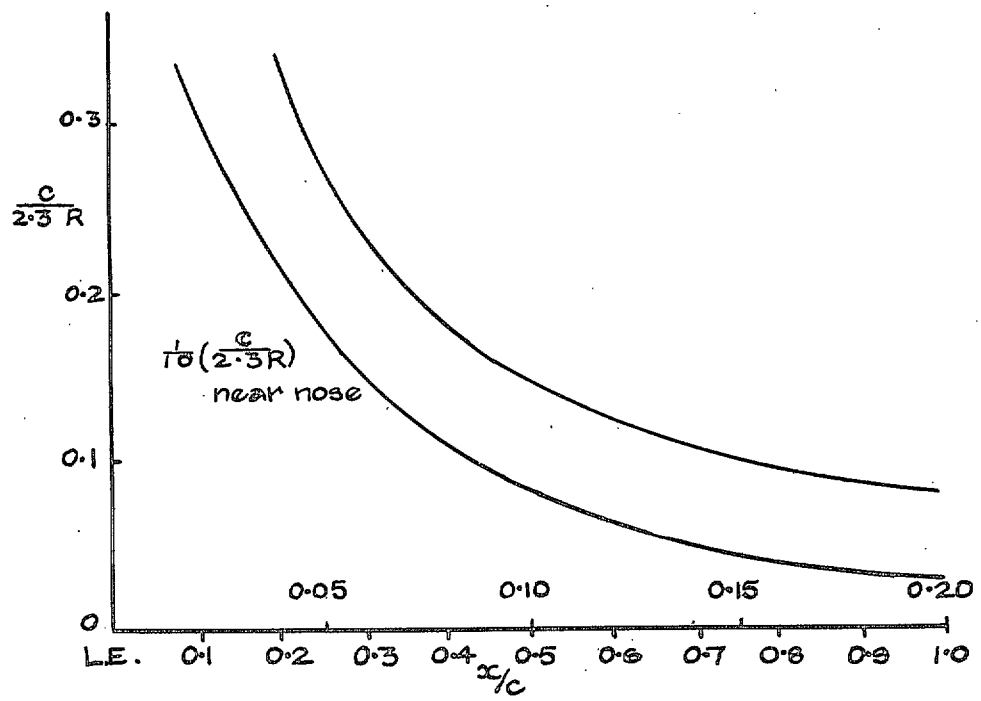

FIG. 4. Piercy-Preston-Piper aerofoil.

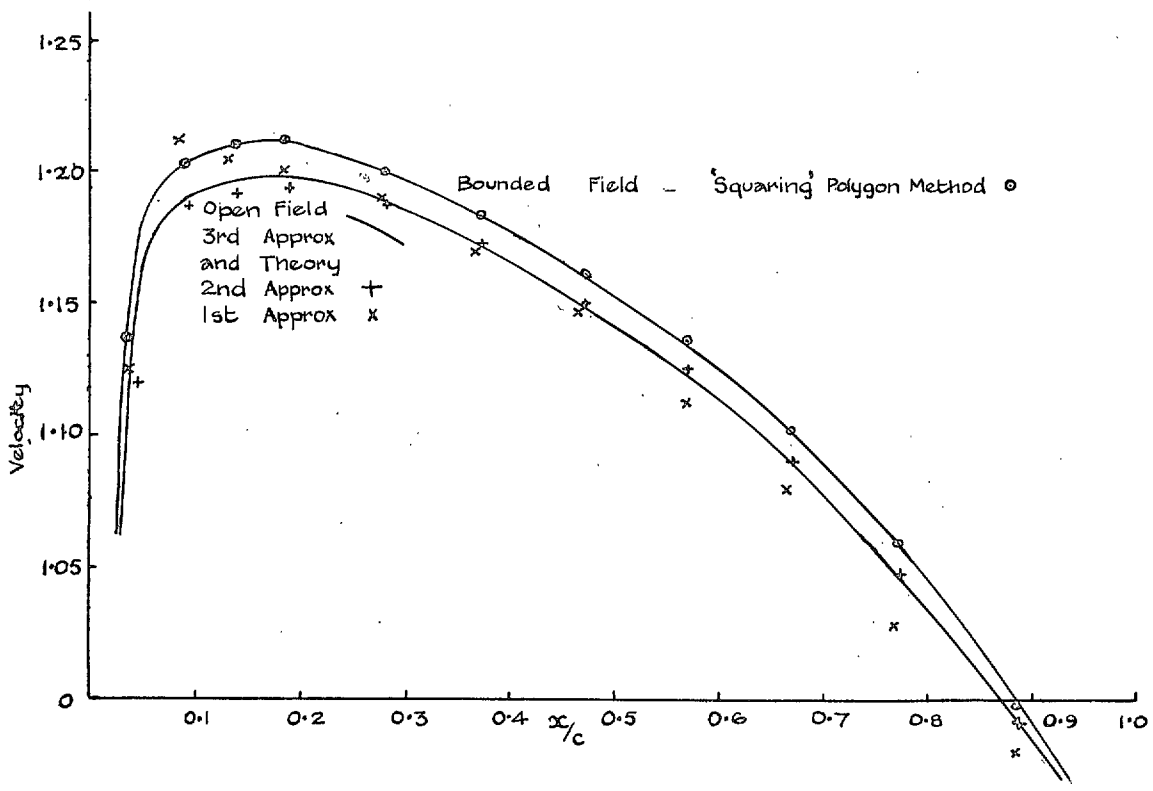

FIG. 5. Velocity distributors.

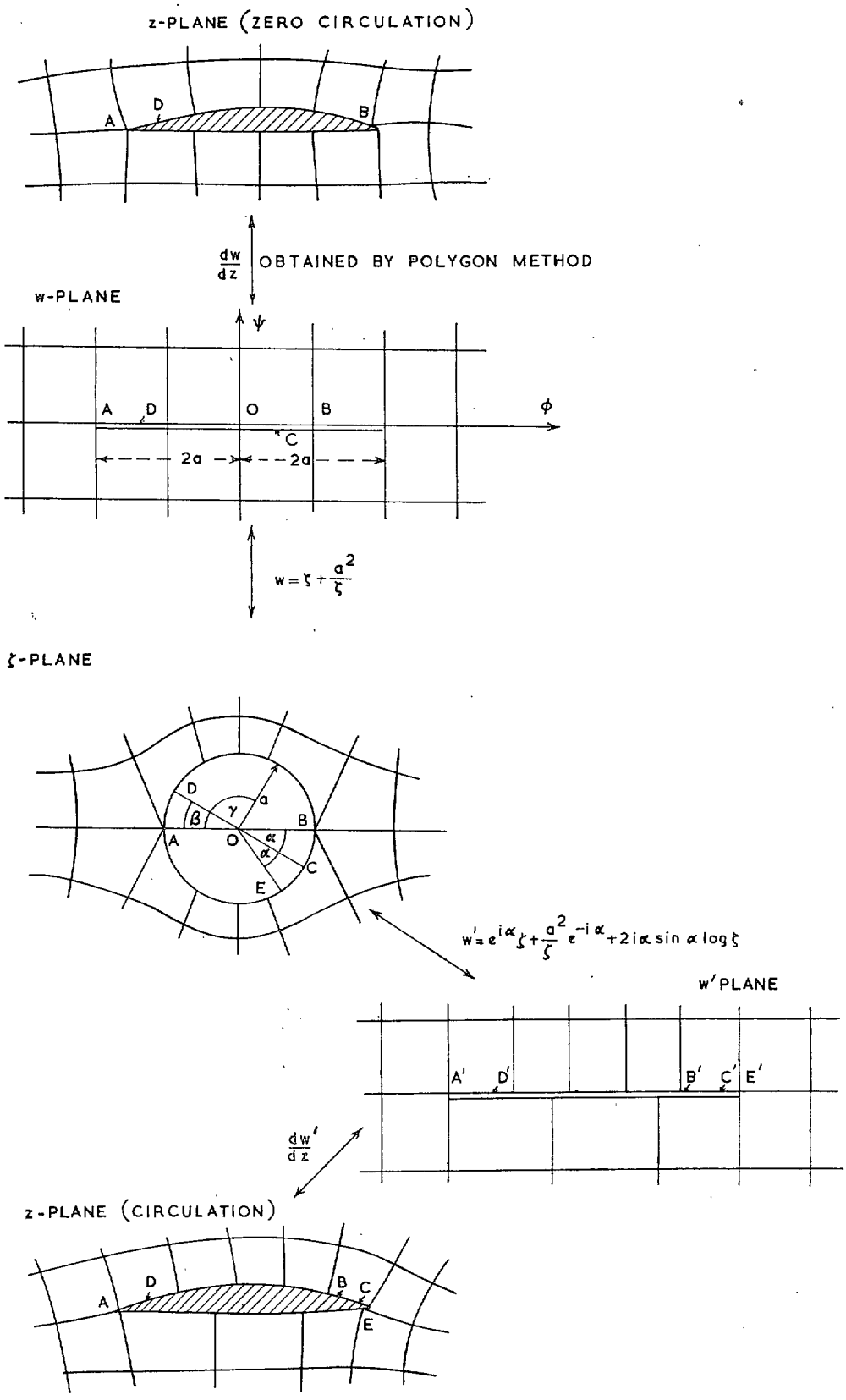
z-PLANE (ZERO CIRCULATION)
A
D
B
dw/dz
OBTAINED BY POLYGON METHOD
w-PLANE
ψ
A
D
O
B
C
φ
2a
2a
w = ζ + a²/ζ
ζ-PLANE
D
β
γ
a
B
A
O
α
α
C
E
w' = e^{iα} ζ + (a²/ζ) e^{-iα} + 2iα sin α log ζ
w'PLANE
A'
D'
B'
C'
E'
dw'/dz
z-PLANE (CIRCULATION)
A
D
B
C
E

FIG. 6.

PART 2

Incompressible Flow about an Asymmetric Aerofoil in a Free Stream

10. *Introduction.*—In section 12 equation (10) is generalised to apply to an asymmetric aerofoil at zero circulation. It is necessary to work in the plane of zero circulation because only in this flow plane are distances defined uniquely, *i.e.*, are independent of the path taken. In section 11 it is shown that once the problem has been solved at zero absolute incidence (zero circulation) then it is simple to deduce results for any angle of incidence. To complete the solution it is necessary to compute the zero-lift angle. The method is quite simple and is set out in section 14, while section 15 summarizes the application of the polygon method to an asymmetric aerofoil.

The example selected to illustrate the method is a high-speed 10 per cent propeller aerofoil (NACA 16), which has a very small nose radius. In Fig. 8 surface results obtained from the polygon method are compared with results (a) from a previously computed relaxation solution[18] and (b) obtained experimentally at the National Physical Laboratory. There is good agreement with the experimental results except near the trailing edge, where of course the effects of viscosity are not negligible.

11. *Asymmetric Aerofoil with Circulation.*—This section reduces the general problem of an asymmetric aerofoil *with* circulation to the problem of an asymmetric aerofoil *without* circulation. Fig. 6 shows the various transformations used in this section. In this figure

α is the absolute incidence

ζ is the complex variable in the plane in which the aerofoil is transformed into a circle of radius a,

$$\text{i.e.,}\quad w = \zeta + \frac{a^2}{\zeta}, \qquad \ldots\ldots\ldots\ldots\ldots\ldots\ldots\ldots\ldots\ldots \quad (35)$$

and w' is the flow plane with circulation,

$$\text{i.e.,}\quad w' = e^{i\alpha}\zeta + \frac{a^2 e^{-i\alpha}}{\zeta} + 2ia \sin\alpha \log \zeta . \qquad \ldots\ldots\ldots\ldots\ldots\ldots \quad (36)$$

In the w-plane the aerofoil is represented by a slit extending from $2a$ to $-2a$. In (36) the circulation has been selected so that the Joukowski condition holds, *i.e.*, the rear stagnation point H coincides with the trailing edge.

It is required to express the velocity in the w-plane in terms of the velocity in the w-plane. From (35) and (36)

$$q'e^{-i\theta'} = \frac{dw'}{dz} = \frac{dw'}{d\zeta}\frac{d\zeta}{dw}\frac{dw}{dz}$$

$$= qe^{-i\theta}\left(e^{i\alpha} - \frac{a^2}{\zeta^2}e^{-i\alpha} + \frac{2ia\sin\alpha}{\zeta}\right)\Big/\left(1 - \frac{a^2}{\zeta^2}\right),$$

where $qe^{-i\theta} = \dfrac{dw}{dz}$. From (35) $2\zeta = w + (w^2 - 4a^2)^{1/2}$, the positive sign being selected so that the ζ and w-planes are identical at infinity. Thus *

$$q'e^{-i\theta'} = \left\{\cos\alpha + i\sin\alpha\left(\frac{w+2a}{w-2a}\right)^{1/2}\right\} qe^{-i\theta}, \qquad \ldots\ldots\ldots\ldots\ldots \quad (37)$$

*An alternate proof of this result appears in Ref. 21

in which the first factor is the well-known solution for a flat plate at an angle of incidence α. Thus if the solution at zero incidence can be determined, that at incidence is found by multiplying by the corresponding flat plate solution. This simple rule can be expressed concisely in terms of elliptic co-ordinates (η,γ) defined by

$$w = -2a \cosh t,\ t = \eta + i\gamma, \quad \ldots \quad (38)$$

when (37) reduces to

$$q' e^{-i\theta'} = \{\cos\alpha \times i \sin\alpha \tanh(t/2)\}\, q e^{-i\theta}. \quad \ldots \quad (39)$$

$\gamma = 0$, defines the stagnation streamline, while $\eta = 0$, or $w = \phi = -2a \cos\gamma$, $\ldots$ (40)

defines the slit representing the aerofoil. Thus on the aerofoil (39) becomes

$$q_0' = (\cos\alpha + \sin\alpha \tan\tfrac{1}{2}\gamma)\, q_0 \quad \ldots \quad (41)$$

The angle γ is shown in Fig. 6. At the trailing edge $\gamma = 0$, and at the front stagnation point corresponding to zero circulation, $\gamma = \pi$. From (41), when $\gamma = 0$, $q_0' = q_0 \cos\alpha$, but when $\gamma = \pi$, $q_0' = \infty \times q_0$. However q_0' remains finite since at $\gamma = \pi$, $q_0 = 0$.

12. *Asymmetric Aerofoil at Zero Incidence.*—The method already developed for a symmetrical aerofoil at zero incidence, together with the equations given above, solves the problem with flow with circulation about a symmetrical aerofoil. It remains now to determine $dw/dz = qe^{-i\theta}$ for an asymmetric aerofoil at zero incidence.

Consider the transformation

$$w = -2a \cosh t,\ t = \eta + i\gamma,$$

already used in the previous section. Fig. 7 shows the relation between the w and t-planes. The whole of the w–plane maps into each of the semi-infinite strips

$$0 \leqslant \eta \leqslant \infty, \quad 2\pi r \leqslant \gamma \leqslant 2\pi(r+1),$$

$$0 \geqslant \eta \geqslant -\infty, \quad 2\pi r \leqslant \gamma \leqslant 2\pi(r+1),$$

where $r = 0, \pm 1, \pm 2, \ldots$. Eliminating γ from

$$\phi + i\psi = -2a \cosh\eta \cos\gamma - 2ai \sinh\eta \sin\gamma,$$

we have $\dfrac{\phi^2}{4a^2\cosh^2\eta} + \dfrac{\psi^2}{4a^2\sinh^2\eta} = 1,$

and so $\eta = \pm$ constant, is an ellipse in the w-plane.

The only singularities in f occur on the aerofoil surface at simple discontinuities in θ. The transformation (38) is conformal except at points B and D (Fig. 7), and so f, being analytic in the w-plane in which points B and D and the surface singularities are excluded by indentations, will be analytic in the corresponding region of the t-plane. As in section 3 the contributions to Cauchy's integral, taken around the contour indicated in Fig. 7, from the indentations excluding the singularities will tend to zero as the radius of the indentation tends to zero. We can therefore omit further consideration of these singularities.

It is clear that f and its derivatives are continuous across the family of lines AB, but while f is continuous across $\eta = 0$, its derivatives are not. However this does not affect the application of Cauchy's integral to the rectangles $0 \leqslant \eta \leqslant k$, $2\pi r \leqslant \gamma \leqslant 2\pi(r+1)$, since

$\eta = 0$ lies only on the contours. Suppose P(t) is a point inside the rectangle $0 \leqslant \gamma \leqslant 2\pi$, $0 \leqslant \eta \leqslant k$, then P($-\bar{t}$) (the bar denoting 'conjugate') is a point inside the rectangle $0 \leqslant \gamma \leqslant 2\pi$, $0 \geqslant \eta \geqslant -k$, *i.e.*, *outside* the first rectangle. Thus for P(t) we have

$$f(t) = \frac{1}{2\pi i}\left\{\int_0^{2\pi} \frac{f(0,\beta)}{i\beta - t} i\,d\beta + \int_0^{k'} \frac{f(\eta,2\pi)}{\eta + 2i\pi - t}\,d\eta + \int_{2\pi}^{0} \frac{f(k,\beta)}{k + i\beta - t} i\,d\beta + \int_k^0 \frac{f(\eta,0)}{\eta - t}\,d\eta\right\},$$

which, since $f(\eta,\gamma) = f(\eta,\gamma + 2\pi)$, we can write

$$f(t) = \frac{1}{2\pi i}\left\{\int_0^{2\pi}\left(\frac{f(0,\beta)}{i\beta - t} - \frac{f(k,\beta)}{k + i\beta - t}\right) i\,d\beta + \int_0^k \left(\frac{1}{\eta + 2i\pi - t} - \frac{1}{\eta - t}\right) f(\eta,0)\,d\eta\right\}. \quad .. \quad (42)$$

Also for P($-\bar{t}$) we have

$$0 = \frac{1}{2\pi i}\left\{\int_0^{2\pi}\left(\frac{f(0,\beta)}{i\beta + \bar{t}} - \frac{f(k,\beta)}{k + i\beta + \bar{t}}\right) i\,d\beta + \int_0^k \left(\frac{1}{\eta + 2i\pi + \bar{t}} - \frac{1}{\eta + \bar{t}}\right) f(\eta,0)\,d\eta\right\}. \quad .. \quad (43)$$

Adding the conjugate of equation (43) to (42) we have

$$f(t) = \frac{1}{2\pi i}\left\{\int_0^{2\pi}\left(\frac{2i\theta(0,\beta)}{i\beta - t} - \frac{f(k,\beta)}{k + i\beta - t} - \frac{\bar{f}(k,\beta)}{k - i\beta + t}\right) i\,d\beta \right.$$
$$\left. + \int_0^k \left(\frac{f(\eta,0)}{\eta + 2i\pi - t} - \frac{f(\eta,0)}{\eta - t} - \frac{\bar{f}(\eta,0)}{\eta - 2i\pi + t} + \frac{\bar{f}(\eta,0)}{\eta + t}\right) d\eta\right\}. \quad .. \quad .. \quad (44)$$

Similarly, taking Cauchy integrals around the rectangles $2\pi r \leqslant \gamma \leqslant 2(r+1)$, $0 \leqslant \eta \leqslant k$, $r = \pm 1, \pm 2, \ldots \pm n$, and adding the results (all zero on the left-hand side) to (44) we find

$$f(t) = \frac{1}{2\pi i}\left\{\int_0^{2\pi} \sum_{r=-n}^{n}\left(\frac{2i\theta(0,\beta)}{2\pi ir + i\beta - t} - \frac{f(k,\beta)}{k + 2\pi ir + i\beta - t} - \frac{\bar{f}(k,\beta)}{k + 2\pi ir - i\beta + t}\right) i\,d\beta \right.$$
$$\left. + \int_0^k \sum_{r=-n}^{n}\left(\frac{f(\eta,0)}{\eta + 2i\pi + 2\pi ir - t} - \frac{f(\eta,0)}{\eta + 2\pi ir - t} - \frac{\bar{f}(\eta,0)}{\eta + 2\pi ir - 2\pi i + t} - \frac{\bar{f}(\eta,0)}{\eta + 2\pi ir + t}\right) d\eta\right\}.$$

In the limit as $n \to \infty$ this becomes

$$f(t) = \frac{i}{2\pi}\int_0^{2\pi} \theta(0,\beta)\coth \tfrac{1}{2}(i\beta - t)\,d\beta - \frac{1}{4\pi}\int_0^{2\pi} \{f(k,\beta)\coth \tfrac{1}{2}(k + i\beta - t)$$
$$+ \bar{f}(k,\beta)\coth \tfrac{1}{2}(k - i\beta + t)\}\,d\beta.$$

Suppose $f(\infty,\beta) = i\theta_\infty$, *i.e.*, $q_\infty = U$, then when $k \to \infty$, we have finally

$$f(t) = \frac{i}{2\pi}\int_{-\pi}^{\pi} \theta(\beta)\coth \tfrac{1}{2}(i\beta - t)\,d\beta, \quad .. \quad .. \quad .. \quad .. \quad .. \quad .. \quad .. \quad (45)$$

where $$\theta_\infty = -\frac{1}{2\pi}\int_{-\pi}^{\pi} \theta(\beta)\,d\beta. \quad .. \quad .. \quad .. \quad .. \quad .. \quad .. \quad .. \quad .. \quad (46)$$

The range alteration is permissible since $\theta(\beta) = \theta(\beta + 2\pi)$.

If instead of *adding* the conjugate of (43) to (42), we subtract it, we can derive the conjugate equation to (45):—

$$f(t) = \frac{1}{2\pi}\int_{-\pi}^{\pi} L(\beta) \coth \tfrac{1}{2}(i\beta - t)\, d\beta - i\theta_\infty, \quad \ldots \quad (47)$$

where $L(\beta)$ satisfies $\int_{-\pi}^{\pi} L(\beta)\, d\beta = 0.$ $\ldots$ (48)

Equation (47) is a more general form of an equation due to Lighthill[8]*. His equation, the basis of his method of aerofoil design, is obtained by putting $t = i\gamma$ in (47):—

$$\theta_0(\gamma) = \frac{1}{2\pi}\int_{-\pi}^{\pi} L(\beta) \cot \tfrac{1}{2}(\beta - \gamma)\, d\beta.$$

13. *Numerical Solution of the Equations.*—Integrating (45) by parts

$$f(t) = -\frac{1}{\pi}\int_{\beta=-\pi}^{\pi} \log \sinh \tfrac{1}{2}(i\beta - t)\, d\theta\ (\beta). \quad \ldots \quad (49)$$

Now $\theta(\beta)$ is continuous except at a number of points $\beta = \beta_s$, where there is a jump in θ of τ_s, say. From (38) and (16) $\phi_0 = -2a\cos\beta$, *i.e.*, $d\theta(\beta) = -\left(\frac{1}{Rq}\right)_0 2a \sin\beta\, d\beta$, and so the Stieltjes integral in (49) can be written

$$f(t) = \frac{2a}{\pi}\int_{-\pi}^{\pi}\left(\frac{1}{Rq}\right)_0 \sin\beta \log \sinh \tfrac{1}{2}(i\beta - t)\, d\beta - \frac{1}{\pi}\sum_s \tau_s \log \sinh \tfrac{1}{2}(\beta_s - t). \quad \ldots \quad (50)$$

On the aerofoil surface, $\eta = 0$, this becomes

$$L_0(\gamma) = \frac{2a}{\pi}\int_{-\pi}^{\pi}\left(\frac{1}{Rq}\right)_0 \sin\beta \log \sin \tfrac{1}{2}(\beta - \gamma)\, d\beta - \frac{1}{\pi}\sum_s \tau_s \log \sin \tfrac{1}{2}(\beta_s - \gamma), \quad \ldots \quad (51)$$

an integral equation which can be solved by the iterative method set out in section 15 below. When this has been done $\left(\frac{1}{Rq}\right)_0$ will be known as a function of β and so (50) can be solved directly.

Of course if $\theta = \theta(\beta)$ is specified algebraically, (45) could be used directly to calculate $f(t)$. However since an aerofoil of arbitrary shape can be much more closely approximated to by assuming that Rq_0 remains constant over small intervals of β than by assuming the same for θ, equation (50) has an obvious advantage over (45).

As in Part 1 we divide the range of integration into $n - 1$ small intervals, $\phi_{j+1} - \phi_j$, $j = 1, 2, \ldots n - 1$, in each of which Rq_0 can be taken, with negligible error, to be constant. The size of the intervals at any point on the aerofoil chord is determined by the rate of change of $(1/Rq)_0$, and needs to be quite small in the neighbourhood of a nose of small radius. This point is illustrated in the example of section 17 below.

Suppose that in the j^{th} interval $(1/Rq)_0 = (1/Rq)_j$, and that $\phi_{j+1} - \phi_j = \delta\phi_j$, then (51) can be written

$$L_0(\gamma) = \frac{1}{\pi}\left\{\sum_{j=1}^{n-1}\left(\frac{\delta\phi}{Rq}\right)_j [\log \sin \tfrac{1}{2}(\beta - \gamma)]_{mj} - \sum_s \tau_s \log \sin \tfrac{1}{2}(\beta_s - \gamma)\right\}, \quad \ldots \quad (52)$$

* See Ref. 23 for an extension of Lighthill's method to compressible flow.

in which 'mj' indicates the mean value of the logarithm in the j^{th} range. The mid-range value can be used except near the singularity $\beta = \gamma$, when, in the absence of special tables, we must use

$$[\log \sin \tfrac{1}{2}(\beta - \gamma)]_{mj} = \frac{1}{2\,\delta\phi_j}\left[\cos\beta - \beta\sin\gamma - 2(\cos\beta - \cos\gamma)\log\sin\frac{\gamma-\beta}{2}\right]_{\phi j}^{\phi j+1}. \qquad (53)$$

Equations (52) and (53) prove a little laborious to use. The following procedure reduces the work and avoids the need to use (53).

We can write (49) as $f(t) = -\frac{1}{\pi}\int_{\beta=-\pi}^{\pi} \log\sinh\tfrac{1}{2}(t - i\beta)\,d\theta(\beta)$, in virtue of

$$\int_{\beta=-\pi}^{\pi} d\theta(\beta) = 0, \qquad \ldots\ \ldots\ \ldots\ \ldots\ \ldots\ \ldots\ \ldots\ \ldots\ \ldots \qquad (54)$$

which is one of the conditions that the profile is closed (*cf.* equation (11)). Thus using (54)

$$f(t) = -\frac{1}{\pi}\int_{\beta=0}^{\pi} \log\sinh\tfrac{1}{2}(t - i\beta)\,d\theta(\beta) - \frac{1}{\pi}\int_{\beta=0}^{\pi} \log\sinh\tfrac{1}{2}(t + i\beta)\,d\theta(-\beta)$$

$$= -\frac{1}{\pi}\int_{\beta=0}^{\pi} \log\{\sinh\tfrac{1}{2}(t - i\beta)\sinh\tfrac{1}{2}(t + i\beta)\}\,d\{\tfrac{1}{2}(\theta(\beta) + \theta(-\beta))\}$$

$$-\frac{1}{\pi}\int_{\beta=0}^{\pi} \log\left\{\frac{\sinh\frac{1}{2}(t - i\beta)}{\sinh\frac{1}{2}(t + i\beta)}\right\}d\{\tfrac{1}{2}(\theta(\beta) - \theta(-\beta))\}$$

$$= \frac{1}{\pi}\int_{\phi_0=H}^{A} \log(\phi_0 - w)\,dF + \frac{1}{\pi}\int_{\beta=0} \log\frac{\sinh\frac{1}{2}(t - i\beta)}{\sinh\frac{1}{2}(t + i\beta)}\,dG,$$

where $F \equiv -\tfrac{1}{2}\{\theta(\beta) + \theta(-\beta)\}$, $\quad G \equiv -\tfrac{1}{2}\{\theta(\beta) - \theta(-\beta)\}$,

and we have assumed that in the w-plane the aerofoil lies between the stagnation points A and H, which are at $\phi_0 = 2a$, and $\phi_0 = -2a$ respectively (*see* equation (38)). If the only discontinuities in θ are τ_A and τ_H at the stagnation points (the usual case), then subdividing the range, and writing

$$dF = T\,d\phi = \tfrac{1}{2}\left\{\frac{1}{Rq}(\beta) + \frac{1}{Rq}(-\beta)\right\}d\phi; \quad dG = C\,d\phi = \tfrac{1}{2}\left\{\frac{1}{Rq}(\beta) - \frac{1}{Rq}(-\beta)\right\}d\phi,$$

where T and C are taken to be constant in each interval, we find

$$f = \frac{1}{\pi}\sum_{j=1}^{n-1}\left(T_j\,[\log(\phi_0 - w)]_{mj}\,\delta\phi_j + C_j\left[\log\frac{\sinh\frac{1}{2}(t - i\beta)}{\sinh\frac{1}{2}(t + i\beta)}\right]_{mj}\delta\phi_j\right)$$

$$-\frac{1}{\pi}\tau_A\log(2a - w) - \frac{1}{\pi}\tau_H\log(2a + w). \qquad \ldots\ \ldots\ \ldots\ \ldots\ \ldots\ \ldots \qquad (55)$$

On the aerofoil surface

$$L_0 = \frac{1}{\pi}\sum_{j=1}^{n-1}\left(T_j\,[\log(\phi_0 - \phi)]_{mj}\,\delta\phi_0 \pm C_j\left[\log\frac{\sin\frac{1}{2}(\gamma - \beta)}{\sin\frac{1}{2}(\gamma + \beta)}\right]_{mj}\delta\phi_j\right)$$

$$-\frac{1}{\pi}\tau_A\log(2a - \phi) - \frac{1}{\pi}\tau_H\log(2a + \phi), \qquad \ldots\ \ldots\ \ldots\ \ldots\ \ldots\ \ldots \qquad (56)$$

in which the range of γ is reduced to $(0,\pi)$ and the positive sign gives values on the upper surface and the negative sign values on the lower surface.

For a symmetrical aerofoil $C_j = 0$, and so the T_j give the effect of thickness, and the C_j the effect of camber. In the absence of special tables

$$\left[\log \frac{\sin \frac{1}{2}(\gamma - \beta)}{\sin \frac{1}{2}(\gamma + \beta)}\right]_{mj} = [\log(\phi - \phi_0)]_{mj} - \log 4a - 2\,[\log \sin \tfrac{1}{2}(\gamma + \beta)]_{mj},$$

in which it is sufficiently accurate to use mid-range values for the last term.

Equation (54) can be written

$$2\int_{\beta=0}^{\pi} d\{\tfrac{1}{2}(\theta(\beta) + \theta(-\beta))\} = 2\int_{\beta=0}^{\pi} dF(\beta) = 0,$$

corresponding to which we have

$$\sum_{j=1}^{n-1} T_j\,\delta\phi_j + \tau_A + \tau_H = 0 \qquad \ldots\ldots\ldots\ldots\ldots\ldots\ldots\ldots \quad (57)$$

assuming that the only finite angles are τ_A and τ_H.

14. *The Zero-Lift Angle.*—Integrating (46) by parts we have $\theta_\infty = \dfrac{1}{2\pi}\displaystyle\int_{\beta=-\pi}^{\pi} \beta\, d\theta(\beta)$,

$$i.e., \quad \theta_\infty = -\frac{a}{\pi}\int_{-\pi}^{\pi} \frac{\beta \sin\beta}{Rq_0} d\beta + \frac{1}{2\pi}\sum_s \tau_s \beta_s,$$

the last term of which vanishes if $\frac{1}{2}\tau_A$ at $\beta = \pi$, $\frac{1}{2}\tau_A$ at $\beta = -\pi$, and τ_H at $\beta = 0$ are the only finite angles on the profile. Thus in this case $\theta_\infty = -\dfrac{a}{\pi}\displaystyle\int_{-\pi}^{\pi} \frac{\sin\beta}{Rq_0}\,\beta\, d\beta$.

The angle between the chord and the streamlines at infinity, *i.e.*, the zero-lift angle α_0, is given by

$$\alpha_0 = \theta_\infty$$

$$= -\frac{a}{\pi}\int_{\pi}^{\pi} \frac{\sin\beta}{Rq_0}\,\beta\, d\beta, \qquad \ldots\ldots\ldots\ldots\ldots\ldots\ldots\ldots \quad (58)$$

$$= -\frac{1}{\pi}\int_{\beta=0}^{\pi} \beta\, d\{\tfrac{1}{2}(\theta(\beta) - \theta(-\beta))\}$$

$$= \frac{1}{\pi}\int_{\beta=0}^{\pi} \beta\, dG(\beta)$$

$$= \frac{1}{\pi}\sum_{j=1}^{n-1} \beta_j C_j\,\delta\phi_j, \qquad \ldots\ldots\ldots\ldots\ldots\ldots\ldots\ldots \quad (59)$$

where β_j is the value of β at the mid-point of the j^{th} range, $\phi_{j+1} - \phi_j$.

From (58) we can deduce an approximate equation for α_0, by assuming that $4a = cq_0$, where c is the aerofoil chord, when

$$\alpha_0 = -\frac{1}{4\pi}\int_{-\pi}^{\pi} \frac{\beta c}{R} \sin\beta \, d\beta. \quad .. \quad .. \quad .. \quad .. \quad .. \quad .. \quad .. \quad .. \quad (60)$$

15. *Summary of the Method.*—Following is a summary of the steps to be taken to find the incompressible flow about an asymmetric aerofoil with circulation. In practice, of course, all the differentiations and integrations of this section are performed numerically. It will be convenient to take the origin for s and ϕ at the trailing edge, H.

(a) Determine from the profile co-ordinates

$$\text{(i)} \ \frac{s}{c} = \int_0^{x/c} \left\{1 + \left(\frac{dy}{dx}\right)^2\right\}^{1/2} d\left(\frac{x}{c}\right), \quad .. \quad .. \quad .. \quad .. \quad .. \quad .. \quad .. \quad .. \quad (61)$$

(ii) semi-perimeter $p = mc$, say, from $p = \frac{1}{2}\oint\left\{1 + \left(\frac{dy}{dx}\right)^2\right\}^{1/2} d\left(\frac{x}{c}\right)$,

and $$\text{(iii)} \ \frac{c}{R} = c\frac{d^2y}{dx^2}\left\{1 + \left(\frac{dy}{dx}\right)^2\right\}^{-3/2}. \quad .. \quad .. \quad .. \quad .. \quad .. \quad .. \quad .. \quad .. \quad (62)$$

(b) Assume an approximate relation $q_0 = q_0(\phi)$, ... (63)
from which $q_0 = q_0(\beta)$ follows immediately.

$$\text{Since } s(\phi) = \int_0^{\phi} \frac{d\phi}{q_0}, \text{ and } c = \frac{1}{2m}\oint \frac{d\phi}{q_0}, \quad .. \quad .. \quad .. \quad .. \quad .. \quad .. \quad .. \quad (64)$$

$$\text{then } \frac{s}{c}(\phi) = 2m\int_0^{\phi} d\phi/q_0 \Big/ \left(\oint d\phi/q_0\right),$$

$$\text{and hence } \frac{c}{R} = \frac{c}{R}(\phi), \quad .. \quad .. \quad .. \quad .. \quad .. \quad .. \quad .. \quad .. \quad .. \quad (65)$$

follows from (61) and (62). The infinities occurring in $d\phi/q_0$ at the stagnation points are dealt with in the appendix. An approximate value of the boundary gradient $\left(\frac{c}{R}\right)\frac{1}{cq_0}$ .. (66) follows from (63), (64) and (65).

(c) Intervals $\phi_{j+1} - \phi_j$ are selected so that the aerofoil will be adequately represented, and approximate T_j, C_j, $j = 1, 2, \ldots n-1$, are calculated using the values (66). τ_A and τ_H must now be selected so that (57) is satisfied. Only when the number of intervals, $n-1$, tends to infinity will τ_A and τ_H become equal to the *actual* leading and trailing edge angles. Otherwise τ_H will usually be very nearly the exact trailing-edge angle, but even with a relatively fine mesh, τ_A will have a value quite different from π, except perhaps for very large nose-radius aerofoils. In practice τ_H is made equal to the sum of the $(\delta\phi/Rq)_j$ between the points of contact of parallel tangents on the aerofoil and the trailing edge. τ_A is then selected to satisfy (57), when clearly it will be equal to the sum of the $(\delta\phi/Rq)$ between the points of contact of the parallel tangents and the leading edge.

(d) L_0 is found from (56), and a new and more accurate relation $q_0 = q_0(\phi)$ is deduced to use in step (e).

(e) Steps (b), (c) and (d) are repeated until there is no further change in q_0.

(f) The values of T_j and C_j found in the last round of this iterative process are now used in (55) to find values of L in the outer field, *i.e.*, $L = L(\eta,\gamma)$, and hence from (38)

$$L = L(\phi,\psi) \quad .. \quad .. \quad .. \quad .. \quad .. \quad .. \quad .. \quad .. \quad .. \quad .. \quad (67)$$

can be deduced.

(g) $\theta(\phi,\psi)$ follows from

$$\theta(\phi,\psi) = \theta(\phi_0,0) + \int_0^{\psi} \frac{\partial L}{\partial \phi} d\psi - \int_{\phi_0}^{\phi} \frac{\partial L}{\partial \psi} d\phi, \quad .. \quad .. \quad .. \quad .. \quad .. \quad .. \quad (68)$$

which holds in virtue of the Cauchy-Riemann equations relating L and θ. $\theta(\phi_0,0)$ is the value of θ on the aerofoil and is thus known.

(h) The (ϕ,ψ) and (x,y)-planes are now related by

$$x = x(\phi,\psi) = \int_{\phi_0}^{\phi} \frac{\cos\theta}{q} d\phi - \int_0^{\psi} \frac{\sin\theta}{q} d\psi,$$

$$y = y(\phi,\psi) = \int_{\phi_0}^{\phi} \frac{\sin\theta}{q} d\phi + \int_0^{\psi} \frac{\cos\theta}{q} d\psi, \quad .. \quad .. \quad .. \quad .. \quad .. \quad .. \quad .. \quad (69)$$

and hence from (67) and (68) we have the solution

$$q = q(x,y), \quad \theta = \theta(x,y). \quad .. \quad .. \quad .. \quad .. \quad .. \quad .. \quad .. \quad .. \quad (70)$$

(i) The zero-lift angle α_0, is now calculated from (59).

10. If α_c is the angle of incidence measured from the chord, then putting $\alpha = \alpha_c + \alpha_0$ in (41) and using (38), (69) and (70) we can find $q' = q'(x,y)$, $\theta' = \theta'(x,y)$, for any given α_c.

In the iterative process described above, the position of A, the front stagnation point, is determined by an integration commencing at the trailing edge. Initially it can be assumed with little error that A is at the semi-perimeter point, P say. Suppose a subsequent integration indicates that A should be moved a small distance δs^* from P, then, since both R and q change rapidly in the neighbourhood of an aerofoil nose, this small movement will result in a relatively large change in T_j and C_j near the nose. When $q_0 = q_0(\phi)$ is calculated and the integration performed, it may be found that according to this integration A should be placed at a distance greater than δs^* on the other side of P. This diverging oscillation of A about P certainly occurs for an aerofoil of small nose radius such as that of section 17 below, and so another method must be used to help locate the position of A. This is given in the next section, but during the early stages of the calculation it is better to maintain A fixed at P until the velocity distribution has ' settled ', and only then to allow A to move.

16. *Location of Front Stagnation Point* A.—From equation (56) it follows that the difference in velocity between the upper and lower surface of the aerofoil is due entirely to the coefficients C_j. We shall calculate an approximate value of the displacement of A (δs) due to a small change δC_j in the values of C_j, $j = 1, 2, \ldots n - 1$.

Consider the effect of one δC_j at $\phi = -2a\cos\beta_j$, on the velocity at $\phi = -2a\cos\gamma$. Suppose this velocity q is increased to $q + \delta q$, then, with $\delta\phi$ constant, if δs was the original length of an element, $(\delta s)q/(q + \delta q)$ will be the new length of the element, *i.e.*, the element changes in length approximately $\frac{\delta s\,\delta q}{q} = \frac{\delta q\,\delta\phi}{q^2}$ (since $\delta\phi = q\,\delta s$).

Now $\delta L = -\log(q + \delta q) + \log q \simeq -\delta q/q$,

$$i.e., \text{ from (56)} \quad \frac{\delta q}{q} = \frac{\delta C_j}{\pi} \log \frac{\sin \frac{1}{2}(\gamma - \beta_j)}{\sin \frac{1}{2}(\gamma + \beta_j)}.$$

Therefore change in length of element at $\phi = -2a \cos \gamma$

$$= \frac{1}{q} \frac{\delta C_j}{\pi} \log \frac{\sin \frac{1}{2}(\gamma - \beta_j)}{\sin \frac{1}{2}(\gamma + \beta_j)} \delta\phi.$$

Thus the total displacement of A due to δC_j is approximately

$$\frac{2a}{\pi} \delta C_j \int_0^{\pi} \log \frac{\sin \frac{1}{2}(\gamma - \beta_j)}{\sin \frac{1}{2}(\gamma + \beta_j)} \frac{\sin \gamma}{q} d\gamma \simeq \frac{2a}{\bar{q}} \delta C_j \sin \beta_j,$$

where $\bar{q}$ is an average velocity over the aerofoil.

Hence, since $4a/\bar{q} = c$, the displacement δs due to all the δC_j is

$$\frac{\delta s}{c} \simeq \frac{1}{2} \sum_{j=1}^{n-1} \delta C_j \sin \beta_j. \qquad (71)$$

We use this equation in the following way. Suppose that initially A is taken to be at P, the semi-perimeter point, and that a subsequent integration indicates that A should be moved a distance δs^*, which movement will change the C_j to $C_j + \delta C_j$. Equation (71) gives immediately the approximate displacement δs that will result. This displacement will probably be larger than δs^* and of opposite sign. If however a smaller displacement of A is made in the direction of δs^*, then δs calculated from (71) will be reduced and even changed in sign. It is clear that the *actual* displacement $\delta s'$ should be selected so that it and the δs subsequently calculated from (71) are equal. This method involves a small amount of trial and error, but the process does converge, and it only takes a small time to calculate beforehand, with reasonable accuracy, the effect of any given displacement of A. The method was applied to the aerofoil discussed in the next section.

17. *An Example: NACA* 16.—This aerofoil received some attention in a previous paper[18]. Table 6 gives the profile co-ordinates, and Table 7 sets out the values of q_0 at $\alpha = 0$ deg, 2·15 deg and 4·3 deg. Equation (41) was used to calculate the values of $q_0 = 2{\cdot}15$ deg and 4·3 deg from the value of q_0 at $\alpha = 0$ deg. This equation can be written $q_0' = q_p(\alpha) \times q_0$, where $q_p = \cos \alpha + \sin \alpha \tan \frac{1}{2}\gamma$. Values of q_p are shown in the table.

Fig. 8 shows the velocity distribution curves. From these it is clear that the aerofoil was designed for an absolute angle of incidence of about 2·15 deg. There is reasonably close agreement between the results found using relaxation at $\alpha = 4{\cdot}3$ deg, and the polygon method. The experimental curve shown was deduced from a curve for which the stream Mach number was 0·4 by using the Glauert factor (in the absence of low-speed results). Agreement is good over the front part of the chord, but as can be expected, there is increasing disagreement towards the trailing edge, where viscosity effects cannot be ignored.

There is another important difference between the experimental and theoretical results. The experimental value of α_0 is 2·3 deg, whereas equation (59) yields $\alpha_0 = 2{\cdot}72$ deg. Thus theoretically at $\alpha = 2{\cdot}72$ deg $- 2{\cdot}3$ deg $= 0{\cdot}42$ deg, the aerofoil should give about 10 per cent of the lift it has at $\alpha = 4{\cdot}3$ deg, whereas in fact it gives zero lift. The experimental lift at $\alpha = 4{\cdot}3$ deg is about 16 per cent less than the theoretical value, and it would seem that in this case the boundary layer is still causing an appreciable loss in lift near the zero-lift angle.

TABLE 6

Ordinates for 10 *per cent Aerofoil NACA* 16, 5 *in. Chord*

(Figures supplied by the National Physical Laboratory)

1 Distance from L.E.	2 Upper Surface	3 Lower Surface	1	2	3
			(All measurements in inches)		
0·000	0·0000	0·0000	1·6	0·3052	0·1555
0·005	0·0165	0·0146	1·7	0·3100	0·1579
0·010	0·0236	0·0202	1·8	0·3151	0·1601
0·015	0·0292	0·0243	1·9	0·3206	0·1620
0·02	0·0339	0·0277	2·0	0·3244	0·1636
0·025	0·0382	0·0306	2·1	0·3274	0·1649
0·03	0·0420	0·0332	2·2	0·3299	0·1659
0·035	0·0455	0·0356	2·3	0·3316	0·1666
0·04	0·0489	0·0377	2·4	0·3325	0·1671
0·05	0·0550	0·0416	2·5	0·3327	0·1673
0·06	0·0605	0·0450	2·6	0·3324	0·1671
0·07	0·0657	0·0481	2·7	0·3313	0·1666
0·08	0·0705	0·0509	2·8	0·3295	0·1658
0·09	0·0750	0·0535	2·9	0·3269	0·1645
0·10	0·0793	0·0599	3·0	0·3235	0·1628
0·125	0·0893	0·0613	3·1	0·3192	0·1607
0·15	0·0982	0·0660	3·2	0·3140	0·1580
0·175	0·1065	0·0702	3·3	0·3079	0·1548
0·2	0·1142	0·0741	3·4	0·3007	0·1511
0·25	0·1283	0·0809	3·5	0·2925	0·1467
0·3	0·1410	0·0868	3·6	0·2832	0·1417
0·35	0·1526	0·0921	3·7	0·2729	0·1361
0·4	0·1634	0·0968	3·8	0·2614	0·1299
0·45	0·1734	0·1012	3·9	0·2487	0·1231
0·5	0·1828	0·1052	4·0	0·2345	0·1156
0·6	0·2001	0·1125	4·1	0·2188	0·1076
0·7	0·2156	0·1189	4·2	0·2016	0·0989
0·8	0·2296	0·1245	4·3	0·1829	0·0897
0·9	0·2424	0·1297	4·4	0·1627	0·0797
1·0	0·2540	0·1345	4·5	0·1410	0·0690
1·1	0·2647	0·1389	4·6	0·1177	0·0576
1·2	0·2744	0·1429	4·7	0·0927	0·0455
1·3	0·2833	0·1465	4·8	0·0658	0·0327
1·4	0·2914	0·1498	4·9	0·0366	0·0192
1·5	0·2987	0·1528	5·0	0·0050	0·0050

Trailing-edge radius = 0·005 in.

TABLE 7

Velocity Distributions

(a) *Upper Surface.*

ϕ	$\frac{x}{c}$	$\frac{\delta\phi}{Rq_0}$	q_0	$a = 2{\cdot}15$ deg		$a = 4{\cdot}3$ deg	
				q_p	q_0'	q_p	q_0'
0	0·0016	—	0	∞	—	∞	—
0·020	0·0056	0·2100	0·543	0·843	1·001	2·685	1·458
0·040	0·0098	0·0680	0·660	1·591	1·050	2·182	1·440
0·075	0·0144	0·0900	0·747	1·446	1·080	1·890	1·412
0·125	0·0206	0·0402	0·810	1·332	1·089	1·663	1·347
0·225	0·0327	0·0658	0·879	1·247	1·096	1·492	1·311
0·40	0·053	0·0525	0·946	1·183	1·119	1·365	1·291
0·75	0·093	0·0585	1·003	1·1309	1·134	1·2605	1·264
1·25	0·145	0·0356	1·042	1·0985	1·145	1·1957	1·246
2	0·222	0–0428	1·076	1·0744	1·156	1·1474	1·235
3	0·320	0·0358	1·106	1·0566	1·169	1·1118	1·230
4	0·417	0·0327	1·125	1·0451	1·176	1·0889	1·225
5	0·512	0·0237	1·138	1·0368	1·180	1·0722	1·220
6	0·607	0·0413	1·149	1·0297	1·183	1·0581	1·216
7	0·700	0·0498	1·149	1·0239	1·176	1·0463	1·202
8	0·795	0·0680	1·133	1·0180	1·153	1·0347	1·172
9	0·890	0·0735	1·067	1·0119	1·080	1·0223	1·091
9·75	0·970	0·0508	0·930	1·0035	0·933	1·0056	0·935
10	1·000	—	0	0·9993	0	0·9972	0

(b) *Lower Surface.*

0	−0·0016	—	0	∞	—	∞	—
0·020	−0·0001	0·4700	0·802	0·155	0·138	0·691	0·617
0·040	+0·0002	0·3080	1·230	0·407	0·476	0·188	0·220
0·075	0·0020	0·3930	1·508	0·552	0·803	0·104	0·151
0·125	0·0050	0·1680	1·480	0·666	0·939	0·331	0·470
0·225	0·0123	0·1770	1·379	0·751	1·006	0·502	0·672
0·40	0·0263	0·0770	1·271	0·815	1·017	0·629	0·785
0·75	0·060	0·0522	1·183	0·8677	1·015	0·7339	0·859
1·25	0·106	0·0228	1·141	0·9001	1·020	0·7987	0·905
2	0·178	0·0214	1·110	0·9242	1·020	0·8470	0·935
3	0·276	0·0152	1·096	0·9420	1·028	0·8826	0·963
4	0·375	0·0144	1·088	0·9535	1·035	0·9055	0·982
5	0·475	0·0149	1·083	0·9617	1·040	0·9222	0·997
6	0·575	0·0208	1·077	0·9689	1·043	0·9363	1·007
7	0·675	0·0296	1·070	0·9747	1·042	0·9481	1·014
8	0·776	0·0317	1·045	0·9806	1·023	0·9597	1·001
9	0·882	0·0370	0·994	0·9867	0·980	0·9721	0·965
9·75	0·970	0·0205	0·902	0·9951	0·898	0·9888	0·892
10	+1·000	—	0	0·9993	0	0·9972	0

Other Results. $c = 9{\cdot}268$, $C_L = \frac{8\pi a}{c}\sin a = \frac{20\pi}{9{\cdot}286}\sin a$

i.e., $C_L = 0{\cdot}253$ for $\alpha = 2{\cdot}15$ deg; $C_L = 0{\cdot}507$ for $\alpha = 4{\cdot}3$ deg

$\alpha_0 = 2{\cdot}72$ deg.

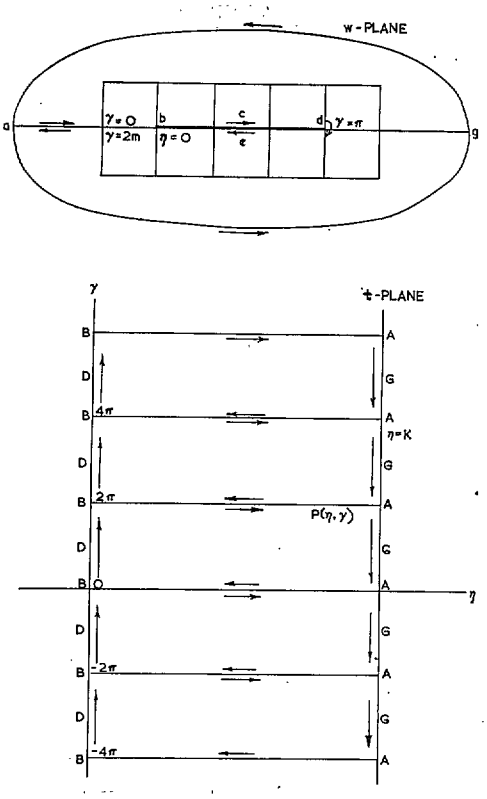

FIG. 7. The transformation $w = -2a \cosh t$.

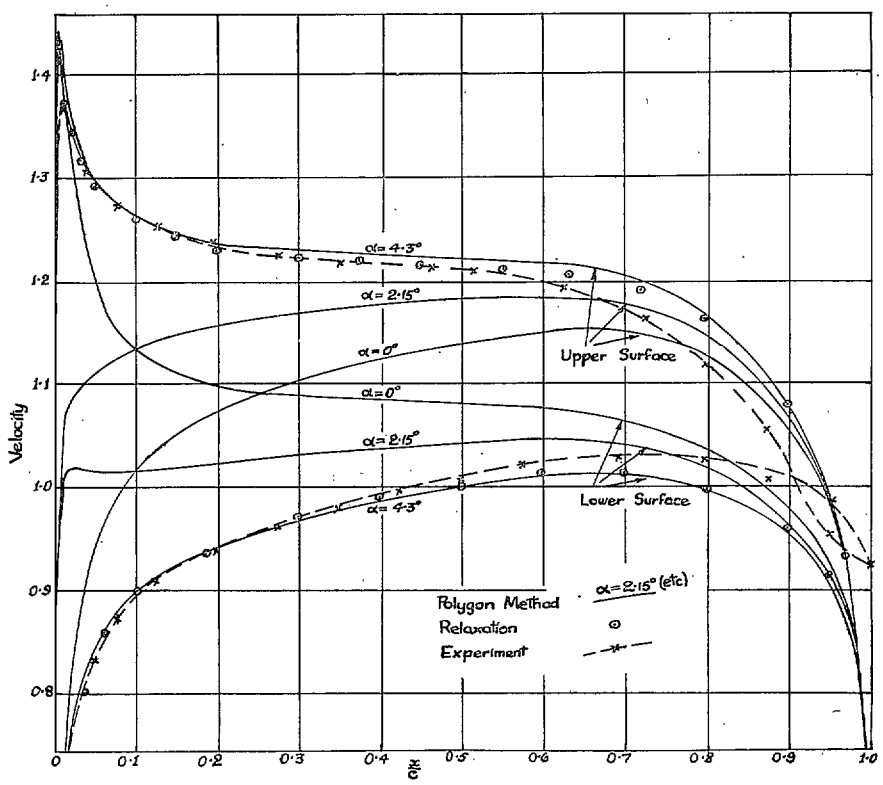

FIG. 8. Velocity distributions for NACA 16.

PART 3

The Influence Factor Method of Calculating Incompressible Flow

18. *Introduction.*—Thom[13] developed a method for calculating the incompressible flow about a symmetrical body at zero incidence in an open or bounded stream. The author's polygon method has points of similarity with Thom's influence factor method. The calculations to both methods are performed in the (ϕ,ψ) or flow plane, instead of the more usual (x,y) or physical plane. Thom uses the conjugate harmonic functions x and y as dependent variables in the (ϕ,ψ)-plane and obtains a solution $x = x(\phi,\psi)$, $y = y(\phi,\psi)$; whereas in the author's method the conjugate harmonic functions $\log (U/q)$ and θ are the dependent variables in the (ϕ,ψ)-plane. Since the boundary conditions are usually specified in the (x,y)-plane an iterative method of solution is required for both the polygon and influence factor methods. However convergence to the exact solution is rapid. Details of the iteration for the polygon method, and a demonstration of the rapidity of convergence was given in Part 1.

Some time after this paper was written it was discovered that Goldstein and Lighthill[5] had established equations equivalent to (74), (75) and (76) for what they termed the ' complementary function ' in the Janzen-Rayleigh method of computing compressible flow. They did not however link these equations with the incompressible flow or make any use of them to find the flow about aerofoils of arbitrary shape.

Thom, whose original work appeared in an unpublished R.A.E. report in 1942, used a semi-empirical method to develop his equations, and while the majority of these are correct, a few, as he states himself, are approximations only. In the following sections the equations are derived mathematically, and several extensions are made. An iterative method of solving the integral equations for an arbitrary aerofoil is given in section 23, and applied in section 26 to the aerofoil already considered by the polygon method in section 9.

19. *The Influence Factor Equations.*—We define a ' displacement ' function

$$\bar{z} = \bar{x} + i\bar{y} = \{Ux(\phi,\psi) - \phi\} + i\{Uy(\phi,\psi) - \psi\} = Uz - w, \quad .. \quad .. \quad .. \quad (72)$$

for which $\nabla_{\phi,\psi}{}^2\bar{z} = \nabla_{\phi,\psi}{}^2(Uz - w) = U\nabla_{\phi,\psi}{}^2 z = 0,$

since z is an analytic function in the (ϕ,ψ)-plane. From (72) we have on the boundaries

$$\bar{y}(\phi,0) = Uy_0, \text{ and } \bar{y}(\phi,\tfrac{1}{2}h) = Uy^* - \tfrac{1}{2}h, \quad .. \quad .. \quad .. \quad .. \quad .. \quad .. \quad (73)$$

where $h = UH$ (H is the channel width), y_0 refers to the aerofoil, and y^* refers to the channel wall.

Now in the proof of equation (8) it was assumed only that L and θ were conjugate harmonic functions in the (ϕ,ψ)-plane, such that $f(w)$ was finite at infinity. Suppose that near infinity $w = Ve^{i\theta}z +$ constant, *i.e.*, $\bar{z} = z(Ve^{i\theta} - U) -$ constant, then if $\bar{z}$ is to remain finite at infinity, $\theta = 0$, $U = V$, *i.e.*, the flow at infinity must be parallel to the x-axis, and U must be the velocity in the channel at both $+\infty$ and $-\infty$. With this limitation, $\bar{z}$, being harmonic and having boundary conditions similar to $f(w)$, must satisfy an equation of the same form as (8), *i.e.*, using (72) and (73)

$$z = \frac{w}{U} + \frac{1}{UH}\int_{-\infty}^{\infty} \{y_0 \coth \frac{\pi}{UH}(\phi_0 - w) - (y^* - \tfrac{1}{2}H)\tanh \frac{\pi}{UH}(\phi_0 - w)\}\, d\phi_0. \quad .. \quad (74)$$

The origin is selected so that $\bar{x}(\infty) + \bar{x}(-\infty) = 0$, and y_0 and y^* must satisfy

$$\bar{x}(\infty) - \bar{x}(-\infty) = \frac{2}{H}\int_{-\infty}^{\infty} (y^* - \tfrac{1}{2}H - y)\, d\phi_0.$$

Equation (74) can be regarded as an equation for the flow in an asymmetric channel of width $\frac{1}{2}H$. Putting $y^* = \frac{1}{2}H$ and taking the limit as $H \longrightarrow \infty$, we find for a symmetrical aerofoil in an open stream

$$z = \frac{w}{U} + \frac{1}{\pi}\int_{-\infty}^{\infty} \frac{y_0\, d\phi_0}{\phi_0 - w}. \qquad \text{(75)}$$

For an asymmetric aerofoil in an open stream we have in a similar way corresponding to (45) the result

$$z = \frac{w}{U} - \frac{i}{2\pi}\int_{-\infty}^{\infty} y_0 \coth \tfrac{1}{2}(t - i\beta)\, d\beta, \qquad \text{(76)}$$

of which (75) is only a special case.

Since there is no circulation $w = Uz + O\left(\frac{1}{z}\right)$,

$$i.e., \quad z - \frac{w}{U} = O\left(\frac{1}{w}\right) \to 0 \text{ as } w \to \infty.$$

Using this in (76) we find y_0 must be measured from a chord selected to make $\int_{-\pi}^{\pi} y_0(\beta)d\beta = 0$.

Equations (75) and (76) are only true for zero circulation. The effect of circulation is given in section 23.

20. *The Iterative Method of Solution.*—The equations developed above require that $y_0 = y_0(\phi_0)$ be known, whereas in fact the given aerofoil profile yields the relation

$$y_0 = y_0(x_0) \qquad \text{(77)}$$

only. This difficulty is readily overcome as follows.
Consider for example equation (75) on $\psi = 0$:—

$$x_0(\phi) = \frac{\phi}{U} + \frac{1}{\pi}\int_{-\infty}^{\infty} \frac{y_0\, d\phi_0}{(\phi_0 - \phi)}. \qquad \text{(78)}$$

$y_0 = y_0(\phi_0)$ can be determined from (77) and (78), but since this solution occurs under the integral sign in (78), the equations taken together define an integral equation, which can be solved by the following iterative process:—

(a) Assume a relation $y_0 = y_0(\phi_0)$, *e.g.*, assume $\phi_0 \simeq x_0$, then $y_0 = y_0(\phi_0)$ is simply the profile equation.

(b) Solve (77) and (78) to find a first approximation $y_0^1(\phi_0)$.

(c) Use $y_0^1(\phi_0)$ in (77) and (78) to determine a second approximation $y_0^2(\phi_0)$.

(d) Repeat these steps until $y_0^{i+1}(\phi_0) - y_0^i(\phi_0)$ is negligible.

Only two or three iterations are required for normally shaped aerofoils. When $y_0(\phi_0)$ is finally determined in this way, equation (75) can be used directly to find $z(\phi,\psi)$ away from the aerofoil. A similar treatment is applicable to (74) and (76), but with this latter equation, as in section 15, some difficulty may be experienced in locating the front stagnation point. A procedure along the lines of section 16 could probably be developed to obviate this.

Suppose that we have to solve (75) for an aerofoil for which the profile (77) is defined numerically. If the aerofoil lies in the range $a \geqslant \phi_0 \geqslant b$, which is subdivided into $n-1$ intervals, as in section 4, such that $\left(\frac{d^2y}{d\phi^2}\right)_0$ can be taken to have the constant value $\delta m_i/(\phi_{i+1} - \phi_i)$ in the i^{th} interval with negligible error, then integrating (75) twice by parts, we find

$$z(w) = \frac{w}{U} - \frac{1}{\pi}\left\{\left[\left(\frac{dy}{d\phi}\right)_0(\phi_0 - w)\{\log(\phi_0 - w) - 1\}\right]_b^a - \sum_{i=1}^{n-1}\delta m_i[(\phi_0 - w)\{\log(\phi_0 - w) - 1\}]_{mi}\right\}, \quad \ldots\ldots\ldots\ldots \quad (79)$$

where $[\ ]_{mi}$ denotes the mean value of the function in the i^{th} range. The other equations can be treated similarly.

21. *Calculation of Velocities.*—Since $dz/dw = e^{i\theta}/q$ we could use the solution $z = z(w)$ found above to deduce the values of q and θ, but it is more convenient to calculate these by directly differentiating the equations for z. Equations (75), (74) and (76) become respectively

$$\frac{e^{i\theta}}{q} = \frac{1}{U} + \frac{1}{\pi}\int_{-\infty}^{\infty}\frac{y_0\,d\phi_0}{(\phi_0 - w)^2}. \quad \ldots\ldots\ldots\ldots\ldots\ldots\ldots\ldots \quad (80)$$

$$\frac{e^{i\theta}}{q} = \frac{1}{U} + \frac{\pi}{(UH)^2}\int_{-\infty}^{\infty}\left\{y_0\,\mathrm{cosech}^2\frac{\pi}{UH}(\phi_0 - w) - (y^* - \tfrac{1}{2}H)\,\mathrm{sech}^2\frac{\pi}{UH}(\phi_0 - w)\right\}d\phi_0 \quad \ldots\ldots\ldots\ldots \quad (81)$$

$$\frac{e^{i\theta}}{q} = \frac{1}{U} - \frac{i}{8a\pi\sinh t}\int_{-\pi}^{\pi}\frac{y_0\,d\beta}{\sinh^2\frac{1}{2}(t - i\beta)}. \quad \ldots\ldots\ldots\ldots\ldots\ldots \quad (82)$$

Alternative forms of (76) and (82) are of some interest. Equation (76) may be written

$$z = \frac{w}{U} - \frac{i}{2\pi}\int_0^{\pi}\{y_0(\beta)\coth\tfrac{1}{2}(t - i\beta) + y_0(-\beta)\coth\tfrac{1}{2}(t + i\beta)\}\,d\beta$$

$$= \frac{w}{U} + \frac{1}{\pi}\int_0^{\pi}\frac{d\phi_0}{(\phi_0 - w)}\left(T - iC\frac{\sinh t}{\sin\beta}\right), \quad \ldots\ldots\ldots\ldots\ldots\ldots \quad (83)$$

where T is a ' thickness parameter ', i.e., $T = \frac{1}{2}\{y_0(\beta) - y_0(-\beta)\}$,

and C is a ' camber parameter ', i.e., $C = \frac{1}{2}\{y_0(\beta) + y_0(-\beta)\}$.

Differentiating (83) we have

$$\frac{e^{i\theta}}{q} = \frac{1}{U} + \frac{1}{\pi}\int_0^{\pi}\frac{d\phi_0}{(\phi_0 - w)^2}\left[T + iC\frac{(1 - \cos\beta\cosh t)}{\sin\beta\sinh t}\right], \quad \ldots\ldots\ldots\ldots \quad (84)$$

which enables the efiects of thickness and camber to be investigated separately.

Approximate Theory.—Useful approximate equations can be derived from those given above by assuming that on the aerofoil $\cos\theta \doteq 1$, and that $d\phi_0 \doteq \bar{q}\, ds \doteq \bar{q}\, dx_0$, where $\bar{q}$ is the mean velocity over the chord. For example on the aerofoil equation (80) becomes

$$\frac{1}{q} = \frac{1}{U}\left(1 + \frac{U}{\bar{q}\pi}\int_{-c/2}^{c/2} \frac{y_0\, dx_0}{(x_0 - x)^2}\right),$$

in which the origin is taken at the midpoint of the chord, c, and $y_0 = 0$ when $|x_0| > \frac{1}{2}c$. We shall write

$$\frac{1}{q} = \frac{1}{U}\left(1 - \delta\frac{U}{q}\right) \text{ where } \delta(x) = -\frac{1}{\pi}\int_{-c/2}^{c/2} \frac{y_0\, dx_0}{(x_0 - x)^2}, \quad \ldots\ \ldots\ \ldots\ \ldots \quad (85)$$

i.e., $$q \doteq U\left\{1 + \delta\frac{U}{\bar{q}} + \delta^2\left(\frac{U}{\bar{q}}\right)^2\right\}.$$

Now $\bar{q} \doteq U(1 + \bar{\delta})$, and so ignoring terms $O(\delta^3)$ we find

$$q \doteq U\{1 + \delta + \delta(\delta - \bar{\delta})\}. \quad \ldots\ \ldots\ \ldots\ \ldots\ \ldots\ \ldots\ \ldots\ \ldots \quad (86)$$

From (85) we have $\bar{\delta} = -\frac{1}{c\pi}\int_{-c/2}^{c/2}\left\{\int_{-c/2}^{c/2}\frac{dx}{(x_0 - x)^2}\right\} y_0\, dx_0$

$$i.e.,\ \bar{\delta} = \frac{4}{\pi c^2}\int_{-c/2}^{c/2}\frac{y_0\, dx_0}{1 - (2x_0/c)^2}. \quad \ldots\ \ldots\ \ldots\ \ldots\ \ldots\ \ldots \quad (87)$$

A similar treatment for equation (81), in the special case $y^* = \frac{1}{2}H$, yields

$$\delta(x) = -\frac{\bar{q}\pi}{(UH)^2}\int_{-c/2}^{c/2} \operatorname{cosech}^2\left\{\frac{\bar{q}\pi}{UH}(x_0 - x)\right\} y_0\, dx_0, \text{ and}$$

$$\bar{\delta} = \frac{\bar{q}\pi}{(UH)^2}\int_{-c/2}^{c/2}\frac{\sinh(c\pi/UH)y_0\, dx_0}{\sinh(\bar{q}\pi/UH)(x_0 - \frac{1}{2}c)\sinh(\bar{q}\pi/UH)(x_0 + \frac{1}{2}c)}.$$

The assumption $\phi_0 \doteq qx_0 \doteq -2a\cos\beta$ can similarly be used in (84).

Example.—If t is the thickness of a symmetrical circular-arc aerofoil, then,

$$y_0 = \tfrac{1}{2}t\left\{1 - \left(\frac{2x_0}{c}\right)^2\right\}.$$

Using this in (85) and (87) we find $\delta(0) = \frac{4}{\pi}\left(\frac{t}{c}\right)$, $\bar{\delta} = \frac{2}{\pi}\left(\frac{t}{c}\right)$, which substituted in (86) yield

$$q(0) \doteq U\left(1 + \frac{4}{\pi}\left(\frac{t}{c}\right) + \frac{8}{\pi^2}\left(\frac{t}{c}\right)^2\right). \quad \ldots\ \ldots\ \ldots\ \ldots\ \ldots\ \ldots\ \ldots \quad (88)$$

Comparing this with equation (31), which was based on exact theory, we find there is an error of only 11 per cent in the coefficient of the last term, which demonstrates that even the first approximation of the iterative process described in section 20 will be reasonably accurate.

The corresponding calculation for the same aerofoil in a straight-walled channel yields

$$q(0) \simeq U\left\{1 + \frac{4}{\pi}\left(\frac{t}{c}\right) + \left(\frac{\pi}{9}\right)\left(\frac{t}{c}\right)\left(\frac{c}{H}\right)^2\right\}.$$

Comparing this result with (88) we see that the blockage factor (*see* equation (27)) is given by

$$\frac{\Delta q}{q_u} \simeq \left(\frac{\pi}{9}\right)\left(\frac{t}{c}\right)\left(\frac{c}{H}\right)^2 \simeq \frac{\pi A}{6H^2}, \text{ where } A\left(\simeq \tfrac{2}{3}ct\right) \text{ is the area of the profile.}$$

This is the accepted value.

For the asymmetric circular-arc aerofoil $y_0(\beta) = \frac{1}{2}t\sin^2\beta$, i.e., $C(\beta) = \frac{1}{2}t\sin^2\beta$, $T = 0$, we find from the approximate equation corresponding to (84)

$$q\left(\frac{\pi}{2}\right) \simeq U\left(1 + \frac{Ut}{a}\right) = U(1 + 2\Gamma), \text{ where } \Gamma \text{ is the camber.}$$

Similarly $q\left(-\frac{\pi}{2}\right) \simeq U(1 - 2\Gamma)$. These results agree to the first power of Γ with the exact theoretical results:—

$$q\left(\frac{\pi}{2}\right) = U(1 + \sin e), \quad q\left(-\frac{\pi}{2}\right) = U(1 - \sin e), \text{ where } \tan e = 2\Gamma.$$

22. *Numerical Solution of the Velocity Equations.*—Consider for example equation (80). Proceeding as in section 20 we obtain

$$\frac{e^{i\theta}}{q} = \frac{1}{U} + \frac{1}{\pi}\left\{[m(\phi_0)\log(w - \phi_0)]_b^a - \sum_{i=1}^{n}\delta m_i\,[\log(w - \phi_0)]_{mi}\right\}, \quad \ldots \quad (89)$$

where $m = (dy/d\phi)_0$. We notice further that closure of the profile requires that

$$m_{\phi=a} + m_{\phi=b} - \sum_{n=i}^{n}\delta m_i = 0, \quad \ldots \quad (90)$$

which is the corresponding equation to (28) for the polygon method. Starting from an assumed $y_0 = y_0(\phi_0)$, we find $\delta m = \delta m(\phi_0)$, and from (89), $q = q(\phi)$. From equation (3), *i.e.*,

$$s(\phi) = \int_0^{\phi} d\phi_0/q,$$

and $y_0 = y_0(s)$, which follows from the profile equation, we then obtain a new relationship $y_0 = y_0(\phi_0)$. The process is repeated a number of times until no further change occurs.

The other velocity equations can be treated similarly.

23. *The Effect of Circulation.*—Equation (39) gives the relation between the velocity vector (q',θ') for an angle of incidence α, and the velocity vector (q,θ) for zero incidence. It can be written

$$\frac{e^{i\theta'}}{q'} = \frac{\cosh\frac{1}{2}t}{\cosh(\frac{1}{2}t + i\alpha)}\,\frac{e^{i\theta}}{q},$$

and hence from (82) we have for an asymmetric aerofoil in an open stream at an angle of incidence α :—

$$\frac{e^{i\theta'}}{q'} = \frac{\cosh \frac{1}{2}t}{\cosh (\frac{1}{2}t + i\alpha)} \left\{ \frac{1}{U} - \frac{i}{8a\pi \sinh t} \int_{-\pi}^{\pi} \frac{y_0(\beta)\, d\beta}{\sinh^2 \{\frac{1}{2}(t - i\beta)\}} \right\}. \quad .. \quad .. \quad .. \quad (91)$$

Thus once the problem has been solved for zero incidence it is a simple matter to find the solution at a given angle of incidence. The incidence referred to here is of course the ' absolute incidence ' measured from the zero-lift angle. On the aerofoil surface (91) assumes the form

$$\frac{\cos \theta}{q} = \frac{\cos \frac{1}{2}\gamma}{\cos (\frac{1}{2}\gamma + d)} \left\{ \frac{1}{U} + \frac{1}{8a\pi \sin \gamma} \int_{-\pi}^{\pi} \frac{y_0\, d\beta}{\sin^2 \{\frac{1}{2}(\gamma - \beta)\}} \right\}. \quad .. \quad .. \quad .. \quad .. \quad (92)$$

24. *A Comparison with Equations given by Thom.*—The miscellaneous comments in this section refer to equations given by Thom[13]. Throughout this section U is taken to be unity.

(a) *A Solution to Laplace's Difference Equation.*—

$$H(\phi,\psi) = \sum_{n=1}^{\infty} \frac{\psi\{\Gamma(\psi + 2n - 1)\}^2 2^{4-4n-2\psi}}{(\psi + 2n - 2)\Gamma(n)\Gamma(n + \psi)\Gamma(n + \frac{1}{2}(\phi + \psi))\Gamma(n + \frac{1}{2}(\psi - \phi))},$$

is an equation which applies to a point loading of $y_0 = 1$, at the origin in the (ϕ,ψ)-plane on a square mesh of size 2, *i.e.*, H satisfies

$$H(\phi + 1,\psi + 1) + H(\phi + 1,\psi - 1) + H(\phi - 1,\psi + 1) + H(\phi - 1,\psi - 1) = 4H(\phi,\psi).$$

Thom's ' H ' function corresponds to the y of this paper, and so from equation (75) we can deduce the corresponding solution for Laplace's differential equation (in which the loading has been distributed from $\phi = -1$ to $\phi = 1$),

$$\bar{y}(\phi,\psi) = \frac{1}{\pi} \int_{-1}^{1} \frac{\psi\, d\phi_0}{(\phi - \phi_0)^2 + \psi^2} = \frac{1}{\pi} \left\{ \tan^{-1} \left(\frac{1 - \phi}{\psi} \right) + \tan^{-1} \left(\frac{1 + \phi}{\psi} \right) \right\},$$

a result which Thom obtained by letting the mesh size tend to zero.

(b) *An Approximate Equation for Channel Flow.*—For flow about a symmetrical aerofoil at zero incidence between straight and parallel channel walls Thom gives the approximation (written here in our notation)

$$d\bar{y}(\phi,\psi) = \frac{y_0}{\pi} \left(\frac{\psi}{\phi^2 + \psi^2} - \frac{\psi}{\phi^2 + (\frac{1}{2}H)^2} \right), \quad .. \quad .. \quad .. \quad .. \quad .. \quad .. \quad (93)$$

whereas the correct form, from the real part of equation (74) in which $y^* = \frac{1}{2}H$, is

$$d\bar{y}(\phi,\psi) = \frac{y_0}{H} \left(\frac{\sin (2\pi\psi/H)\, d\phi_0}{\cosh (2\pi\phi/H) - \cos (2\pi\psi/H)} \right).$$

Comparing these forms we find that Thom's equation, besides satisfying the boundary conditions, is reasonably accurate in the field close to the aerofoil. The greatest error is likely to occur midway between the boundaries.

Take for example $H = 2\pi$, then $\psi = \frac{1}{2}\pi$ is midway between the boundaries. If we define $f_1 = \frac{3}{8}\pi^2 \frac{1}{(\phi^2 + (\pi/2)^2)(\phi^2 + \pi^2)}$ (from Thom's equation on $\psi = \frac{1}{2}\pi$) and $f_2 = (\operatorname{sech} \phi)/2\pi$ (exact

form of $\psi = \frac{1}{2}\pi$), then the following table gives some idea of the error in Thom's form:—

ϕ	0	1	2	4	6
f_1	0·152	0·098	0·0413	0·0078	0·00021
f_2	0·159	0·103	0·0422	0·0058	0·00079

Miss K. Britten[1], who established the influence factor equations for a symmetrical aerofoil in straight-walled channel by use of a Green's function, has made a detailed comparison of Thom's approximation with the exact form.

(c) *Displacement of Equipotentials in a Channel at Infinity.*—Thom gives $\bar{x}(\infty,\psi) = -\frac{A}{2H}$ (where A is the profile area) which is a very close approximation for the displacement of the equipotentials at infinity. From (74)

$$\bar{z}(\infty,\psi) = \frac{1}{H}\int_{-\infty}^{\infty} y_0(\phi_0) \lim_{\phi \to 0} \coth \frac{\pi}{H}(\phi_0 - \phi - i\psi)\, d\phi_0,$$

$$\text{i.e., } \bar{x}(\infty) = \frac{1}{H}\int_{-\infty}^{\infty} y_0(\phi_0)\, d\phi_0. \qquad \ldots\ \ldots\ \ldots\ \ldots\ \ldots\ \ldots\ \ldots\ \ldots \quad (94)$$

If the mean velocity over the aerofoil can be written $\bar{q} = (1 + \bar{\delta})$, then a close approximation to (94) is

$$\bar{x}(\infty) = -(1 + \bar{\delta})\frac{A}{2H}.$$

which verifies Thom's result.

(d) *Solution to Poisson's Difference Equation at Infinity in a Bounded Field.*—In our notation Thom's solution can be written

$$L(\infty,\psi) = -\frac{1}{H}\sum_j \phi_j x_j,$$

where $L(\infty,\psi)$ is the contribution at infinity obtained by ' relaxing ' the residuals x_j at (ϕ_j,ψ_j). The field is bounded by straight and parallel lines of symmetry distance H apart. The equation can be established as follows:—

Suppose that in the derivation of equation (20) we had had logarithmic singularities not only on the boundary but also in the field, such that for $j = 1,2, \ldots n$, $(n < \infty)$

$$\underset{w \to w_j}{f(w)} \to -\frac{\tau_j}{\pi}\log \sinh \frac{\pi}{H}(w_j - w), \quad (\tau_j \text{ independent of arg } (w_j - w)),$$

then the contour must be modified to exclude these singularities. Doing this we find that the term $-\frac{1}{\pi}\sum_{j=1}\tau_j \log \sinh \frac{\pi}{H}(w_j - w)$ must be added to the right-hand side of (22). Thus for small values of $\frac{\pi}{H}|w_j - w_j|$, *i.e.*, in the neighbourhood of w_j,

$$L(w) \doteq -\frac{1}{\pi}\tau_j \log \left|\sinh \frac{\pi}{H}(w_j - w)\right|$$

$$\doteq -\frac{1}{\pi}\tau_j \log \left|\frac{\pi}{H}\right|(w_j - w) = -\frac{1}{\pi}\tau_j \log\left(\frac{\pi}{H}r\right), \qquad \ldots\ \ldots\ \ldots\ \ldots \quad (95)$$

where $re^{i\theta} = w - w_j$.

Now for Poisson's equation $\nabla^2 L = k(\phi,\psi)$, we define the relaxation residual on a square mesh at w_j by

$$R_j = \sum_{s=1}^{4} L_s - 4L_j - a^2 k_j,$$

where L_s, $s = 1,2,3,4,j$ are the values of L at the points of the mesh labelled in Fig. 9, and k_j is the mean value of $k(\phi,\psi)$ over the square of side a centred at w_j. If initially $L = 0$ throughout the field, $R_j = -a^2 k_j \equiv X_j$, say, and 'relaxation' is the systematic process of modifying the L field to reduce the residuals R_j to zero (or near zero). We can relate the τ to the initial residuals X_j thus:—

$$X_j = a^2 k_j = \iint k\, dS = \iint \nabla^2 L\, dS = \oint \frac{\partial L}{\partial n}\, ds,$$

where the integrals apply to the square about w_j and ds is an element of distance along the square contour. Distorting this contour into a circle (the only singularities are at the mesh points), we have, using (95)

$$X_j = \int_0^{2\pi} \frac{\partial L}{\partial r} r\, d\theta = -\frac{\tau_j}{\pi} \int_0^{2\pi} d\theta = -2\tau_j.$$

Thus the additional term due to the singularities can be written

$$f(w) = \frac{1}{2\pi} \sum_{j=1}^{n} X_j \log \sinh \frac{\pi}{H} (w_j - w).$$

For large values of ϕ, $f(w) = \frac{1}{2}\pi \sum_j X_j \{\log (\frac{1}{2}i) + \frac{\pi}{H} (\phi - \phi_j)\}$.

If $f(w)$ is to remain finite at infinity ΣX_j must be zero, when

$$L(\infty) = -\frac{1}{2H} \sum_j X_j \phi_j. \qquad \text{(96)}$$

Thom's equation was deduced for the special case of antisymmetry in X_j about $\phi = 0$. In this special case (96) assumes the form

$$L(\infty) = -\frac{1}{H} \Sigma X_j \phi_j,$$

since only half of the residuals occur in the summation. Thus Thom's equation is verified mathematically.

25. *Example: A Symmetrical Aerofoil.*—The example is the one already used to illustrate the polygon method in section 9. Only surface values for the velocity for the unbounded stream have been calculated by the influence factor method and since the iteration described in section 22 is similar to that of section 9, for present purposes the exact relationship $y_0 = y_0(\phi_0)$ was adopted immediately from the theoretical solution. Thus the correct value of q should have been obtained in the first and only application of equation (89).

We shall describe the tables setting out the calculations to the problem.

Table 8: Calculation of δm_i

Columns 2 and 3 set out the true values of x_0 and y_0 as functions of ϕ.

Column 4 is $m_i = (y_{i+1} - y_i)/(\phi_{i+1} - \phi_i)$.

Column 5 is $\delta m_i = m_{i+1} - m_i$, except for the values opposite $\phi = 0$, and $\phi = 10$. These values are simply $m_{\phi=0}$ and $m_{\phi=10}$ (*cf.* equation (89)).

Column 6 is the value of $\cos\theta$ determined from columns 2 and 3.

Table 9: Calculation of $(\cos\theta)/q$

To save space this table is set out in the form of a matrix equation:—$[A_{ij}][B_j] = [C_i]$. With the exception mentioned below, the elements of the first matrix are defined by $A_{ij} = 10^3 (\log \phi_i - \phi_0)_M$. For convenience the logarithms in the table are to base 10. The values of ϕ_i and ϕ_j are shown bordering the matrix. The exceptional elements of $[A]$ are those in the first and last columns. Mean values of the logarithms are not taken for these elements (*cf.* equation(89)). The elements of B_j are δm_j, except $B_1 (= m_{\phi=0})$ and $B_{13} (= m_{\phi=10})$. Values of the function

$$[A_{ij}][B_j] \times \frac{\log 10}{\pi} = 10^3 \left(\frac{\cos\theta}{q} - 1\right)_i$$

are shown in the column matrix $[C_i]$. Using the values of $\cos\theta$ given in Table 8, q can be deduced immediately.

Table 10: Comparison of Velocities

This table sets out the surface velocities obtained from (a) exact theory, (b) the polygon method, and (c) the influence factor method. The results indicate that the polygon method is more accurate in the neighbourhood of the nose for a given size of interval than the influence factor method.

PART 4

Compressible Flow

26. *Introduction.*—The following additional notation will be used in this part:—

(ϕ,ψ) the compressible-flow plane for zero circulation (such that the aerofoil is a slit along $\psi = 0$)

i as a suffix to denote incompressible quantities

M_0 undisturbed stream Mach number; M, the Mach number

ρ_0 stagnation point density; ρ the density

a_0 stagnation point sound velocity

The theory will be based on the equations[7]

$$\frac{\partial\theta}{\partial n} + (1 - M^2)\frac{1}{q}\frac{\partial q}{\partial s} = 0, \qquad \frac{\partial\theta}{\partial s} - \frac{1}{q}\frac{\partial q}{\partial n} = 0,$$

i.e.,
$$\frac{\partial\theta}{\partial n} - (1 - M^2)\frac{\partial L}{\partial s} = 0, \qquad \frac{\partial\theta}{\partial s} + \frac{\partial L}{\partial n} = 0, \qquad \ldots\ \ldots\ \ldots\ \ldots\ \ldots \quad (97)$$

in which s and n are distances measured along and normal to a streamline. The boundary conditions are

(a) $L \equiv \log (q/U) = 0$, at infinity, and

(b) $\dfrac{\partial q}{\partial n} = -\dfrac{q}{R}$ (zero vorticity condition),

i.e., $$\frac{\partial L}{\partial n} = \frac{1}{R} = -\frac{\partial \theta}{\partial s}, \quad \ldots \quad (98)$$

on the aerofoil boundary.

Now since $$d\phi = q\,ds, \quad d\psi = \frac{\rho}{\rho_0} q\,dn, \quad \ldots \quad (99)$$

we have $$\frac{\partial L}{\partial n} = \frac{\rho}{\rho_0} q \frac{\partial L}{\partial \psi}, \qquad \text{i.e., from (98)} \quad \frac{\partial L}{\partial \psi} = \frac{\rho}{\rho_0} \frac{1}{Rq}. \quad \ldots \quad (100)$$

From (99) it follows that

$$dx = \frac{\cos\theta}{q} d\phi - \frac{\rho_0}{\rho} \frac{\sin\theta}{q} d\psi, \qquad dy = \frac{\sin\theta}{q} d\phi + \frac{\rho_0}{\rho} \frac{\cos\theta}{q} d\psi,$$

i.e., if $z = x + iy$, $$dz = \frac{e^{i\theta}}{q}\left(d\phi + i\frac{\rho_0}{\rho} d\psi\right),$$

and so the (x,y) and (ϕ,ψ)-planes are related by

$$z = \int \frac{e^{i\theta}}{q}\left(d\phi + i\frac{\rho_0}{\rho} d\psi\right). \quad \ldots \quad (101)$$

27. *An Approximate Solution in the Incompressible-Flow Plane.*—For incompressible flow $d\phi_i = q_i\,ds_i$, $d\psi_i = q_i\,dn_i$. We shall assume that $ds_i = ds$, $dn_i = dn$, *i.e.*, the angle between the incompressible-flow vector and the compressible-flow vector is negligible. (For a cylinder at $M = 0{\cdot}4$ this angle is less than 3 deg throughout the field.) With the additional approximation that $(1 - M^2)^{1/2} = (1 - M_0^2)^{1/2} \equiv \beta_0$, say, equations (97) become

$$\frac{\partial \theta}{\partial \psi_i} - \beta_0^2 \frac{\partial L}{\partial \phi_i} = 0, \qquad \frac{\partial \theta}{\partial \phi_i} + \frac{\partial L}{\partial \psi_i} = 0.$$

Cross-differentiating and writing $f = L + i\theta$ we find

$$\frac{\partial^2 f}{\partial \psi_i^2} + \beta_0^2 \frac{\partial^2 f}{\partial \phi_0^2} = 0. \quad \ldots \quad (102)$$

Applying the transformation $\phi_e = \lambda\phi_i$, $\psi_e = \lambda\beta_0\psi_i$, $f_e = \nu f$, $\ldots \quad (103)$
to (102) we obtain Laplace's equation

$$\frac{\partial^2 f_e}{\partial \psi_e^2} + \frac{\partial^2 f_e}{\partial \phi_e^2} = 0. \quad \ldots \quad (104)$$

λ and ν are constants in this affine transformation.

Thus if $f_e = F(\phi_e, \psi_e)$ is a solution of (104), then

$$f = \frac{1}{\nu} F(\lambda\phi_i, \lambda\beta_0\psi_i) \quad \ldots \quad \ldots \quad \ldots \quad \ldots \quad \ldots \quad \ldots \quad \ldots \quad \ldots \quad \ldots \quad (105)$$

is a solution of (102). In the next section we shall solve equation (104) by the polygon method, and then with the aid of (105) we shall have the solution to equation (102).

28. *Integral Equation Solutions.*—(a) *Symmetrical Aerofoil at Zero Incidence in an Open Stream.*—Equation (10) gives the solution of (104) in this case,

$$\text{i.e.,} \quad f_e(\phi_e, \psi_e) = \frac{1}{\pi} \int_{-\infty}^{\infty} \frac{\theta_e' \, d\phi_e'}{\phi_e' - \phi_e - i\psi_e}.$$

θ_e' is the boundary value of θ_e, and is a function of ϕ_e'. Hence from (105) we find

$$f(\phi_i, \psi_i) = \frac{1}{\nu\pi} \int_{-\infty}^{\infty} \frac{\theta_e' \, d(\lambda\phi^{1\prime})}{\lambda\phi_i' - \lambda\phi_i - i\lambda\beta_0\psi_i}. \quad \ldots \quad \ldots \quad \ldots \quad \ldots \quad \ldots \quad \ldots \quad (106)$$

It still remains to transform θ_e'. There are two ways of doing this: either θ_e' transforms in the same way as the solution θ_e, *i.e.*, from (103)

$$\theta_e' = \nu\theta', \quad \ldots \quad \ldots \quad \ldots \quad \ldots \quad \ldots \quad \ldots \quad \ldots \quad \ldots \quad \ldots \quad \ldots \quad (107)$$

or θ_e' transforms as a consequence of the application of (103) to its conjugate function L_e', *i.e.*,

$$\theta_e' = \int \frac{\partial\theta_e'}{\partial\phi_e} d\phi_e = -\int \frac{\partial L_e'}{\partial\psi_e} d\phi_e = -\int \frac{\partial(\nu L')}{\partial(\lambda\beta_0\psi_i)} d(\lambda\phi_i) = -\frac{\nu}{\beta_0}\int \frac{\partial L'}{\partial\psi_i} d\phi_i.$$

Now from (98) it follows that on the aerofoil surface

$$\frac{\partial L'}{\partial\psi_i} = \frac{\partial L'}{\partial n}\frac{\partial n}{\partial\psi_i} = \frac{1}{Rq},$$

a result which is clearly true for both compressible and incompressible flow,

$$\text{i.e.,} \quad \frac{\partial L'}{\partial\psi_i} = \frac{\partial L_i'}{\partial\psi_i} = -\frac{\partial\theta_i'}{\partial\phi_i} = -\frac{\partial\theta'}{\partial\phi_i},$$

since on the aerofoil boundary $\theta_i' = \theta'$. Using this in the expression for θ_e' we find

$$\theta_e' = \frac{\nu}{\beta_0}\theta'. \quad \ldots \quad \ldots \quad \ldots \quad \ldots \quad \ldots \quad \ldots \quad \ldots \quad \ldots \quad \ldots \quad \ldots \quad (108)$$

If we are using equation (106) to calculate θ in the field then to be consistent with (103) we must use (107) to transform θ_e', whereas if we are calculating L we must use (108) to transform θ_e'. Combining these calculations we find that

$$L(\phi_i, \psi_i) + \frac{i}{\beta_0}\theta(\phi_i, \mu_i) = \frac{1}{\beta_0\pi}\int_{-\infty}^{\infty} \frac{\theta' \, d\phi_i'}{\phi_i' - \phi_i - i\beta_0\psi_i}. \quad \ldots \quad \ldots \quad \ldots \quad \ldots \quad \ldots \quad (109)$$

Full details of the solution of (109) in the case of $\beta_0 = 1$ for an arbitrary aerofoil have been given in section 4, and will not be repeated here for this slightly different form of the equation.

For incompressible flow

$$L_i(\phi_i, \beta_0\psi_i) + i\theta_i(\phi_i, \beta_0\psi_i) = \frac{1}{\pi}\int_{-\infty}^{\infty} \frac{\theta'\, d\phi_i'}{\phi_i' - \phi_i - i\beta_0\psi_i},$$

and so from (109) $L(\phi_i, \psi_i) = \frac{1}{\beta_0} L_i(\phi_i, \beta_0\psi_i),$

i.e., $$\frac{q}{U}(\phi_i, \psi_i) = \left(\frac{q_i(\phi_i, \beta_0\psi_i)}{U}\right)^{1/\beta_0}, \quad \ldots\ldots\ldots\ldots\ldots\ldots \quad (110)$$

and $$\theta(\phi_i, \psi_i) = \theta_i(\phi_i, \beta_0\psi_i). \quad \ldots\ldots\ldots\ldots\ldots\ldots \quad (111)$$

On the aerofoil surface $\frac{q}{U} = \left(\frac{q_i}{U}\right)^{1/\beta_0}$. $\ldots\ldots\ldots\ldots\ldots\ldots$ (112)

It is interesting to compare (112) with the Glauert-Prandtl law for the pressure coefficients,

i.e., $C_p = (C_p)_i/\beta_0$. $\ldots\ldots\ldots\ldots\ldots\ldots\ldots\ldots$ (113)

Now to the same order of accuracy $C_p = -2(q - U)/U$, and $(C_p)_i = -2(q_i - U)/U$, and so (113) can be written $q = U + \frac{(q_i - U)}{\beta_0}$. Equation (112) can be expanded:—

$$q = U + \frac{q_i - U}{\beta_0} + \frac{(q_i - U)^2}{2!}\frac{(1 - \beta_0)}{\beta_0^2} + \ldots,$$

to which (113) can be regarded as a first approximation. The Glauert-Prandtl law underestimates the effect of compressibility. This is also true of equation (112) but there is some improvement as can be seen from Fig. 10, in which the equations are compared for $M_0 = 0{\cdot}7$.

(b) *Symmetrical Aerofoil at Zero Incidence in a Channel.*—If h_e is the channel width in the (ϕ_e,ψ_e)–plane, then, from equation (8), a solution for (104) in the case of a straight-walled channel is

$$f_e(\phi_e, \psi_e) = \frac{1}{h_e}\int_{-\infty}^{\infty} \theta_e' \coth\frac{\pi}{h_e}(\phi_e' - \phi_e - i\psi_e)\, d\phi_e',$$

i.e., from (103), (107) and (108)

$$L(\phi_i, \psi_i) + \frac{i}{\beta_0}\theta(\phi_i, \psi_i) = \frac{\lambda}{\beta_0 h_e}\int_{-\infty}^{\infty} \theta' \coth\frac{\lambda\pi}{h_e}(\phi_i' - \phi_i - i\beta_0\psi_i)\, d\phi_i'.$$

Now h_e is a fixed distance measured in units of ψ_i, and so from (103) transforms into $\lambda\beta_0 h$. Further if H is the channel width in the (x, y)-plane, by considering the conditions at infinity we find that $h = UH$. Using these results we have finally

$$L(\phi_i, \psi_i) + \frac{i}{\beta_0}\theta(\phi_0,\psi_0) = \frac{1}{\beta_0^2 HU}\int_{-\infty}^{\infty} \theta' \coth\frac{\pi}{HU\beta_0}(\phi_i' - \phi_i - i\beta_0\psi_i)\, d\phi_i'. \quad \ldots\ldots \quad (114)$$

Now $$f_i(\phi_i, \beta_0\psi_i)_{H\beta_0} = \frac{1}{\beta_0 HU}\int_{-\infty}^{\infty} \theta' \coth\frac{\pi}{HU\beta_0}(\phi_i' - \phi_i - i\beta_0\psi_i)\, d\phi_i',$$

where $f_i(\phi_i, \beta_0\psi_i)_{H\beta_0}$ denotes the incompressible value of f at $(\phi_i, \beta_0\psi_i)$ in a channel of width $H\beta_0$ in the (x,y)-plane.

Thus $$L(\phi_i, \psi_0)_H = \frac{1}{\beta_0} L_i(\phi_0, \beta_0\psi_i)_{H\beta_0},$$

i.e., $$\frac{q}{U}(\phi_i\psi_i)_H = \left\{\frac{q_0}{U}(\phi_i\beta_0\psi_i)_{H\beta_0}\right\}^{1/\beta_0}, \quad \ldots\ldots\ldots\ldots\ldots\ldots\ldots\ldots \quad (115)$$

and $$\theta(\phi_i, \psi_i)_H = \theta_i(\phi_i, \beta_0\psi_i)_{H\beta_0}. \quad \ldots\ldots\ldots\ldots\ldots\ldots\ldots\ldots \quad (116)$$

Channel Blockage:—

On $\psi_i = 0$, (109) and (114) become

$$L = \frac{1}{\beta_0\pi}\int_{-\infty}^{\infty} \frac{\theta'\, d\phi_i'}{\phi_i' - \phi_i}, \quad \text{and} \quad L_c = \frac{1}{U_c\beta_0{}^2H}\int_{-\infty}^{\infty} \theta_c' \coth\frac{\pi}{H\beta_0U_c}(\phi_i' - \phi_i)\, d\phi_i',$$

respectively, where 'c' denotes channel values. Little error is introduced by assuming that $\theta(\phi_i') = \theta_c(\phi_i')$. Now the channel blockage ε is defined by the simultaneous equations

$$U_c(1 + \varepsilon) = U, \; q_c(\phi_i') = q(\phi_i'),$$

i.e., $\log(1 + \varepsilon) = L_c - L$, and so

$$\log(1 + \varepsilon) = \frac{1}{U_c\beta_0{}^2H}\int_{-\infty}^{\infty} \theta'\left[\frac{1}{\frac{\pi}{U_c\beta_0H}(\phi_i' - \phi_i)} - \coth\frac{\pi}{U_c\beta_0H}(\phi_i' - \phi_i)\right] d\phi_i'$$

$$\simeq \frac{-\pi}{3\beta_0{}^3H^2U_c{}^2}\int_{-\infty}^{\infty} (\phi_i' - \phi_i)\theta'\, d\phi_i'. \quad \ldots\ldots\ldots\ldots\ldots \quad (117)$$

On the aerofoil surface we can write approximately $\phi_i = \bar{q}_i x$, where $\bar{q}_i$ is the mean incompressible velocity over the surface in the open stream. If in addition we write

$$\bar{q}_i = U(1 + \delta) = U_c(1 + \varepsilon)(1 + \delta) \simeq U_c(1 + \varepsilon + \delta), \text{ and } \theta' \simeq dy'/dx,$$

then equation (117) assumes the form

$$\log(1 + \varepsilon) = -\frac{\pi}{3\beta_0{}^3H^2}(1 + 2\delta + 2\varepsilon)\int_{-\infty}^{\infty} (x' - x)\, dy',$$

i.e., $$\varepsilon \simeq \frac{\pi A}{6\beta_0{}^3H^2}(1 + 2\delta), \quad \ldots\ldots\ldots\ldots\ldots\ldots\ldots\ldots \quad (118)$$

where A is the cross-sectional area of the aerofoil. This equation, without the δ term, is the result obtained by the linear pertubation theory[4]. Incompressible and compressible blockage has been dealt with at length in another paper[20].

(c) *Asymmetric Aerofoil at Zero Incidence in a Free Stream.*—In this case a solution of (104) is (*see* equation (45)),

$$f_e(t_e) = -\frac{i}{2\pi}\int_{-\pi}^{\pi} \theta_e' \coth\tfrac{1}{2}(t_e - ib_e)\, db_e, \quad \ldots\ldots\ldots\ldots\ldots\ldots \quad (119)$$

where $\phi_e + i\psi_e = -2a_e\cosh t_e$, $t_e = \eta_e + i\gamma_e$, $\phi_e' = -2a_e\cos b_e$, and $4a_e$ is the length of the slit representing the aerofoil in the (ϕ_e,ψ_e)-plane. We shall write

$$\phi_i + i\beta_0\psi_i = -2a\cosh t, \; t = \eta + i\gamma, \text{ and } \phi_i' = -2a\cos b. \quad \ldots\ldots\ldots \quad (120)$$

λ disappears since a_e is measured in units of ϕ_e, and so transforms to λa. Using (103), (107) and (108) in equation (119) we have

$$L(t) + \frac{i}{\beta_0}\theta(t) = -\frac{i}{2\pi\beta_0}\int_{-\pi}^{\pi} \theta' \coth \tfrac{1}{2}(t - ib)\, db, \quad \ldots \quad \ldots \quad \ldots \quad \ldots \quad \ldots \quad (121)$$

an equation of which (109) is a special case. Equations (110) and (111) are also true in this general case.

(d) *The Effect of Incidence in a Free Stream.*—If α_e is the angle of incidence in the (ϕ_e, ψ_e)-plane, then from equation (39),

$$q_e'' \, e^{-i\theta_e''} = (\cos \alpha_e + i \sin \alpha_e \tanh \tfrac{1}{2}t_e)\, q_e \, e^{-i\theta_e},$$

where (q_e'', θ_e'') is the velocity vector at incidence α_e, and (q_e, θ_e) is the velocity vector at zero incidence. Dividing by the velocity at infinity and taking logarithms we have

$$f_e''(t_e) = f_e(t_e) - \log(\cos \alpha_e + i \sin \alpha_e \tanh \tfrac{1}{2}t_e). \quad \ldots \quad \ldots \quad \ldots \quad \ldots \quad \ldots \quad (122)$$

At $\eta = \infty$, *i.e.*, at infinity in the (ϕ_e, ψ_e)-plane, $f_e''(\infty) = f_e(\infty) - i\alpha_e$, which shows that the flow at infinity is at an angle α_e to its original direction. Now α_e is a boundary condition and so must transform either by equation (107) (when it is required to calculate θ) or by equation (108) (when it is required to calculate $\log(U/q)$), *i.e.*,

either $\quad vf''(\infty) = vf(\infty) - iv\alpha$, or $vf''(\infty) = vf(\infty) - i\alpha\dfrac{v}{\beta_0}$.

Comparing these equations with (122) we deduce that

$$L''(t) = L(t) - \log\left|\cos\frac{\alpha}{\beta_0} + i \sin\frac{\alpha}{\beta_0}\tanh\tfrac{1}{2}t\right|,$$

and $$\theta''(t) = \theta(t) - \arg\{\log(\cos\alpha + i \sin\alpha \tanh \tfrac{1}{2}t)\}. \quad \ldots \quad \ldots \quad \ldots \quad \ldots \quad \ldots \quad (123)$$

Now $L_i''(\phi_i, \beta_0\psi_i)_{\alpha/\beta_0} = L_i(\phi_i, \beta_0\psi_i) - \log|\cos\alpha/\beta_0 + i \sin\alpha/\beta_0 \tanh\tfrac{1}{2}t|$, where $L_i''(\phi_i, \beta_0\psi_i)_{\alpha/\beta_0}$ denotes the incompressible L'' at the point $(\phi_i, \beta_0\psi_i)$ at an angle of incidence α/β_0.

Therefore $L''(\phi_i', \psi_i)_\alpha = L(\phi_i, \psi_i) + L_i''(\phi_i, \beta_0\psi_i)_{\alpha/\beta_0} - L_i(\phi_i, \beta_0\psi_i)$,

$$\text{i.e.,} \quad \frac{q''}{q}(\phi_i, \psi_i)_\alpha = \frac{q_i''}{q_i}(\phi_i, \beta_0\psi_i)_{\alpha/\beta_0}. \quad \ldots \quad \ldots \quad \ldots \quad \ldots \quad \ldots \quad \ldots \quad (124)$$

Similarly $\quad (\theta'' - \theta)(\phi_i, \psi_i)_\alpha = (\theta_i'' - \theta_i)(\phi_i, \beta_0\psi_i)_\alpha$. $\quad \ldots \quad \ldots \quad \ldots \quad \ldots \quad \ldots \quad (125)$

From equation (124) we deduce that, since circulation and lift are proportional to incidence, compressibility increases both in the ratio $1/\beta_0$.

29. *A More Accurate Treatment in the Compressible-Flow Plane.*—Returning to equations (97), we see that with the aid of (99) they assume the form

$$\frac{\partial\theta}{\partial\psi} - \frac{\rho_0}{\rho}(1 - M^2)\frac{\partial L}{\partial\phi} = 0, \quad \frac{\partial\theta}{\partial\phi} + \frac{\rho}{\rho_0}\frac{\partial L}{\partial\psi} = 0. \quad \ldots \quad \ldots \quad \ldots \quad \ldots \quad \ldots \quad (126)$$

We shall write $$dr = (1 - M^2)^{1/2}\, dL, \quad \ldots \quad (127)$$

and $$m = \frac{\rho_0}{\rho}(1 - M^2)^{1/2}, \quad \ldots \quad (128)$$

when (126) becomes $$\frac{\partial \theta}{\partial \psi} - m\frac{\partial r}{\partial \phi} = 0, \quad \frac{\partial \theta}{\partial \phi} + \frac{1}{m}\frac{\partial r}{\partial \psi} = 0, \quad \ldots \quad (129)$$

Now from (128), $m = \{1 + \frac{1}{2}(\gamma - 1)M^2\}^{1/(\gamma-1)}(1 - M^2)^{1/2}$, where γ is the ratio of the specific heats.

Therefore $$m = 1 - \frac{\partial \gamma + 1}{8} M^4 + \frac{(\gamma + 1)(\gamma - 3)}{24} M_0^6 + \ldots,$$

and so it is sufficiently accurate to write for subsonic flow

$$m \doteq m_0 \equiv \{1 + \tfrac{1}{2}(\gamma - 1)M_0^2\}^{1/(\gamma-1)}(1 - M_0^2)^{1/2}, \quad \ldots \quad (130)$$

except near the sonic speed. With this approximation in (129) we can deduce that

$$\frac{\partial^2 g}{\partial \psi^2} + m_0^2 \frac{\partial^2 g}{\partial \phi^2} = 0, \quad \ldots \quad (131)$$

where we have written $g = r + i\theta$. This equation has the solution

$$g = \frac{1}{\nu} G(\lambda\phi, \lambda m_0 \psi), \quad \ldots \quad (132)$$

where $G(\phi_e, \psi_e)$ is a solution of $\frac{\partial^2 g_e}{\partial \psi_e^2} + \frac{\partial^2 g_e}{\partial \phi_e^2} = 0$, in which

$$\phi_e = \lambda\phi, \quad \psi_e = \lambda m_0 \psi, \quad g_e = \nu g. \quad \ldots \quad (133)$$

The transformation for θ_e' is easily found. As before it either transforms directly, *i.e.*,

$$\theta_e' = \nu\theta, \quad \ldots \quad (134)$$

or it transforms through its conjugate function r_e',

i.e., $\theta_e' = \int \frac{\partial \theta_e'}{\partial \phi_e} d\phi_e = -\int \frac{\partial r_e}{\partial \psi_e} d\phi_e = \frac{\nu}{m_0}\int \frac{\partial r}{\partial \psi} d\phi$, from (133). With the aid of equation (127) equation (100) can be written

$$\frac{\partial r}{\partial \psi} = \frac{\partial L}{\partial \psi}\frac{\partial r}{\partial L} = \frac{\rho_0}{\rho}\frac{1}{Rq}(1 - M^2)^{1/2} = \frac{m}{Rq} \doteq \frac{m_0}{Rq}. \quad \ldots \quad (135)$$

Using this result in the equation for θ_e' we find

$$\theta_e' = -\int \frac{d\phi}{Rq} = -\int \frac{ds}{R} = \nu\theta,$$

which is conveniently the same as the direct transformation (134). Integrating (127) we have

$$r = \int (1 - M^2)^{1/2}\, dL. \quad \ldots \quad (136)$$

Now since $M^2 = \dfrac{(q/a_0)^2}{1 - \frac{1}{2}(\gamma - 1)(q/a_0)^2}$, $dL = -\dfrac{dq}{q}$, $\gamma \simeq 1{\cdot}4$,

and $$\beta^2 = 1 - M^2 = 1 - \frac{(q/a_0)^2}{1 - 0{\cdot}2(q/a_0)^2},$$

(136) can be written $r = \int \dfrac{\beta^2\, d\beta}{(1-\beta^2)(6-\beta^2)}$.

Therefore $$r = \frac{\sqrt{6}}{2} \log \left| \frac{1 - (\beta/\sqrt{6})}{1 - (\beta_0/\sqrt{6})} \times \frac{1 + (\beta_0/\sqrt{6})}{1 + (\beta/\sqrt{6})} \right| + \tfrac{1}{2} \log \left| \frac{1-\beta_0}{1-\beta} \frac{1+\beta}{1+\beta_0} \right| . \quad .. \quad .. \quad (137)$$

in which the constant of integration has been selected so that $r = 0$, when $L = 0$, *i.e.*, when $\beta = \beta_0$. Thus, since β is a known function of L we have from (137) a relationship

$$r = r(L). \quad .. \quad .. \quad .. \quad .. \quad .. \quad .. \quad .. \quad .. \quad .. \quad .. \quad (138)$$

Finally we note from (136) that at an infinite distance from the aerofoil,

$$r(\infty) = \int \beta_0\, dL = \beta_0 L(\infty) = 0. \quad .. \quad .. \quad .. \quad .. \quad .. \quad .. \quad .. \quad (139)$$

30. *The Corresponding Integral Equation Solutions.*—These can be deduced immediately from the incompressible equations (10), (8), (45) and (122) with the aid of (133) and (134).

(a) *A Symmetrical Aerofoil at Zero Incidence.*—In this case we find from equation (10)

$$g(\phi, \psi) = \frac{1}{\pi} \int_{-\infty}^{\infty} \frac{\theta'\, d\phi'}{\phi' - \phi - i m_0 \psi}. \quad .. \quad .. \quad .. \quad .. \quad .. \quad .. \quad .. \quad (140)$$

(b) *Symmetrical Aerofoil at Zero Incidence in a Straight-Walled Channel.*—Equation (8) becomes

$$g(\phi, \psi) = \frac{1}{\beta_0 U H} \int_{-\infty}^{\infty} \theta' \coth \frac{\pi}{\beta_0 U H} (\phi' - \phi - i m_0 \psi)\, d\phi' \quad .. \quad .. \quad .. \quad .. \quad (141)$$

in which we have used $h = (\beta_0 U H)/m_0$, which comes from (99) applied to the channel at infinity.

(c) *Asymmetric Aerofoil at Zero Incidence in a Free Stream.* Equation (45) becomes

$$g(t) = -\frac{i}{2\pi} \int_{-\pi}^{\pi} \theta' \coth \tfrac{1}{2}(t - ib)\, db, \quad .. \quad .. \quad .. \quad .. \quad .. \quad .. \quad .. \quad (142)$$

where $$\phi + i m_0 \psi = -2a \cosh t, \quad \phi' = -2a \cos b. \quad .. \quad .. \quad .. \quad .. \quad .. \quad (143)$$

(d) *The Effect of Circulation in a Free Stream.*—Equation (122) assumes the form

$$g''(t) = g(t) - \log (\cos \alpha + i \sin \alpha \tanh \tfrac{1}{2} t), \quad .. \quad .. \quad .. \quad .. \quad .. \quad .. \quad (144)$$

where t is defined as in (143).

When these integral equations have been solved, equation (101), with the aid of (138), enables the relationship between the (ϕ,ψ) and (x,y)-planes to be established, and then the solution is complete.

If we assume that the relation between the (ϕ_i, ψ_i) and (ϕ,ψ)-planes is approximately the same as that between them at infinity, then using (99) we can write

$$\phi = \phi_i, \quad \psi = \beta_0\psi_i/m_0. \quad .. \quad .. \quad .. \quad .. \quad .. \quad .. \quad .. \quad .. \quad .. \quad (145)$$

With this approximation we find that equation (140) becomes

$$g(\phi_i, \psi_i) = \frac{1}{\pi}\int_{-\infty}^{\infty} \frac{\theta'\, d\phi_i'}{\phi_i' - \phi_i - i\beta_0\psi_i},$$

i.e., $$g(\phi_i, \psi_i) = f_i(\phi_i, \beta_0\psi_i), \quad .. \quad .. \quad .. \quad .. \quad .. \quad .. \quad .. \quad .. \quad .. \quad (146)$$

the real and imaginary parts of which yield

$$\theta(\phi_i, \psi_i) = \theta_i(\phi_i, \beta_0\psi_i), \text{ (cf. (111))},$$

and $$r(\phi_i, \psi_i) = L_i(\phi_i, \beta_0\psi_i). \quad .. \quad .. \quad .. \quad .. \quad .. \quad .. \quad .. \quad .. \quad .. \quad (147)$$

These equations also apply to an asymmetric aerofoil in a free stream.

Similarly for channel flow we find

$$g(\phi_i, \psi_i)_H = f_i(\phi_i, \beta_0\psi_i)_{H\beta_0}, \quad .. \quad .. \quad .. \quad .. \quad .. \quad .. \quad .. \quad .. \quad (148)$$

while the effect of incidence is given by

$$(g'' - g)(\phi_i, \psi_i)_a = (f'' - f)(\phi_i, \beta_0\psi_i)_a. \quad .. \quad .. \quad .. \quad .. \quad .. \quad .. \quad .. \quad (149)$$

On the aerofoil surface (147) yields $r = L_i$, i.e., $q_i = U\mathrm{e}^{-r}$. .. .. (150)

This approximate solution for compressible flow was first obtained by von Kármán[6], whose method is discussed in the next section. Equations (146) to (148) should be compared with the corresponding equations of section 28. It will be found that the equations for θ are the same in each method, but that L calculated *by the first method* is related to the r of the second method by

$$L = r/\beta_0. \quad .. \quad .. \quad .. \quad .. \quad .. \quad .. \quad .. \quad .. \quad .. \quad .. \quad (151)$$

Of course the correct relation between r and L for the second method is given by equation (138), an equation which leads to an appreciably larger value of L than does (151). This is illustrated in Fig. 10, in which equations (112) and (150) are compared at $M_0 = 0{\cdot}7$.

Integral equations of the same form as those given above have received detailed treatment in Parts 1 and 2; for example on the aerofoil surface (140) becomes

$$r(\phi) = \frac{1}{\pi}\int_{-\infty}^{\infty} \frac{\theta'\, d\phi}{\phi' - \phi},$$

which, by a similar argument to that of section 4, can be written

$$r(\phi) = \frac{1}{\pi}\int_{-\infty}^{\infty} \frac{1}{Rq'} \log(\phi' - \phi)\, d\phi' - \frac{1}{\pi}\sum_j \tau_j \log(\phi_j - \phi), \quad .. \quad .. \quad .. \quad .. \quad (152)$$

and the calculation proceeds just as in section 4. However one new point does arise in the calculation of the distance along the aerofoil surface,

$$s = \int_0^{\phi^*} \frac{d\phi}{q}, \qquad \ldots \ldots \ldots \ldots \ldots \ldots \ldots \ldots \ldots \ldots \quad (153)$$

measured from a stagnation point at which the discontinuity in θ is $-\tau$, say (*e.g.*, at a trailing-edge angle of 2τ). The integrand becomes infinite at the stagnation point. The problem has been solved for incompressible flow[16], the solution being $s = \phi_i^*/q_i^*(1 - \tau/\pi)$ where q_i^* is the velocity at ϕ_i^*, *see* equation (165). From (152) we see that sufficiently near a discontinuity in θ' of amount $-\tau$,

$$r(\phi) \doteq -\frac{\tau}{\pi} \log |\phi|,$$

where we have taken the origin at the discontinuity. The complexity of equation (138) renders further algebraic progress impossible, but if we accept the approximation (151), we can write

$$L(\phi) = -\frac{\tau}{\pi\beta_0} \log |\phi|, \text{ i.e., } \frac{q}{q^*} = \left(\frac{\phi}{\phi^*}\right)^k, \text{ where } k = \frac{\tau}{\pi\beta_0}.$$

Using this in (153) we find

$$s \doteq \frac{\phi^*}{q^*(1 - \tau/\pi\beta_0)}. \qquad \ldots \ldots \ldots \ldots \ldots \ldots \ldots \ldots \ldots \quad (154)$$

Of course this approximation is only used over the first mesh interval, which should be reasonably small, adjacent to a stagnation point (or sharp corner, if any).

31. *Comparison with von Kármán's Approximation.*—Briefly von Kármán's method is as follows. Equations (126) are transformed so that q and θ are the independent variables. This transformation to the hodograph-plane linearizes the equations. Then with the use of (127), (128) and the approximation (130) the equations

$$\frac{\partial^2\phi}{\partial r^2} + \frac{\partial^2\phi}{\partial\theta^2} = \frac{\partial^2\psi}{\partial r^2} + \frac{\partial^2\psi}{\partial\theta^2} = 0,$$

follow, but since these equations also hold for incompressible flow if r is replaced by L_i, it is concluded that $r = L_i$, and so $q_i = U\mathrm{e}^{-r}$ (cf. (150)). Then with the same degree of approximation as in (130) von Kármán deduces that

$$L_i = m_0\left(L + \frac{q^2 - U^2}{4a_0^2}\right),$$

i.e., $$\left(\frac{q_i}{U}\right)^{1/m_0} = \left(\frac{q}{U}\right)\mathrm{e}^{-(q^2-U^2)/4a_0^2}. \qquad \ldots \ldots \ldots \ldots \ldots \ldots \ldots \quad (155)$$

Von Kármán's theory was developed initially for the case of zero circulation, but Lin[9] later extended the theory to flows with circulation. The author's theory is quite general. Experimental evidence shows that (155) is reasonably accurate for slender bodies up to about $M_0 = 0{\cdot}6$, but that it underestimates q at the higher Mach numbers. Further since it is only

a velocity correction factor, it reproduces the compressible velocity peak directly above the incompressible velocity peak, whereas experimental evidence shows that the velocity peak travels towards the trailing edge, with increasing Mach number, slowly at first, but quite rapidly by the time sonic speed is achieved locally.

The author's method is similar to von Kármán's, except that the hodograph transformation is not used. In fact the calculation leading to (150) in the previous section may be considered an alternative approach to von Kármán's approximation. Equations (140) to (144) however should be more accurate, and do not depend upon previous knowledge of the incompressible flow.

Three approximations are made in the von Kármán method:—

(a) $m = m_0$, in the differential equation

(b) $m = m_0$, when calculating the relation between r and L,

(c) changes in the boundary profile due to the approximations are ignored.

Approximation (c) is not made in the author's method. This is a big advantage over von Kármán's method as the flow round a *given* profile can be found directly. If increased accuracy is required in von Kármán's method it is necessary to calculate the distortion to the profile, and then to recalculate the problem starting with a profile so modified that the hodograph transformation distorts it into the desired shape. Of course it is clear that the application of an equation such as (140) to the problem will be a much lengthier process than the *simple* application of von Kármán's approximation, but it would certainly be simpler than the iterations required to apply his method accurately to the problem of the flow around a *given* profile.

Approximations (a) and (b), while apparently equivalent, do not necessarily result in the same magnitude of error in the final answer. Approximation (b) is unnecessary, and has not been made in this paper. This inconsistency can at least be justified empirically. Fig. 10 shows the $(e^{-r}, q/U)$ and $(q_i/U, q/U)$ curves at $M_0 = 0{\cdot}7$ given by (138) and (155). A close examination of (152) reveals that Ue^{-r} calculated from it, will be a little smaller than q_i, but from the figure it can be seen that a given value of Ue^{-r} corresponds to a much larger value of q than does the same value of q_i by von Kármán's method. The overall effect is that the author's method results in larger values of q than does von Kármán's method, and this is certainly supported by the experimental evidence.

32. *Modification to the Method.*—The method of sections 29 and 30 requires that M must be less than unity (*e.g.*, (127)), and this has the disadvantage of not permitting even an approximate solution to be found if a small supersonic patch makes an appearance in the field. Further, from equations (129) we can deduce the exact equation

$$\frac{\partial}{\partial\phi}\left(m\frac{\partial r}{\partial\phi}\right) + \frac{\partial}{\partial\psi}\left(\frac{1}{m}\frac{\partial r}{\partial\psi}\right) = 0, \qquad \ldots\ldots\ldots\ldots\ldots\ldots\ldots \quad (156)$$

which suggests the possibility of an exact relaxation solution for r. This approach would have the advantage that L_i is a close approximation to r, and hence could be used as a starting point for the relaxation. It is clearly desirable to use the best available approximate theoretical solution as a starting point when solving non-linear equations by relaxation. The method suggested amounts to doing this. However, working in the (ϕ,ψ)-plane has the disadvantage that the relation between the (x,y) and (ϕ,ψ)-planes is a function of M_0. If boundary values on the aerofoil are the only objects of the calculation, this disadvantage is negligible. The application of relaxation to the method of this paper, such that there are no difficulties in supersonic patches, requires the modifications given below.

If in (126) we write $dv = \frac{\rho}{\rho_0}\, dL$, the equations become

$$\frac{\partial \theta}{\partial \phi} + \frac{\partial v}{\partial \psi} = \frac{\partial \theta}{\partial \psi} - m^2 \frac{\partial v}{\partial \phi} = 0,$$

and so $$\frac{\partial^2 v}{\partial \psi^2} + \frac{\partial}{\partial \phi}\left(m^2 \frac{\partial v}{\partial \phi}\right) = 0. \quad .. \quad .. \quad .. \quad .. \quad .. \quad .. \quad .. \quad .. \quad (157)$$

Now $$dM^2 = -2M^2\left(\frac{a_0}{a}\right)^2 dL = -2M^2(1 + 0{\cdot}2M^2)\, dL \ (\gamma = 1{\cdot}4), \quad .. \quad .. \quad .. \quad (158)$$

a result obtained with the aid of the equations following (136); and therefore

$$v = \int \frac{\rho}{\rho_0} dL = \int \frac{dL}{(1 + 0{\cdot}2M^2)^{2{\cdot}5}} = -\tfrac{1}{2} \int \frac{dM^2}{M^2(1 + 0{\cdot}2M^2)^{3{\cdot}5}},$$

in which $v = 0$, when $L = 0$, *i.e.*, when $M = M_0$. The solution to this equation is

$$v = \tfrac{1}{2} \log\left(\frac{p + 1}{p - 1}\right) - \frac{1}{5p^5} - \frac{1}{3p^3} - \frac{1}{p}, \text{ where } p = (1 + 0{\cdot}2M^2)^{1/2}, \text{ and so}$$

$$v = v(L) \quad .. \quad .. \quad .. \quad .. \quad .. \quad .. \quad .. \quad .. \quad .. \quad .. \quad .. \quad (159)$$

follows.

Similarly we can make the substitution $du = \frac{\rho_0}{\rho}(1 - M^2)\, dL$ in (126) and find

$$\frac{\partial^2 u}{\partial \phi^2} + \frac{\partial}{\partial \psi}\left(\frac{1}{m^2} \frac{\partial u}{\partial \psi}\right) = 0, \quad .. \quad .. \quad .. \quad .. \quad .. \quad .. \quad .. \quad .. \quad (160)$$

in which $u = \int \frac{\rho_0}{\rho}(1 - M^2)\, dL$. Making the same substitutions as for v we find that

$$u = \tfrac{1}{2} \log\left(\frac{p + 1}{p - 1}\right) + p^5 - \tfrac{1}{3}p^3 - p,$$

from which $$u = u(L), \quad .. \quad .. \quad .. \quad .. \quad .. \quad .. \quad .. \quad .. \quad .. \quad (161)$$

follows.

Now from the definitions of u, v and m we have

$$\tfrac{1}{2}\left(m\, dv + \frac{du}{m}\right) = (1 - M^2)^{1/2}\, dL = dr,$$

and so using the approximation (130) we have

$$r^* = \tfrac{1}{2}\left(m_0 v + \frac{u}{m_0}\right),$$

where the star is introduced to distinguish this modified function from the previous one. Then from (159) and (161) we can deduce a relation

$$r^* = r^*(L), \quad .. \quad .. \quad .. \quad .. \quad .. \quad .. \quad .. \quad .. \quad .. \quad .. \quad (162)$$

which is not of course the same as (138), having real values of r^* for $M_0>1$. $(e^{-r^*}, q/U)$ is plotted in Fig. 10, and can be compared there with $(e^{-r}, q/U)$. There is little difference except close to the sonic speed. $e^{-m_0 v}$ and e^{-u/m_0} are also plotted against q/U for comparison. The former curve, $(e^{-m_0 v}, q/U)$, is indistinguishable from von Kármán's law for $(q_i/U, q/U)$. Some use of this curve is made in the next section.

The modification then, is merely that we use r^* as defined above in place of r to ensure that we obtain real values in supersonic patches.

33. *An Exact Relaxation Solution.*—Equation (157), which is exact, may be solved by relaxation, and without difficulty in the supersonic patches (provided of course a continuous solution does exist[19]). It is clear from the previous section that a first approximation to v is L_i/m_0. L_i can be found by the methods of Parts 1 and 2, in the (ϕ_i, ψ_i)-plane, then using the approximation (145) we will have a reasonably accurate approximation to v in the (ϕ,ψ)-plane.

From (158) and the definition of v we find that $dm^2 = 2{\cdot}4M^4(1 + 0{\cdot}2M^2)^{7{\cdot}5}\,dv$, and so (157) can be expanded

$$\frac{\partial^2 v}{\partial \psi^2} + m^2 \frac{\partial^2 v}{\partial \phi^2} + 2{\cdot}4M^4(1 + 0{\cdot}2M^2)^{7{\cdot}5}\left(\frac{\partial v}{\partial \phi}\right)^2 = 0. \quad \ldots \quad (163)$$

Equation (160) is not suitable for a similar treatment since it follows from the definition of u that a given value of u corresponds to two values of L, one supersonic and the other subsonic. Details of the relaxation treatment of (157) will not be given since it is of the same form as an equation already treated by relaxation[17], and a similar treatment will hold.

From equation (100) we note that the boundary condition for v is

$$\frac{dv}{\partial \psi} = \frac{\partial L}{\partial \psi}\frac{\partial v}{\partial L} = \frac{\rho_0}{\rho}\frac{1}{Rq}\frac{\rho}{\rho_0} = \frac{1}{Rq}. \quad \ldots \quad (164)$$

When v has been found θ can be deduced by integrating the equations preceding (157), while q follows from (162) and $q/U = e^{-L}$. The relation between the (x,y) and (ϕ,ψ)-planes follows from (101), and the solution is complete.

The method outlined in this section would be much quicker than the relaxation method developed elsewhere[17, 18].

34. *An Example.*—The aerofoil selected as an example is one used by Emmons (1946) in a relaxation treatment of compressible flow. Fig. 11 shows the velocity distributions given by Emmons for this aerofoil at $M_0 = 0$, and $M_0 = 0{\cdot}7$. Emmons' solution for $M_0 = 0$ was checked by the polygon method. The results of this calculation are shown in the figure, and are almost identical with Emmons' results. Results from von Kármán's approximation and the approximation of section 32 are also shown in the figure. The latter approximation is certainly superior to von Kármán's, but it did not displace the velocity peak down the aerofoil as far as was expected. However further work is necessary on this example before definite conclusions can be drawn, since (a) Emmons' compressible solution needs checking by the exact relaxation treatment of section 33, and (b) a much smaller mesh interval than that used in the region of the nose is desirable. This point arises since (154) is not a good approximation, and so if the first interval (over which (154) is used) is too large, the whole velocity distribution will be displaced along the chord. It may well be that such an error has accentuated the discrepancy shown in Fig. 11.

General Conclusions.—The method developed in Parts 1 and 2 obtains with a minimum of computation accurate results for the flow of an incompressible fluid about a two-dimensional body of arbitrary shape. The body, if symmetrical, may be placed in a symmetrical channel

of arbitrary shape. While the examples have been given for a channel with straight walls, the extension to the more general case is quite simple. Integration will have to be performed along both boundaries, and along some suitable equipotential connecting them.

Relaxation becomes very tedious for the type of problem treated in this paper, *i.e.*, a problem that involves a field with a fixed value at infinity only, and with specified boundary gradients. (Fixed boundary values would reduce the work many times.) If results throughout the field are required, the method of this paper should be used to compute values of $\log(U/q)$ on the boundaries of the field, and on a coarse mesh throughout the field. The method is quick and accurate for the calculation of surface velocities, but the elliptic co-ordinates may render the calculation of field values a little tedious, and so from this stage it would be quicker to complete the solution on a fine mesh by relaxation, maintaining the values initially calculated constant.

The influence factor method given in Part 3 is also quick and relatively simple to apply, but the polygon method is more accurate for the direct calculation of velocities, and for the inverse problem of designing an aerofoil (not given in this paper). The influence factor method may be more convenient for the calculation of the actual flow pattern, although if both flow pattern *and* velocity field are required the polygon method followed by integration (equations (69)) would probably be the quickest. The author has not succeeded in extending the influence factor method to compressible flow, whereas, as shown in Part 4, the polygon method can be adapted to the calculation of compressible subsonic flow—a calculation which is a little more accurate than the well-known approximation of von Kármán. It also has the advantages that the calculations can be performed directly for an aerofoil of *given* shape, and that relaxation can be applied subsequently to solve the exact non-linear equation of compressible flow. This would be *possible* in the hodograph-plane but with the disadvantages of curved boundaries and singularities in the mapping.

Both the polygon and influence factor methods appear simpler to apply and more direct than the method due to Theodorsen and Garrick[15]. Their method is based on the conjugate harmonic functions α and β defined by $z = 2a\cosh(\alpha + i\beta)$. These functions are not as fundamental in aerofoil theory as either of the conjugate pairs $(\log(U/q), \theta)$ or $(x - \phi, y - \psi)$. Exact and direct aerofoil design can be achieved by either the polygon or influence factor methods. All that is required is to interchange the roles of the conjugate functions. Theodorsen's method apparently lacks this flexibility, for instead of aerofoil design he discusses the creation of families of wing sections, the properties of each member being unknown until the calculation is complete.

TABLE 8

Calculation of δm_i

1	2	3	4	5	6
ϕ	x	y	m_i	δm_i	$\cos\theta$
0	8·8620	0·0000		(0·6680)	—
			+0·6680		
$\frac{1}{2}$	8·4585	0·3340		0·4346	0·9311
			0·2334		
1	8·0530	0·4507		0·0840	0·9753
			0·1494		
$1\frac{1}{2}$	7·6442	0·5254		0·0551	0·9890
			0·0943		
$2\frac{1}{8}$	7·1311	0·5840		0·0451	0·9952
			0·0492		
3	6·4048	0·6272		0·0439	0·9995
			+0·0053		
4	5·5632	0·6325		0·0359	0·9999
			−0·0306		
5	4·7075	0·6019		0·0307	0·9985
			−0·0613		
6	3·8352	0·5406		0·0283	0·9963
			−0·0896		
7	2·9426	0·4510		0·0274	0·9936
			−0·1170		
8	2·0221	0·3340		0·0294	0·9904
			−0·1464		
9	1·0617	0·1876		+0·0412	0·9866
			−0·1876		
10	0·0000	0·0000		(−0·1876)	—

TABLE 9

Calculation of $\left\{\frac{\cos\theta}{q} - 1\right\}$

ϕ	0	$\frac{1}{2}$	1	$1\frac{1}{2}$	$2\frac{1}{8}$	3	4	5	6	7	8	9	10	$\{B_j\}$	$\left(\frac{\cos\theta}{q} - 1\right)10^3$	$\{C_i\}$
	$[A_{ij}]$															
$\frac{1}{2}$	−301	−1036	−323	−5	+206	+397	+544	+653	+740	+813	+875	+925	+978	+0·6680		−2100
1	0	−323	−1036	−323	+40	296	474	600	698	778	845	903	954	−0·4346		−2038
$1\frac{1}{2}$	+176	−5	−323	−1036	−235	+166	397	544	653	740	813	875	929	−0·0840		−1830
2	301	+172	−5	−323	−835	−23	+296	474	600	698	778	845	903	−0·0551		−1718
3	477	397	+299	+173	−73	−735	−23	+296	474	600	698	778	845	−0·0451		−1573
4	602	544	476	397	+270	−23	−735	−23	+296	474	600	698	778	−0·0439		−1446
5	699	653	602	544	458	+296	−23	−735	−23	+296	474	600	699	−0·0359		−1300
6	778	740	699	753	587	474	+296	−23	−735	−23	+296	474	602	−0·0307		−1116
7	845	813	778	740	688	600	474	+296	−23	−735	−23	+296	477	−0·0283		−883
8	903	875	845	813	769	698	600	474	+296	−23	−735	−23	301	−0·0274		−563
9	+954	+929	+903	+875	+837	+778	+698	+600	+474	+296	−23	−735	0	−0·0294		−27
														−0·0412		
														−0·1876		

× $\frac{\pi}{\log_e 10}$ =

TABLE 10

Comparison of Velocities

1	2	3	4
ϕ	Exact	Polygon Method	Influence Factor
0	0·000	0·000	0·000
$\frac{1}{2}$	—	1·125	1·178
1	1·191	1·191	1·224
$1\frac{1}{2}$	—	1·196	1·211
2	1·200	1·199	1·201
3	1·188	1·188	1·188
4	1·171	1·169	1·170
5	1·148	1·148	1·148
6	1·123	1·123	1·121
7	1·090	1·090	1·090
8	1·050	1·051	1·049
9	0·991	0·991	0·989
10	0·000	0·000	0·000

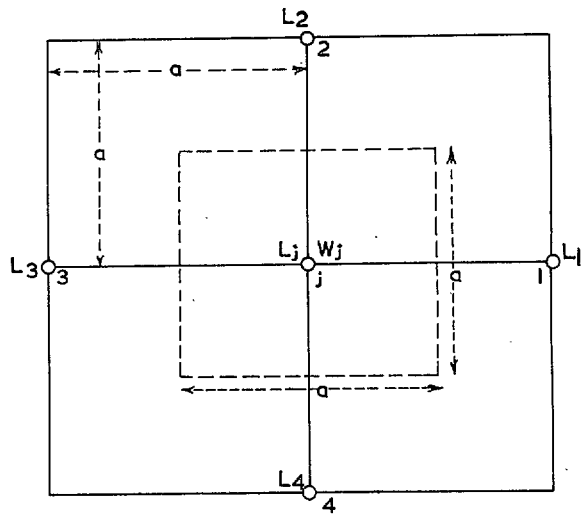

FIG. 9.

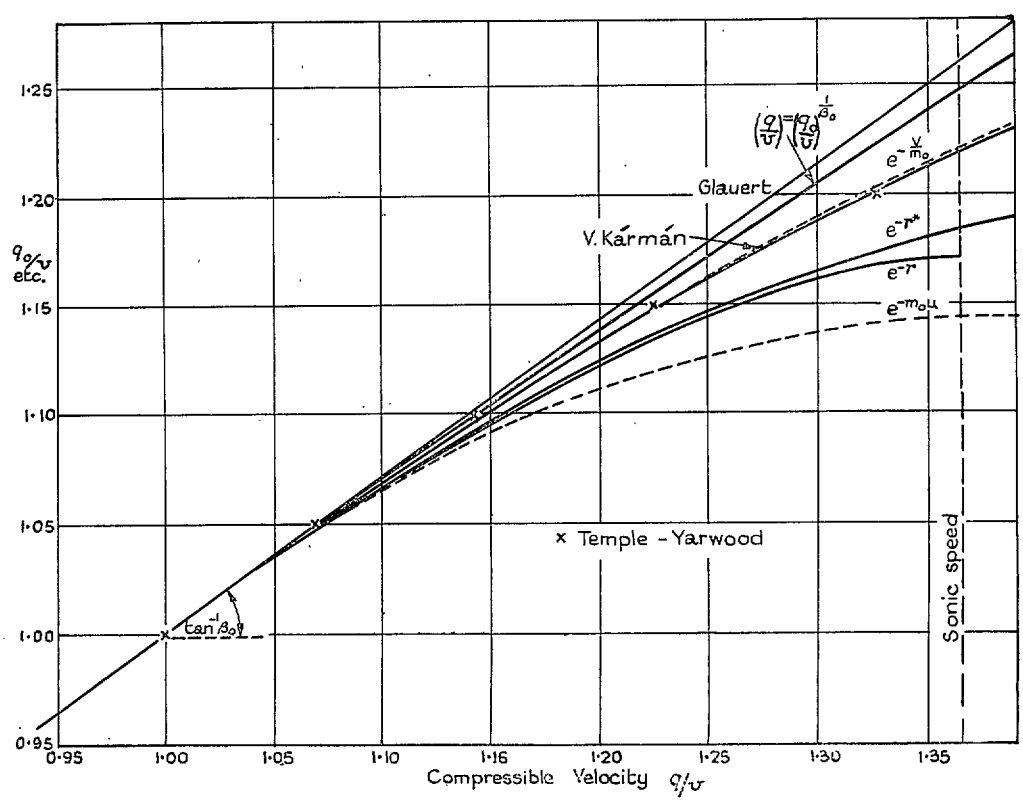

FIG. 10. Comparison of various approximations at $M_0 = 0{\cdot}7$.

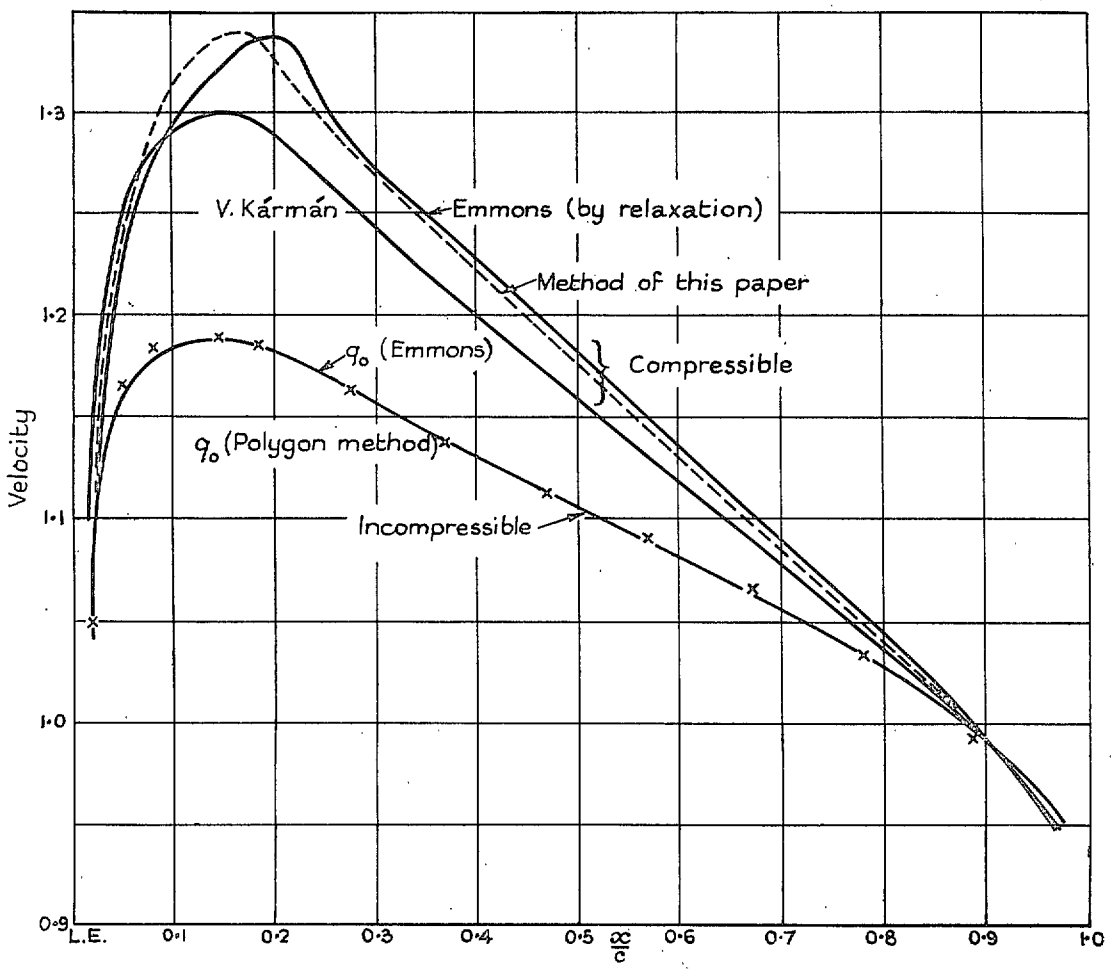

FIG. 11. Velocity distributions at $M_0 = 0, 0{\cdot}7$.

APPENDIX

Singularities in the Relaxation Process

In the w-plane close to a corner of angle τ on an aerofoil, *e.g.*, at the nose or trailing edge, $\log(U/q)$ can be expanded in the form (as in section 3)

$$L = -\frac{\tau}{\pi}\log|w| + a + b|w| + c|w^2| + \ldots,$$

in which the origin is at the corner and $a, b, \ldots$ are independent of $|w|$. The dominant term, $-\tau/\pi \log|w|$, is the contribution to L from the corner itself. In the ϕ-direction

$$L = -\frac{\tau}{\pi}\log\phi + a' + b'\phi + \ldots$$

Therefore $\phi^2\left(\frac{\partial^2 L}{\partial\phi^2}\right) = \frac{\tau}{\pi}$, $\phi^3\left(\frac{\partial^3 L}{\partial\phi^3}\right) = \frac{-2\tau}{\pi}$, $\ldots$ $\phi^n\left(\frac{\partial^n L}{\partial\phi^n}\right) = (-)^n(n-1)!\,\tau/\pi$,

since close enough to the corner the coefficients $a', b', \ldots$ are negligible. Using these relations and similar ones for the ψ-direction, difference equations for L on the mesh points neighbouring the infinity can be found enabling the relaxation to be performed in this region[16].

A further difficulty occurs when the integrand of $\int\frac{d\phi}{q}$ becomes infinite at a stagnation point (or sharp corner). Let $q = 0$ at $\phi = 0$, and $q = q^*$ at $\phi = \phi^*$, then since

$$L \doteq -\frac{\tau}{\pi}\log\phi, \quad q \doteq q^*\left(\frac{\phi}{\phi^*}\right)^{\tau/\pi}.$$

Therefore $s(\phi^*) = \int_0^{\phi^*}\frac{d\phi}{q} = \frac{1}{q^*}\int_0^{\phi^*}\left(\frac{\phi}{\phi^*}\right)^{-\tau/\pi}d\phi = \frac{\phi^*}{q^*(1-\tau/\pi)}$. .. .. (165)

Acknowledgement

The author gratefully acknowledges the help of Professor Temple with the rigorous proof, set out in section 3, of equation (10). Thanks are also due to the National Physical Laboratory for providing the experimental results for NACA 16, quoted in section 17.

REFERENCES

No.	Author(s)	Title, etc.
1	K. H. V. Britten	The use of Influence Factors in Problems of Fluid Flow. R. & M. 2441. April 1947.
2	H. Emmons	Flow of a Compressible Fluid past a Symmetrical Airfoil in a Wind Tunnel and in Free Air. N.A.C.A. Tech. Note 1746. November, 1948.
3	R. G. Gandy and R. V. Southwell..	*Phil. Trans.*, A, Vol. 238, p. 453. 1940.
4	S. Goldstein and A. D. Young ..	The Linear Perturbation Theory of Compressible Flow, with Applications to Wind-tunnel Interference. R. & M. 1909. July, 1943.
5	S. Goldstein and M. J. Lighthill ..	Two-dimensional Compressible Flow past a Solid Body in Unlimited Fluid or symmetrically placed in a Channel. A.R.C. 7184. 1943.
6	Th. von Kármán	Compressibility Effects in Aerodynamics. *Journ. Aero. Sci.*, Vol. 8, No. 9, p. 337. July, 1941.
7	Liepmann and Puckett	*Introduction to the Aerodynamics of a Compressible Fluid.* (p.168). John Wiley and Sons. 1947.
8	M. J. Lighthill	A New Method of Two-dimensional Aerodynamic Design. R. & M. 2112. April, 1945.
9	Lin	*Quart. Journ. Applied Maths.*, Vol. IV, No. 3, p. 291. 1946.
10	Piercy, Piper and Preston	*Phil. Mag.*, Ser. 7, Vol. xxiv, p. 425. 1937.
11	A. Thom	An Investigation of Fluid Flow in Two Dimensions. R. & M. 1194. 1928.
12	A. Thom	Blockage Corrections in a Closed High-speed Tunnel. R. & M. 203 November, 1943.
13	A. Thom	The Method of Influence Factors in Arithmetical Solutions of Certain Field Problems. R. & M. 2440. November, 1947.
14	A. Thom and L. Klanfer	Tunnel Wall Effect on an Aerofoil at Subsonic Speeds. R. & M. 2851. August, 1951.
15	T. Theodorsen and I. E. Garrick ..	General Potential Theory of Arbitrary Wing Sections. N.A.C.A. Report 452. 1932.
16	L. C. Woods	The Numerical Solution of Two-dimensional Fluid Motion in the Neighbourhood of Stagnation Points and Sharp Corners. R. & M. 2726. October, 1949.
17	L. C. Woods	Two-dimensional Aerofoil Design in Compressible Flow. R. & M. 2731. November, 1949.
18	L. C. Woods and A. Thom	A New Relaxational Treatment of the Compressible Two-dimensional Flow about an Aerofoil with Circulation. R. & M. 2727. March, 1950.
19	L. C. Woods	A Relaxation Treatment of Shock-waves. Presented by Prof. A. Thom. A.R.C. 13,242. July, 1950. (Unpublished).
20	L. C. Woods	The Second Order Terms in Two-dimensional Tunnel Blockage (To be published in the *Aero. Quart.*).
21	L. C. Woods	The Application of the Polygon Method to the Calculation of the Compressible Subsonic Flow round Two-dimensional Profiles. C.P. 115, June, 1952.
22	L. C. Woods	Compressible Subsonic Flow in Two-dimensional Channels : The Direct and Indirect Problems. A.R.C. 14,838. April, 1952.
23	L. C. Woods	Aerofoil Design in Two-dimensional Subsonic Compressible Flow. A.R.C. 14,708. (To be published as R. & M. 2845.)

(26167) Wt. 15-680 K9 10/53 F. M. & S. PRINTED IN GREAT BRITAIN

R. & M. No. 2811
(13,240, 13,395, 13,460, 13,533)
A.R.C. Technical Report

Publications of the Aeronautical Research Council

ANNUAL TECHNICAL REPORTS OF THE AERONAUTICAL RESEARCH COUNCIL (BOUND VOLUMES)

1936 Vol. I. Aerodynamics General, Performance, Airscrews, Flutter and Spinning. 40*s.* (40*s.* 9*d.*)
Vol. II. Stability and Control, Structures, Seaplanes, Engines, etc. 50*s.* (50*s.* 10*d.*)

1937 Vol. I. Aerodynamics General, Performance, Airscrews, Flutter and Spinning. 40*s.* (40*s.* 10*d.*)
Vol. II. Stability and Control, Structures, Seaplanes, Engines, etc. 60*s.* (61*s.*)

1938 Vol. I. Aerodynamics General, Performance, Airscrews. 50*s.* (51*s.*)
Vol. II. Stability and Control, Flutter, Structures, Seaplanes, Wind Tunnels, Materials. 30*s.* (30*s.* 9*d.*)

1939 Vol. I. Aerodynamics General, Performance, Airscrews, Engines. 50*s.* (50*s.* 11*d.*)
Vol. II. Stability and Control, Flutter and Vibration, Instruments, Structures, Seaplanes, etc. 63*s.* (64*s.* 2*d.*)

1940 Aero and Hydrodynamics, Aerofoils, Airscrews, Engines, Flutter, Icing, Stability and Control, Structures, and a miscellaneous section. 50*s.* (51*s.*)

1941 Aero and Hydrodynamics, Aerofoils, Airscrews, Engines, Flutter, Stability and Control, Structures. 63*s.* (64*s.* 2*d.*)

1942 Vol. I. Aero and Hydrodynamics, Aerofoils, Airscrews, Engines. 75*s.* (76*s.* 3*d.*)
Vol. II. Noise, Parachutes, Stability and Control, Structures, Vibration, Wind Tunnels. 47*s.* 6*d.* (48*s.* 5*d.*)

1943 Vol. I. (In the press.)
Vol. II. (In the press.)

ANNUAL REPORTS OF THE AERONAUTICAL RESEARCH COUNCIL—

1933-34	1*s.* 6*d.* (1*s.* 8*d.*)	1937	2*s.* (2*s.* 2*d.*)
1934-35	1*s.* 6*d.* (1*s.* 8*d.*)	1938	1*s.* 6*d.* (1*s.* 8*d.*)
April 1, 1935 to Dec. 31, 1936.	4*s.* (4*s.* 4*d.*)	1939-48	3*s.* (3*s.* 2*d.*)

INDEX TO ALL REPORTS AND MEMORANDA PUBLISHED IN THE ANNUAL TECHNICAL REPORTS AND SEPARATELY—

April, 1950 - - - - - R. & M. No. 2600. 2*s.* 6*d.* (2*s.* 7½*d.*)

AUTHOR INDEX TO ALL REPORTS AND MEMORANDA OF THE AERONAUTICAL RESEARCH COUNCIL—

1909-1949 - - - - - R. & M. No. 2570. 15*s.* (15*s.* 3*d.*)

INDEXES TO THE TECHNICAL REPORTS OF THE AERONAUTICAL RESEARCH COUNCIL—

December 1, 1936—June 30, 1939.	R. & M. No. 1850.	1*s.* 3*d.* (1*s.* 4½*d.*)
July 1, 1939—June 30, 1945.	R. & M. No. 1950.	1*s.* (1*s.* 1½*d.*)
July 1, 1945—June 30, 1946.	R. & M. No. 2050.	1*s.* (1*s.* 1½*d.*)
July 1, 1946—December 31, 1946.	R. & M. No. 2150.	1*s.* 3*d.* (1*s.* 4½*d.*)
January 1, 1947—June 30, 1947.	R. & M. No. 2250.	1*s.* 3*d.* (1*s.* 4½*d.*)
July, 1951. - - - - -	R. & M. No. 2350.	1*s.* 9*d.* (1*s.* 10½*d.*)

Prices in brackets include postage.

Obtainable from

HER MAJESTY'S STATIONERY OFFICE

York House, Kingsway, London, W.C.2; 423 Oxford Street, London, W.1 (Post Orders: P.O. Box 569, London, S.E.1); 13a Castle Street, Edinburgh 2; 39 King Street, Manchester 2; 2 Edmund Street, Birmingham 3; 1 St. Andrew's Crescent, Cardiff; Tower Lane, Bristol 1; 80 Chichester Street, Belfast or through any bookseller.

S.O. Code No. 23-2811